Spectrophotometric Determination of Trace Elements by Their Catalytic Effects on the Chlorpromazine-Hydrogen Peroxide Reaction and Its Kinetic-Mechanistic Study

Takashi TOMIYASU

A dissertation submitted to the Doctoral Program
in Chemistry, the University of Tsukuba
in partial fulfillment of the requirements for the degree of
Doctor of Philosophy (Science)

January, 1998

Contents

Chapter 1

Introduction

A chemical determination involves a series of unit operation, including sampling, several sample processing, separation, measurement, data processing and statistical evaluation. Although some determinations will include all the operation while others will include only some of them, all determinations must include a measurement step in which some measurement objectives that are related to concentration or other property of interest are measured. Several variables such as mass, volume of titrant, absorbance, fluorescence, voltammetric diffusion current, etc. have been utilized as the measurement objective. Furthermore, it can be chosen for any measurement objective to measure it either in systems at equilibrium or under dynamic conditions in systems approaching equilibrium. If the first option is chosen, then the resulting procedure is properly classified as an equilibrium method; if the latter option is chosen, then the procedure is properly classified as a kinetic determination. The reaction rate is the most important feature of dynamic systems and the most important factor obtained from the reaction rate is the concentrations of the reactants. This is the basis for kinetic determinations.

Kinetic methods often have some advantages over equilibrium methods in spite of the inherent difficulty of making measurement in a dynamic system [1-3]. The most significant advantages are as follows: the equilibrium differentiations attainable for the reaction

of very closely related compounds such as isomers and homologs are not sufficiently separated to resolve the individual concentrations of a mixture because the characteristic feature of these compounds is very similar, whereas the kinetic features of these compounds are often quite large and permit simultaneous analysis.

Kinetic methods have been classified into catalytic and uncatalytic methods. Catalytic methods are based on the catalytic effect of substances on certain reaction. Broadly speaking, a catalyst can be defined as a substance modifying the rate of a chemical reaction without altering its equilibrium state. Catalytic methods are extremely sensitive, as the catalyst is not consumed during the reaction, but takes part in it in a cyclic manner. The reaction catalyzed by the substance to be determined is termed as the indicator reaction.

Two main approaches have been used for practical treatment of the data in catalytic determinations. These approaches can be distinguished as differential and integral methods. The integral method is subdivided into fixed-time, variable-time and tangent techniques. The fixed time method involves the measurement of the concentration of a reactant and/or product at a predetermined time from the initiation of the reaction. The variable time method, known as the fixed- or constant-concentration method is to measure the time required for a predetermined change. The tangent method is an integral method based on kinetic plots. The dependence of reaction order on the monitored species dictates the kind of plot to

use. For example, for first-order dependence, plots of log[Reactant] versus time yield a family of straight lines whose slopes (generally designated as pseudo-first-order constants) are linearly related to the initial catalyst concentration $[C]_0$. The fixed-time method is most convenient for routine determinations. Application of the tangent method is, however, expected to result in better precision than the use of the fixed- or variable-time methods, since more measurements are performed by the tangent method. The initial-rate method is suitable when the kinetics of the reaction involved is complex and integration of the rate expression is difficult or impossible. This method is the differential variant of the tangent method and involves direct evaluation of d[signal]/dt at a time equal to zero. Although the main difficulty of this method lies in accurate measurement of the initial slope, which is subject to the errors inherent in every graphical method, this method has some advantages generally attributing to that the measurements are performed during the initial very small period: there is no appreciable contribution from the reverse reaction and complications arising from possible side-reactions are negligible.

Because of the growing need for highly sensitive analytical methods, the catalytic kinetic method has become an attractive procedure, as the trace determination can be achieved by relatively simple procedure without expensive or special equipments. Many catalytic methods using various indicator reactions have been reported: there are almost 300 different indicator reactions for determining about 45 elements. However, most of these studies

have been concerned with their analytical applications and little mechanistic studies have been done. This is attributed to the difficulties in evaluation of mechanisms of catalytic reactions arising from their complexity.

Chemical kinetics is concerned with the rate and mechanisms of chemical change. The relation between the rate of a reaction and the concentration of chemical species is termed the rate law or rate equation. The rate law allows much insight into the mechanism, which is always a good guide to the detailed understanding of the reaction process. The interdependence of reaction variables in kinetic methods is commonly rather complicated, so that a large number of experimental runs is required to optimize the analytical conditions. The rate equation describes the quantitative dependence of the reaction rate upon the catalyst and all reactants, and permits an accurate prediction of the mechanism of the reaction over a wide range of reaction conditions. It is often difficult to determine an overall empirical rate law with the reactions utilized for catalytic determinations, because of their complexity. In such a case, the mechanism derived from the results of the experimental observations is utilized to derive an overall kinetic equation. Hence mechanistic studies are important in optimizing the experimental conditions and in extending the analytical utility of the reactions. Moreover, it is expected that the mechanistic studies will lay the foundation for the systematic development of the catalytic methods.

Chlorpromazine (CP) is easily oxidized by several oxidants to

a red intermediate in acidic media, followed by an oxidation to a colorless product by an excess of the oxidants. Because of ease of the formation of the red colored product, CP has been used as an indicator for the detection of various inorganic ions [4,5]. The oxidation of CP by hydrogen peroxide proceeds through two independent parallel reactions; one of which proceeds through the red intermediate, another goes directly to the colorless product. The red intermediate has been designated as a free radical ($C_{17}H_{19}ClN_2SOH\cdot^{2+}$:$CPOH\cdot^{2+}$), which is a bivalent cation having an absorption maximum at 525 nm [6-8]. The colorless product is sulfoxide ($C_{17}H_{19}ClN_2SO^{2+}$:$CP{=}O^{2+}$), which is also bivalent cation having the four absorption maxima at near 240, 270, 300 and 340 nm, respectively [9]. The reactions are written by

$$2C_{17}H_{19}ClN_2S + 3H_2O_2 + 4H^+ = 2C_{17}H_{19}ClN_2SOH\cdot^{2+} + 4H_2O$$

$$C_{17}H_{19}ClN_2S + 2H_2O_2 + 2H^+ = C_{17}H_{19}ClN_2SO^{2+} + 3H_2O$$

It was observed that some trace constituents show a catalytic effect on the oxidation of CP by hydrogen peroxide; iodide and iron catalyzed the red intermediate formation reaction and tungsten(VI) and molybdenum(VI) catalyzed the direct sulfoxide formation reaction. Thus, the analytical and kinetic studies on CP-hydrogen peroxide reaction catalyzed by these species were performed.

The present thesis consists of six chapters.

In Chapter 2, spectrophotometric determination of iodide by its catalytic effect on the red intermediate formation reaction is presented. Kinetic study of the reaction was also performed to elucidate the reaction mechanism for the CP-hydrogen peroxide

reaction and to give a better understanding of the reaction processes.

In Chapter 3, spectrophotometric determination of iron based on its catalytic effect on the formation of red intermediate is presented. According to the results of kinetic study the mechanism of catalyzed reaction is proposed which leads to a rate equation, and analytical implications of the kinetic studies are discussed.

In Chapter 4, spectrophotometric determination of tungsten(VI) by its catalytic effect on the direct sulfoxide formation reaction is developed. The reaction is also investigated kinetically. According to the results, a mechanism is proposed which leads to a rate equation of catalyzed reaction.

It was found that the direct sulfoxide formation reaction was also catalyzed by molybdenum(VI) and the presence of this species caused serious interference for the determination of tungsten(VI). Thus the differential determination of molybdenum(VI) and tungsten(VI) is developed and presented in Chapter 5. The kinetic behavior of these species was investigated in detail. The optimum conditions for differential determination were established by the use of rate equations.

Chapter 2

Spectrophotometric Determination of Trace Amounts of Iodide by Its Catalytic Effect on the Chlorpromazine-Hydrogen Peroxide Reaction. A Mechanistic Study

2.1 Introduction

A number of catalytic methods based on different indicator reactions have been proposed for iodide determination [10-16]. Chlorpromazine is oxidized by hydrogen peroxide to a red intermediate, which has been designated as being a free radical having an absorption maximum at 525 nm [6]. This reagent was first used by Cordoba et al. [17] for the vanadium(V)-catalyzed oxidation of CP by bromate in a phosphoric acid solution. They also applied this indicator reaction to the catalytic determination of iodide in biological samples [18]. This method, however, exhibited a higher reagent blank and was not sufficiently sensitive for the analysis of such samples as natural water having fairly low iodide concentrations, often below 1 $\mu g l^{-1}$; its detection limit was only 5 $\mu g l^{-1}$.

In this work, an iodide-catalyzed oxidation of CP was first examined by using different oxidants (hydrogen peroxide, chloramine T, sodium peroxoborate and potassium bromate) in several acidic media such as hydrochloric, nitric, sulfuric and acetic acids. When hydrogen peroxide was used as an oxidant in sulfuric acid solution, only a slight coloration of CP was observed

in the absence of iodide; this color formation reaction, however, was considerably accelerated by trace amounts of iodide. Thus a kinetic spectrophotometric method for the determination of iodide based on its catalytic effect on the CP-hydrogen peroxide reaction was developed, and the mechanism of catalyzed reaction was also investigated kinetically. The resulting method is highly sensitive and reproducible: as little as 0.2 $\mu g\ l^{-1}$ of iodide can be determined with reasonable reproducibility. This method has been successfully applied to the determination of iodide in natural water samples. The kinetic study was performed to elucidate the reaction mechanisms for the CP-hydrogen peroxide reaction to give a better understanding of the reaction processes and to estimate the extent of the interdependence of variables for allowing the optimal kinetic-catalytic determination of trace iodide.

2.2 Experimental

2.2.1 Apparatus and reagents

A Japan Spectroscopic Co. Ubest-35 spectrophotometer was used with a thermostated cell holder (30 ± 0.1°C) coupled with a Japan Spectroscopic Co. PTL3965 plotter. The temperature was controlled with a Shibata Science Instrument Co. control unit (CU-85) circulating thermostat bath. For the reaction, 1-cm glass cells were used in the recommended procedure and 1-cm quartz cells in the kinetic measurements. The reaction was initiated by the injection of a hydrogen peroxide solution from a Gilson Pipetman

(Model P-1000). For mixing, a remote-controlled magnetic Acrobat stirrer (MS Instrument, Osaka, Japan) was installed at the side of cell holder in the spectrophotometer.

Pure water was prepared by purifying distilled water with a Millipore Milli-Q SP system just before use. Reagent-grade chemicals were used throughout.

A hydrogen peroxide solution was prepared by diluting commercial 31% solution of hydrogen peroxide (10.2 mol l^{-1}) with water. The concentration of this solution was checked by permanganate titration.

A CP solution was prepared by dissolving appropriate amounts of chlorpromazine hydrochloride in water.

A potassium iodide stock solution (0.1 mol l^{-1}) was standardized by Volhard's method. Working solutions were prepared by suitable dilution with water.

A potassium iodate stock solution (1000 mg l^{-1} as iodine) was prepared by dissolving 0.848 g of potassium iodate in water and diluting to 500 ml with water. Working solutions were prepared by diluting this solution.

An iodine (I_2) stock solution was prepared by dissolving 50 mg of elemental iodine in 200 ml of water. The concentration of this solution was determined spectrophotometrically at 350 nm in the presence of excess iodide in an acidic solution just before use. Working solutions were prepared by diluting this solution.

A sulfuric acid (9.0 mol l^{-1}) solution was prepared by diluting concentrated sulfuric acid with water.

2.2.2 Recommended procedure

To 9.0 ml of sample solution in a glass-stoppered tube, 0.30 ml of 0.050 mol l^{-1} CP solution and 2.5 ml of 9.0 mol l^{-1} sulfuric acid were added in this order and thoroughly mixed. This solution was kept at 30℃ in a water bath for about 15 min; a 1.6 ml aliquot was then taken into a 1-cm glass cell. The cell was placed in the holder at 30℃ and the contained solution magnetically stirred. The reaction was initiated by the injection of 0.40 ml of a 10.2 mol l^{-1} hydrogen peroxide solution (30℃). The increase in absorbance of the red intermediate at 525 nm was recorded against a pure-water reference.

2.2.3 Kinetic measurements

A 1.6 ml aliquot of the mixed solution containing the corresponding components except hydrogen peroxide in the appropriate concentrations was taken into a 1-cm cell. The cell was placed in the holder at a given temperature and the contained solution was magnetically stirred. The reaction was initiated by the injection of 0.40 ml of a hydrogen peroxide solution from a Gilson Pipetman (Model P-1000). The increases in absorbance of the red free radical at 525 nm and the colorless sulfoxide at 335 nm were recorded against a pure-water reference. The ionic strength was maintained constant at 1.51 mol l^{-1} by the addition of sodium hydrogen sulfate. Temperature was varied in the range 15.0 to 40.0

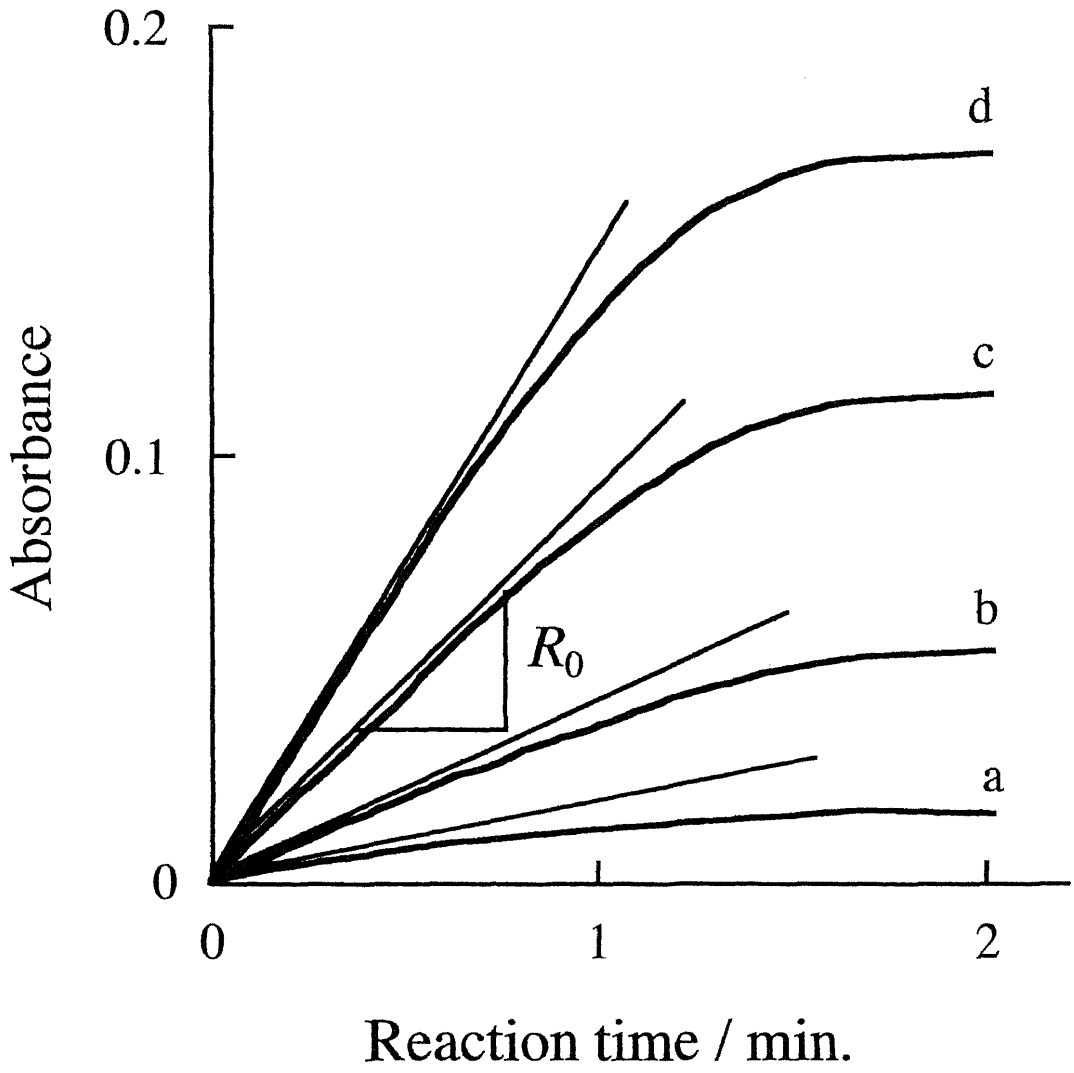

Fig. 2.1 Absorbance-vs.-time curves for the CP/hydrogen peroxide reaction. Concentration of iodide (μg l^{-1}): (a) 0, (b) 2.0, (c) 6.0, (d) 10.0. Conditions: 1.0×10^{-3} mol l^{-1} CP, 1.5 mol l^{-1} sulfuric acid, 2.0 mol l^{-1} hydrogen peroxide, 30℃. R_0: Δ(abs.)/Δ(s) at reaction time zero was used as a measure of the initial reaction rate.

℃. All concentrations given in the tables and figures are the initial analytical concentrations in the reacting mixture at zero time after mixing.

Since the oxidation of CP by hydrogen peroxide proceeds by several parallel pathways, a kinetic investigation of color formation reaction was carried out by the initial-rate method, in which the initial slope of the reaction curves (d(abs.)/dt=R_0) is manually determined and then used as a measure of the initial reaction rate. However, the analysis of the reaction rate curves of the colorless sulfoxide formation reaction was carried out by the integration method, as the formation of the red free radical was negligible under its experimental conditions.

2.3 Results and Discussion

2.3.1 Kinetic determination of iodide

2.3.1.1 Oxidation of CP by hydrogen peroxide and the accelerating effect of iodide on the color formation

In the presence of iodide, CP is oxidized by hydrogen peroxide in a sulfuric acid solution to a red free radical, which is further oxidized to a colorless compound. The reaction can be followed by measuring the increase in absorbance of the red intermediate at 525 nm. As can be seen in Fig. 2.1, the absorbance increases with an increase in the reaction time, and reaches a maximum value at a given time after adding the hydrogen peroxide solution. After the

curves kept maximum values for 20-30 s, the absorbances decrease rather slowly. Since the maximum absorbance increases with an increase in the iodide concentration, this value was used as a parameter for the iodide determination.

Despite the fact that the red intermediate only very slowly decolorized, the absorbance-time curves for the blank and the lower iodide concentrations also reached a maximum at fairly low absorbance. According to this observation, the following behavior was suspected. Chlorpromazine may not only be consumed by the color formation reaction, but also consumed simultaneously by a reaction without any coloration competing with the former one. Iodide accelerates the former reaction. In the absence of iodide a large portion of CP is consumed in the latter reaction, resulting in the development of the maximum on the reaction curve, even in a very low absorbance. This suspicion was confirmed by the following experiments, the results of which are shown in Fig. 2.2. When the iodide solution was added to the reaction mixture for an uncatalyzed reaction (curve A) at a definite time after initiating the reaction (arrow a), an additional increase in the absorbance took place; its value also reached a maximum (curve A'). However, this maximum absorbance (circle d) did not reach a value (circle c) equivalent to the concentration of the added iodide. The maximum value decreased with an increase in the time interval between the start of reaction and the addition of iodide (curve C); no additional increase in the absorbance was observed upon adding the iodide solution when the reaction curve reached the maximum (circle e).

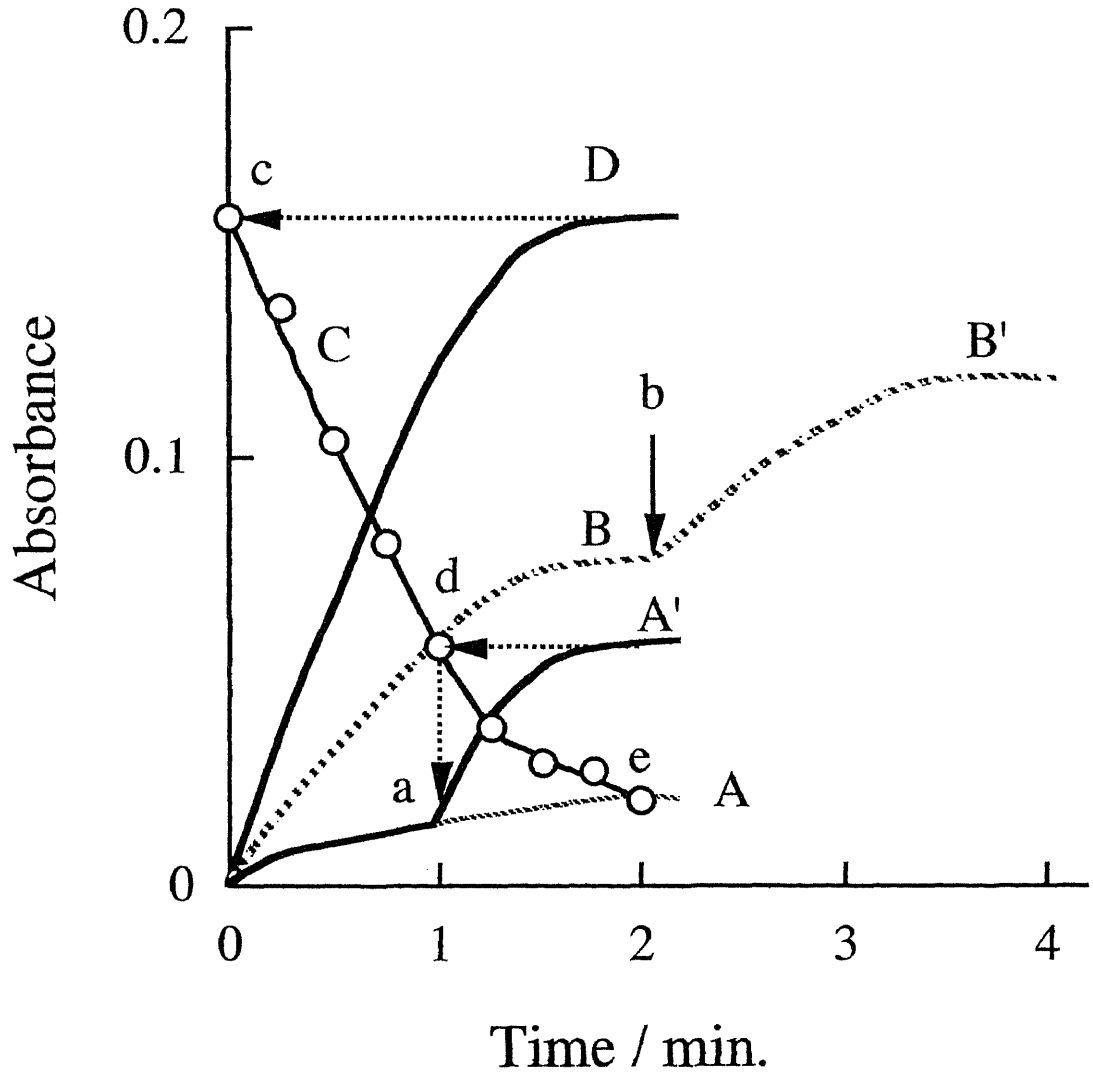

Fig. 2.2 Effect of the subsequent addition of iodide or CP to the reaction mixture. Concentration of iodide in reaction mixture (mol l^{-1}): (A) 0, (B) 1.9×10^{-8}, (D) 3.9×10^{-8}; other conditions as in Fig. 2.1. A 0.010 ml of 7.9×10^{-6} mol l^{-1} iodide solution was added at arrow a to give the iodide concentration in the reaction mixture to be 3.9×10^{-8} mol l^{-1}.; a 0.041 ml of 0.050 mol l^{-1} CP solution was added at arrow b. Curve (A'), (B') and (C); circle (c), (d) and (e): see text.

When the CP solution was added to the reaction mixture for the iodide-catalyzed reaction (curve B) at the maximum on the reaction curve (arrow b), an additional increase in the absorbance also took place, and the reaction curve showed a maximum having an appropriate value for the iodide concentration contained (curve B'). These results suggest that at the maximum absorbance on the reaction curves CP has been exhausted and, thus, its coloration has ceased, even at a fairly low absorbance, such as in the case of the blank.

2.3.1.2 Effects of reaction variables

The influence of temperature on the maximum absorbance for catalyzed and uncatalyzed reactions was studied in the range 15 - 40℃ under the conditions otherwise as in the recommended procedure. The values remained approximately constant in the presence of iodide, while those for the blank increased slightly with an increase in temperature. Although the higher sensitivity was obtained at lower temperatures, there was only a slight increase in the sensitivity upon lowering the temperature. A temperature of 30℃ was chosen because of the convenience for adjusting the temperature throughout the year. The time required for the absorbance to reach a maximum was gradually reduced with temperature from 340 s at 15℃ to 70 s at 40℃. Figure 2.3 shows that there is a complicated relation between the sulfuric acid concentration and the maximum absorbance. In this reaction system CP is consumed by three parallel pathways: catalyzed and

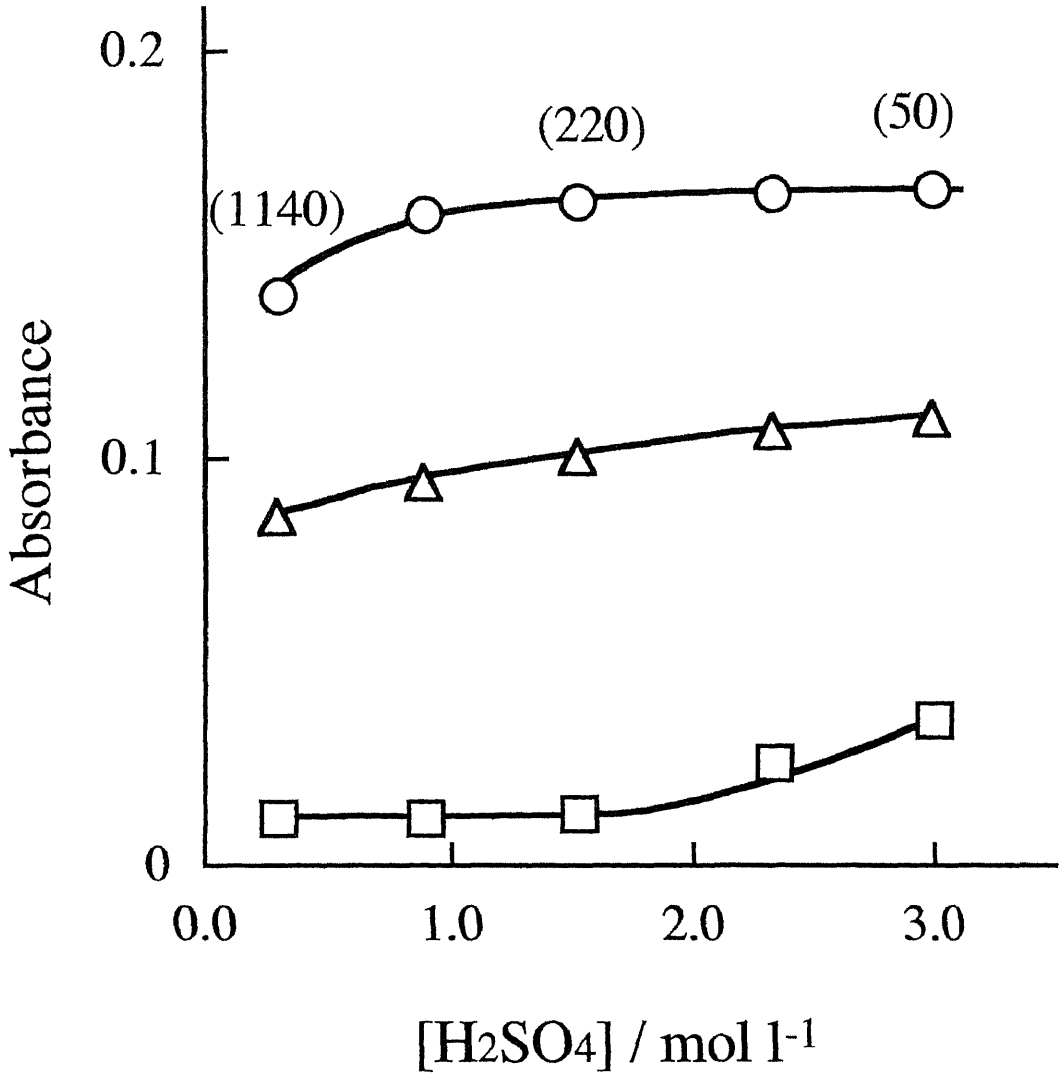

Fig. 2.3 Effect of the sulfuric acid concentration on the catalytic effect of iodide (□ blank, △ 5.0 μg l^{-1}, ○ 10.0 μg l^{-1}). Conditions as in Fig. 2.1, except for the sulfuric acid concentration and hydrogen peroxide concentrations of 1.25 mol l^{-1}.

uncatalyzed color formation reactions, and a side reaction without coloration. Probably, the variation in the hydrogen ion concentration affects the reaction rate by each pathway to a different extent, thus causing the complicated variation in the amount of CP available to the color formation. A sulfuric acid concentration of 1.5 mol l^{-1} was chosen, since it gave the highest sensitivity and the lower blank. The blank absorbance was lowered with increasing hydrogen peroxide concentration (Fig. 2.4). This is probably because an increase in the hydrogen peroxide concentration increases the rate of the side reaction, thus reducing the CP concentration available to color formation. The effect for the catalyzed reaction gradually became less pronounced with increasing iodide concentration. A hydrogen peroxide concentration of 2.0 mol l^{-1} was chosen by considering the sensitivity and the volume of the reagent solution. The time required for the absorbance to reach a maximum decreased with increasing concentration of each of these reagents (sulfuric acid and hydrogen peroxide). The maximum absorbance value increased with an increase in CP concentration in the presence of iodide and in its absence. Since the effect was more pronounced for a catalyzed reaction, a higher sensitivity can be realized at higher CP concentrations (Fig. 2.5). However, at higher CP concentrations the influence of interfering substances increased significantly, due to the susceptibility of CP to react with many oxidizing materials. When a CP solution with higher concentration, along with sulfuric acid, was added to natural water samples, the color formation

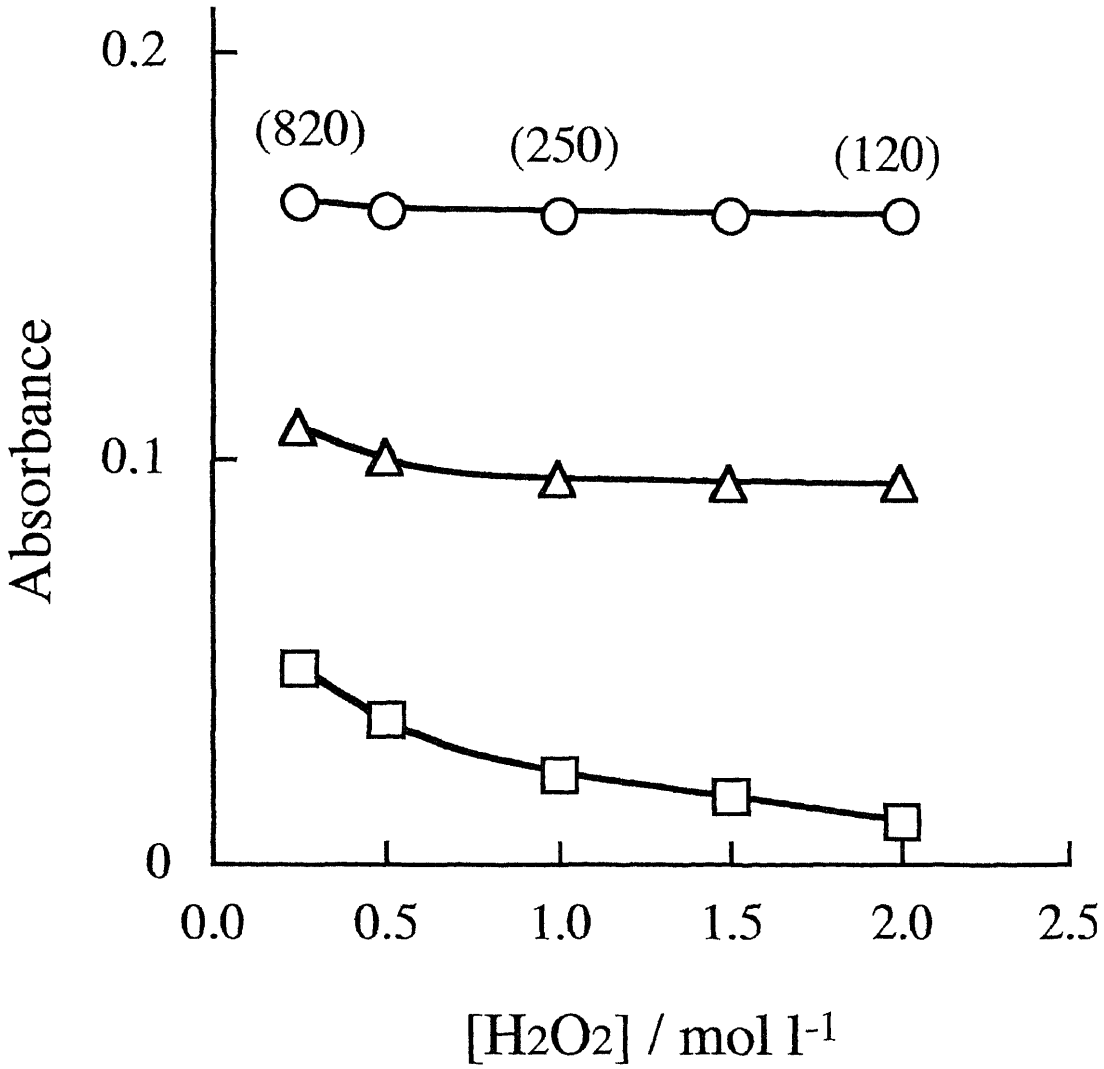

Fig. 2.4 Effect of the hydrogen peroxide concentration on the catalytic effect of iodide (□ blank, △ 5.0 μg l^{-1}, ○ 10.0 μg l^{-1}). Conditions as in Fig. 2.1, except for the hydrogen peroxide concentration.

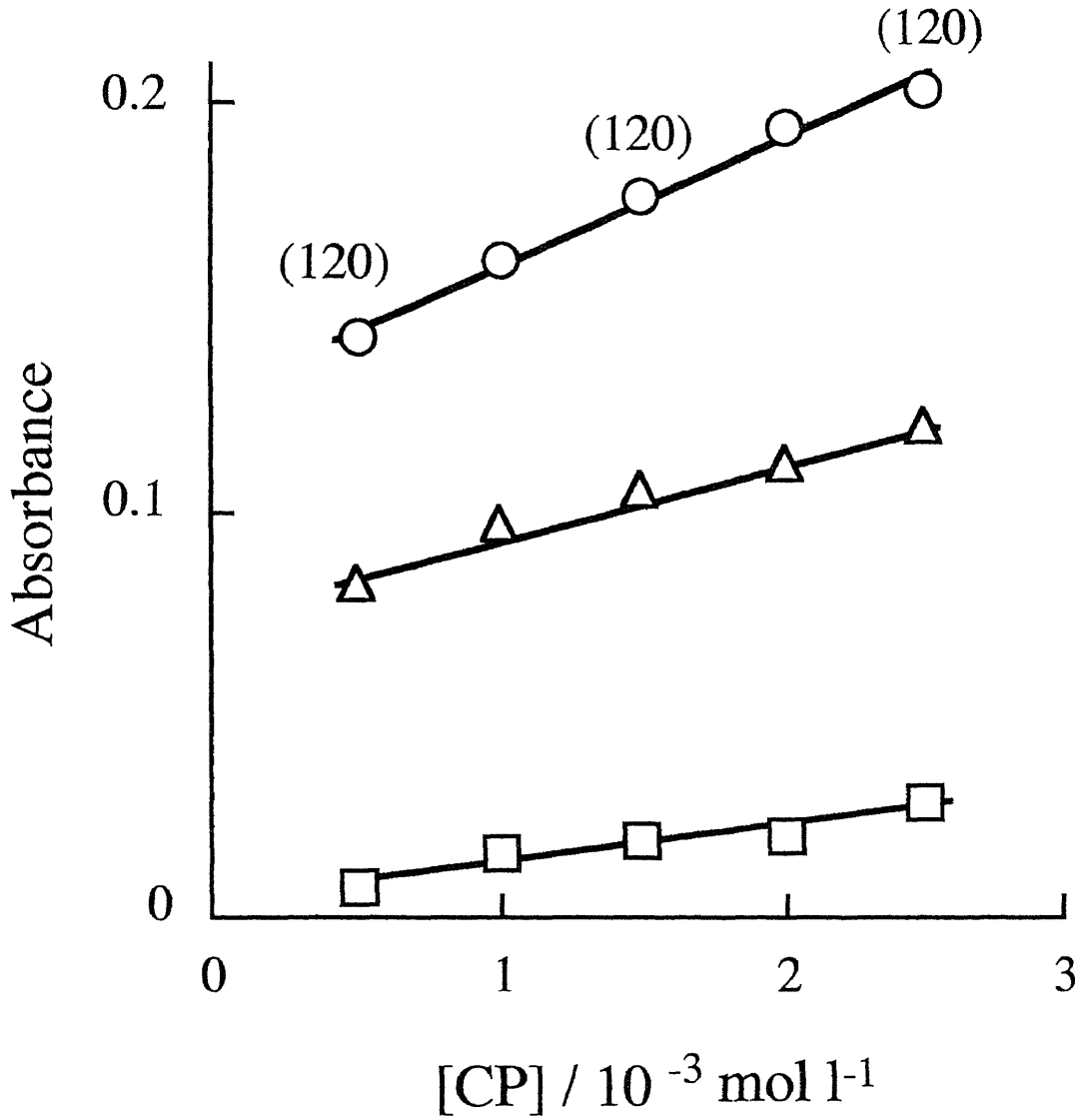

Fig. 2.5 Effect of the CP concentration on the catalytic effect of iodide (□ blank, △ 5.0 μg l^{-1}, ○ 10.0 μg l^{-1}). Conditions as in Fig. 2.1, except for the CP concentration.

occurred to a measurable extent prior to the addition of a hydrogen peroxide solution, causing serious errors in the iodide determinations; thus, CP in the higher concentrations significantly vitiates the applicability of the method to real samples. Hence, a lower CP concentration of 1.0×10^{-3} mol l^{-1} was adopted. No variation in the time required for the absorbance to reach a maximum was observed by varying the CP concentration.

2.3.1.3 Calibration graphs and reproducibility

A series of standard solutions of iodide was treated as in the recommended procedure. The resulting graph shows a slightly negative deviation (Fig. 2.6, ○). The relative standard deviations for 11 replicate determinations of 0.6, 2.0, and 6.0 μg l^{-1} of iodide are 4.2, 2.6 and 0.8%, respectively; it is 10.2% even at concentrations as low as 0.2 μg l^{-1}, which is the lowest concentration that could be determined (Fig. 2.6, inset). Iodate alone can also be determined after iodide was removed by oxidizing to free iodine, followed by heating [19].

2.3.1.4 Catalytic effects of iodide and free iodine

Iodate showed the same catalytic effect (Fig. 2.6, ●) as iodide in the same concentration as iodine, while the catalytic activity of free iodine (Fig. 2.6, □) was slightly lower than that of iodide. Mercury(II) inhibits the catalytic activity of iodide at the same concentration level as iodide ; the larger the mercury(II) concentration, the lower the activity of iodide, and excess

mercury(II) completely inhibits the catalytic effect of iodide. This inhibition probably results from the formation of a complex between mercury(II) and iodide. Iodate was also inhibited by mercury(II) to the same extent as iodide, indicating that iodate has been reduced to iodide by CP and is then introduced into the catalytic cycle. Although free iodine may also be reduced by CP, and then act as a catalyst, the observed negative deviation of the calibration graph for free iodine from that for iodide presumably results from the conversion of a portion of free iodine to a catalytically inactive species, such as the iodinated product of CP, or its escape from the strong acidic solution. If samples contain free iodine, the results obtained by the present procedure should be somewhat lower.

2.3.1.5 Effect of order of reagent addition

In applying this reaction system to the mixture of iodide and iodate, it was observed that the results for the mixture are affected by varying the order of reagent addition. When a CP solution and sulfuric acid were added to the mixture in the same order as in the recommended procedure, the obtained absorbances remained constant at the expected value, regardless of the ratio of iodide and iodate (Fig. 2.6, △). However, when sulfuric acid was first added to the mixture, followed the addition of a CP solution, there was an apparent decrease in the value obtained from that by the recommended procedure; the value varied with varying ratio of iodide and iodate (Fig. 2.6, ▲). When solutions containing free

iodine were analyzed by this order of reagent addition, the obtained results were less reproducible. This is presumably because iodide and iodate reacts partly with each other to form less reactive free iodine, as described above. The order of the addition of the reagents indicated in the recommended procedure was favorable for obtaining reproducible results.

2.3.1.6 Effect of foreign ions

The effect of various ions on the determination of 5 μg l^{-1} iodide was examined. The following ions showed no interference at least at the concentrations (mg l^{-1}) shown in parentheses: K^+ and Na^+ (2000); NO_3^- (1500); NH_4^+ and Ca^{2+} (1000); Mg^{2+} (500); Ni^{2+}, Zn^{2+}, Cd^{2+}, Sn^{4+}, Mn^{2+}, Al^{3+}, Ce^{3+}, As(V), Cl^-, ClO_3^-, ClO_4^-, CO_3^{2-}, $C_2O_4^{2-}$ and CH_3COO^- (100); Cu^{2+}, Pb^{2+} Sn^{2+}, Sb(III), Sb(V), SiO_4^{2-}, SO_3^{2-} and PO_4^{3-} (10). The interfering ions are listed in Table 2.1. Ions which are known to participate in redox reactions as either oxidizing or reducing agents cause serious interference. Mercury and silver ions seriously interfere by combining with iodide. These ions showed no interference at concentrations one order lower than those indicated in Table 2.1.

2.3.1.7 Determination of iodine in natural waters

In order to test the reliability of the present method, it was applied to the determination of iodide in natural water samples. The determinations were made by using samples diluted at different times; the method was also checked by adding a known amount of

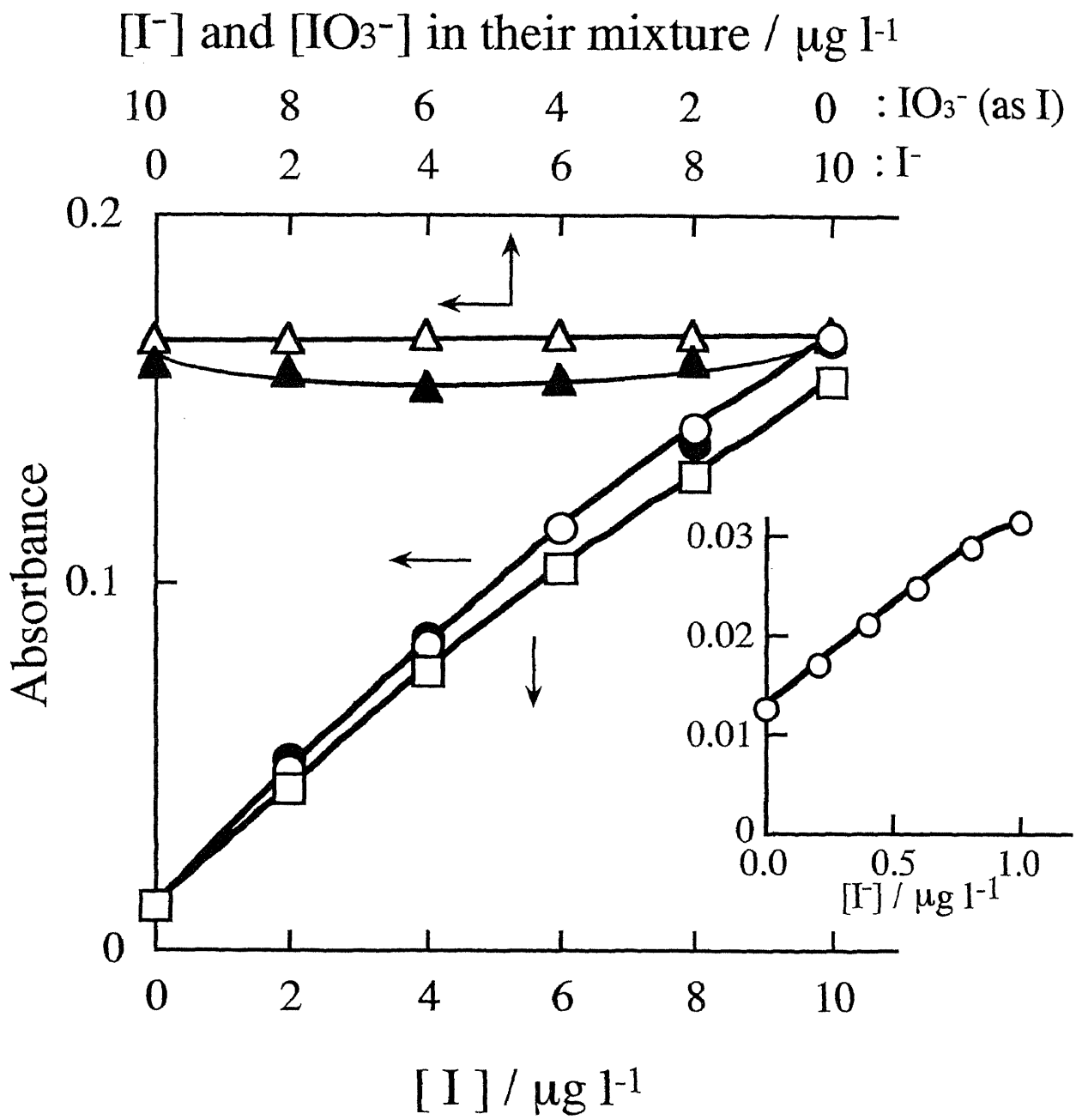

Fig. 2.6 Calibration graphs and effect of order of reagent addition. Conditions as in Fig. 2.1; (○) iodide; (●) iodate; (□) free iodine. Reagents were added to the mixrure of iodide and iodate in the following order: (△) CP/sulfuric acid; (▲) sulfuric acid/CP. The inset provides detail for the lower concentration range of curve for iodide (○).

Table 2.1

Effect of interfering ions on the determination of 5.0 μg l^{-1} of iodide

Ion added	μg l^{-1}	I^- found / μg l^{-1}	Ion added	μg l^{-1}	I^- found / μg l^{-1}
As(III)	10000	4.3	Cr(VI)	100	6.2
V (V)	10000	5.3	Mn(VII)	100	7.1
F^-	10000	5.4	SCN^-	100	7.3
Mo(VI)	5000	2.7	Br^-	100	5.3
Ba^{2+}	1000	7.9	$S_2O_3^{2-}$	100	3.2
Ce(IV)	1000	7.2	NO_2^-	10	5.6
W (VI)	1000	4.2	BrO_3^-	10	5.5
Ag^+	100	0.9	S^{2-}	10	5.6
Fe^{2+}	100	6.6	Hg^{2+}	1	4.4
Fe^{3+}	100	6.7			

Table 2.2 Determination of iodine in natural waters

Sample	Dilution (times)	Added / μg l^{-1}	Found / μg l^{-1}	Recovery, %	In sample / μg l^{-1}	
					Present method	Other method[a]
River water I	-	-	0.45	-	0.45	0.55
	2	-	0.28	-	0.56	
	2	0.50	0.80	103		
	2	1.00	1.35	105		
					av. 0.51	
River water II	-	-	1.95	-	2.0	2.4
	2	-	1.20	-	2.4	
	5	-	0.40	-	2.0	
	5	0.50	0.90	100		
	5	1.00	1.42	101		
	10	-	0.20	-	2.0	
					av. 2.1	
River water III	-	-	3.03	-	3.0	3.9
	2	-	1.55	-	3.1	
	5	-	0.67	-	3.4	
	5	0.50	1.15	98		
	5	1.00	1.65	99		
	10	-	0.33	-	3.3	
					av. 3.2	
Rain water	-	-	0.39	-	0.39	-
	2	-	0.20	-	0.40	
	2	0.20	0.44	110		
	2	0.40	0.58	97		
					av. 0.40	

a. Catalytic (iron(III) thiocyanate) method, by which total iodine can be determined including free iodine and iodate.

iodide to the samples. The results are shown in Table 2.2. The values corrected for dilution showed good agreement, and good recoveries of added iodide were obtained ranging from 97 to 110% (mean 102%). In some cases, a slight coloration was observed upon the addition of the CP and sulfuric acid solutions prior to the addition of hydrogen peroxide. However, the satisfactory results were obtained by subtracting the absorbance (<0.05) measured before starting the reaction from the absorbance finally obtained, and then evaluating the iodide concentration by using the resulting net value. The proposed method is quite suitable for determining iodide at very low concentrations.

These samples were also analyzed by the other method. As can be seen in Table 2.2, the results obtained by the proposed method tended to be somewhat lower than those obtained by the other one. This tendency may suggest that iodine in river water is partly present in the form of free iodine. The speciation of iodine in natural water samples is an interesting subject to be further investigated.

2.3.2 Kinetic and mechanistic study

2.3.2.1 Determination of the molar absorptivity of the red intermediate

For transformation of the initial rate and apparent rate constant evaluated from the absorbance-time curves to those based on the concentration-time dependences, the molar absorptivity at 525 nm

of the red free radical, $C_{17}H_{19}ClN_2SOH^{\bullet 2+}$, was determined as follows. The absorbance was measured by the same procedure as described in Section 2.2.3. When CP in large excess over an oxidant was oxidized by one of several oxidants such as iodate, free iodine, cerium(IV) and dichromate in 1.5 mol l^{-1} sulfuric acid solution, the absorbance of the solution owing to the formation of the red free radical reaches a maximum value within 10 s (at 30℃) and then remains at the maximum value for a few min. This absorbance value was used for the evaluation of the molar absorptivity. The half reaction of the $CPOH^{\bullet 2+}$/CP redox couple may be described as

$$C_{17}H_{19}ClN_2SOH^{\bullet 2+} + H^+ + 3e \rightleftarrows C_{17}H_{19}ClN_2S + H_2O \qquad (2.1)$$

Thus, the reaction between CP and each oxidant has a stoichiometry given by

$$2C_{17}H_{19}ClN_2S + IO_3^- + 4H^+ = 2C_{17}H_{19}ClN_2SOH^{\bullet 2+} + I^- + H_2O \qquad (2.2)$$

$$2C_{17}H_{19}ClN_2S + 3I_2 + 2H_2O = 2C_{17}H_{19}ClN_2SOH^{\bullet 2+} + 6I^- + 2H^+ \qquad (2.3)$$

$$C_{17}H_{19}ClN_2S + 3Ce^{4+} + H_2O = C_{17}H_{19}ClN_2SOH^{\bullet 2+} + 3Ce^{3+} + H^+ \qquad (2.4)$$

$$2C_{17}H_{19}ClN_2S + Cr_2O_7^{2-} + 12H^+ = 2C_{17}H_{19}ClN_2SOH^{\bullet 2+} + 2Cr^{3+} + 5H_2O \qquad (2.5)$$

The concentrations of the red free radical were calculated from the concentrations of the oxidants used according to the stoichiometries in Eqs. (2.2) - (2.5) shown above.

The results obtained together with the experimental conditions are given in Table 2.3. The molar absorptivity of $C_{17}H_{19}ClN_2SOH^{\bullet 2+}$ at 525 nm was evaluated as $\varepsilon_{red} = 3.03 \times 10^4$ l

Table 2.3

Results for the determination of the molar absorptivity at 525 nm of the red free radical (1.5 mol l^{-1} H_2SO_4, 30℃)

oxidant			red free radical		
	($\times 10^{-5}$ mol l^{-1})	concn. of CP ($\times 10^{-3}$ mol l^{-1})	calculated concn. ($\times 10^{-5}$ mol l^{-1})	abs.	ε_{red} ($\times 10^{4}$ l mol^{-1} cm^{-1})
IO_3^-	0.576	1.00	1.15	0.341	2.965
	0.864	1.00	1.73	0.517	2.988
	1.15	1.00	2.30	0.719	3.126
	1.44	1.00	2.88	0.880	3.056
	1.44	2.00	2.88	0.858	2.979
	1.44	3.00	2.88	0.840	2.917
	1.44	4.00	2.88	0.860	2.986
	1.44	5.00	2.88	0.863	2.997
	1.44	10.0	2.88	0.840	2.917
I_2	0.200	1.00	0.133	0.039	2.932
	0.400	1.00	0.267	0.077	2.888
	0.600	1.00	0.400	0.115	2.875
	0.800	1.00	0.533	0.154	2.889
	1.00	1.00	0.667	0.197	2.954
	1.00	0.500	0.667	0.198	2.969
Ce^{4+}	2.00	1.00	0.667	0.208	3.118
	4.00	1.00	1.33	0.421	3.165
	6.00	1.00	2.00	0.647	3.235
	8.00	1.00	2.67	0.878	3.288
	10.0	1.00	3.33	1.098	3.297
$Cr_2O_7^{2-}$	0.200	1.00	0.400	0.127	3.175
	0.400	1.00	0.800	0.237	2.963
	0.800	1.00	1.65	0.479	2.994
	1.20	1.00	2.40	0.710	2.958
					mean 3.026

$mol^{-1}cm^{-1}$ with a standard deviation of 0.13×10^4 l $mol^{-1}cm^{-1}$ (n=24).

2.3.2.2 Kinetics of the iodide-catalyzed red free radical formation reaction

In order to determine the dependence of R_0 on iodide concentration, a series of experiments was performed in which the iodide concentration was varied while the CP, hydrogen ion and hydrogen peroxide concentrations were held constant. The plot of R_0 vs. the total analytical concentration of iodide was linear in the investigated range of 0 - 6.4×10^{-8} mol l^{-1} iodide, as can be seen in Fig. 2.7. It was established that the red free radical formation reaction was first order with respect to iodide ions:

$$R_0 = k_{1(app)}[I^-] + a \qquad (2.6)$$

where $k_{1(app)}$ is the apparent rate constant and a is the intercept on the ordinate which corresponds to the initial rate of an uncatalyzed reaction ($R_{0(uc)}$). $R_{0(uc)}$ was also measured in the absence of iodide under the same conditions as those for the catalyzed reaction. The initial rate of the catalyzed reaction ($R_{0(cat)}$) was obtained by $R_{0(cat)} = R_0 - R_{0(uc)}$. The $k_{1(app)}$ values were determined at different concentrations of both hydrogen peroxide in the range 0.5-2.0 mol l^{-1} and hydrogen ions in the range 0.6 - 1.5 mol l^{-1}. As can be seen in Fig. 2.8, the straight lines obtained by plotting the $k_{1(app)}$ vs. hydrogen peroxide concentration show that the relation is given by $k_{1(app)} = k_{2(app)}[H_2O_2]$, where $k_{2(app)}$ is the slope of the line. The dependence of $k_{2(app)}$ on hydrogen ion concentration is shown in

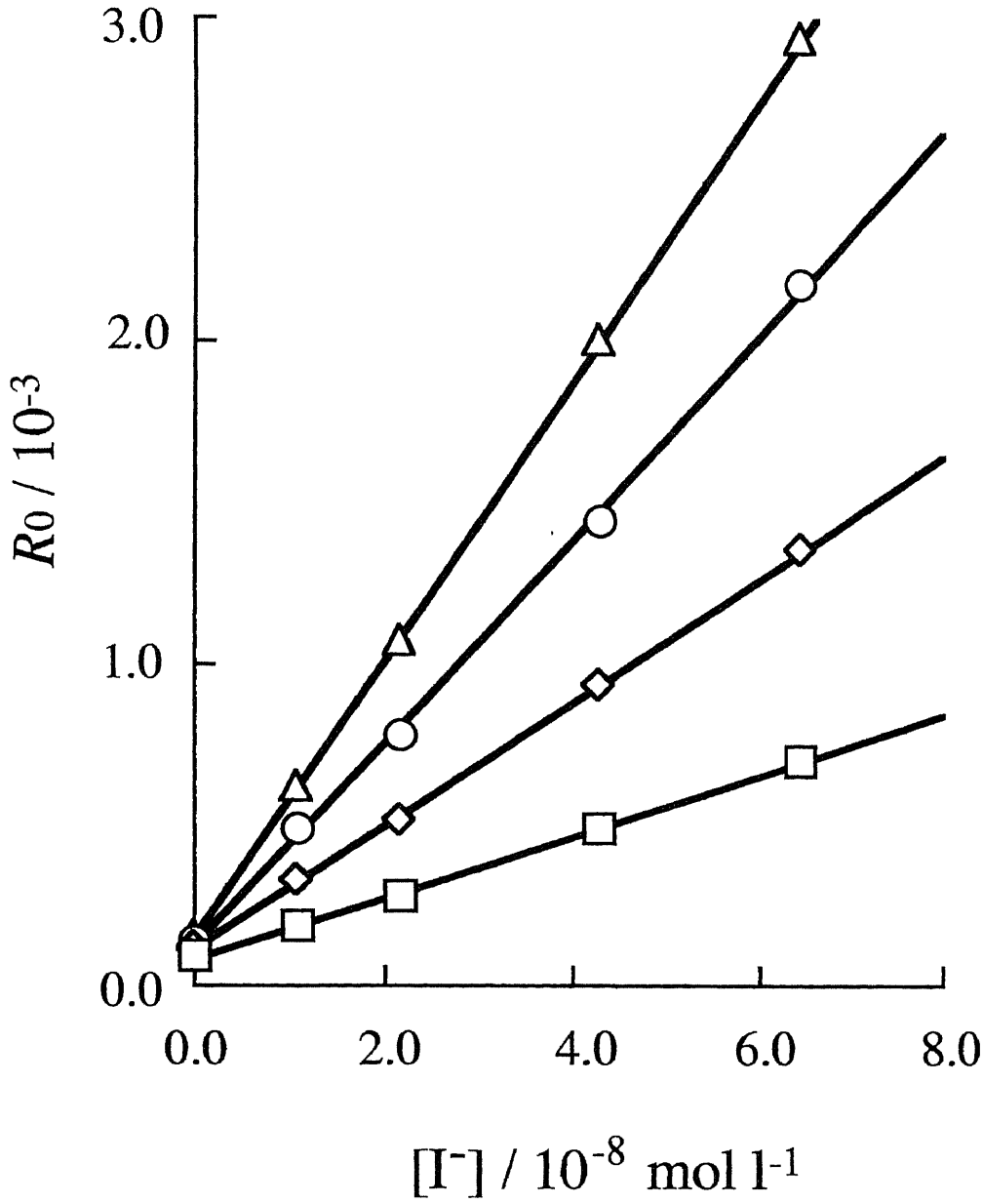

Fig. 2.7 Dependence of initial rate R_0 for iodide catalyzed red free radical formation on iodide concentration. Conditions: 1.0×10^{-3} mol l^{-1} CP, 1.5 mol l^{-1} sulfuric acid, 1.5 mol l^{-1} ionic strength, 30 ℃, hydrogen peroxide concentration (mol l^{-1}) [0.50 (□), 1.00 (◇), 1.50 (○), 2.00 (△)]

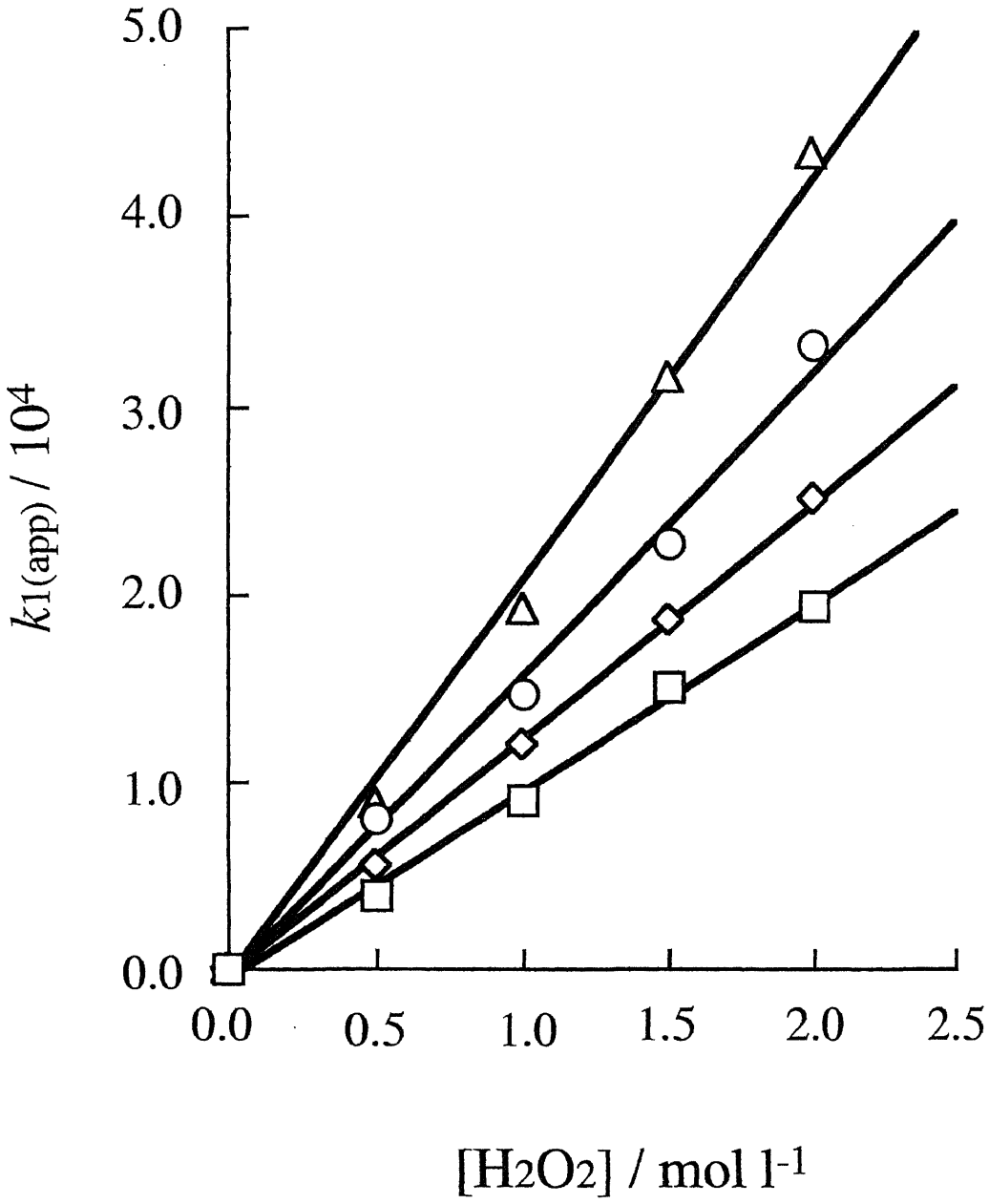

Fig. 2.8 Dependence of apparent rate constant $k_{1(app)}$ on hydrogen peroxide concentration. Conditions: sulfuric acid concentration (mol l^{-1}) [0.60 (□), 0.90 (◇), 1.2 (○), 1.5 (△)], the others as in Fig. 2.7.

Fig. 2.9 (line I), from which the relation is found to be $k_{2(app)}=k_{3(app)}[H^+]$, where $k_{3(app)}$ is the slope. The dependence of the rate on the CP concentration was determined by measuring the initial rate at constant hydrogen peroxide and hydrogen ion concentrations for two iodide concentrations. As can be seen in Table 2.4, the approximate constancy of the initial rate of the catalyzed reaction ($R_{0(cat)}$) shows that $R_{0(cat)}$ is independent of the CP concentration over the wide range 5×10^{-5} - 1×10^{-3} mol l^{-1}. This kinetic behavior suggests that the color formation from CP in the catalyzed reaction occurs rapidly after the rate-determining step. Thus, the rate of the catalyzed reaction is given by:

$$R_{(cat)} = k_{3(app)}[I^-][H_2O_2][H^+] \qquad (2.7)$$

The rate constant k_3 (= $k_{3(app)}/\varepsilon_{red}$) is 0.449 ($1.36\times10^4$ / 3.03×10^4) l^2 mol^{-2} s^{-1} (at 30℃).

2.3.2.3 Kinetics of the uncatalyzed red free radical formation reaction

The kinetics of the uncatalyzed reaction are illustrated in Figs. 2.10 and 2.11. The plots of $R_{0(uc)}$ vs. the initial concentration of CP was linear in the range of 0 - 1.0×10^{-3} mol l^{-1} CP (Fig. 2.10). It was established that the uncatalyzed reaction was first order with respect to CP:

$$R_{0(uc)} = k_{4(app)}[CP]_0 + b \qquad (2.8)$$

where subscript 0 refers to initial concentration, $k_{4(app)}$ is the apparent rate constant and b is the intercept on ordinate which is

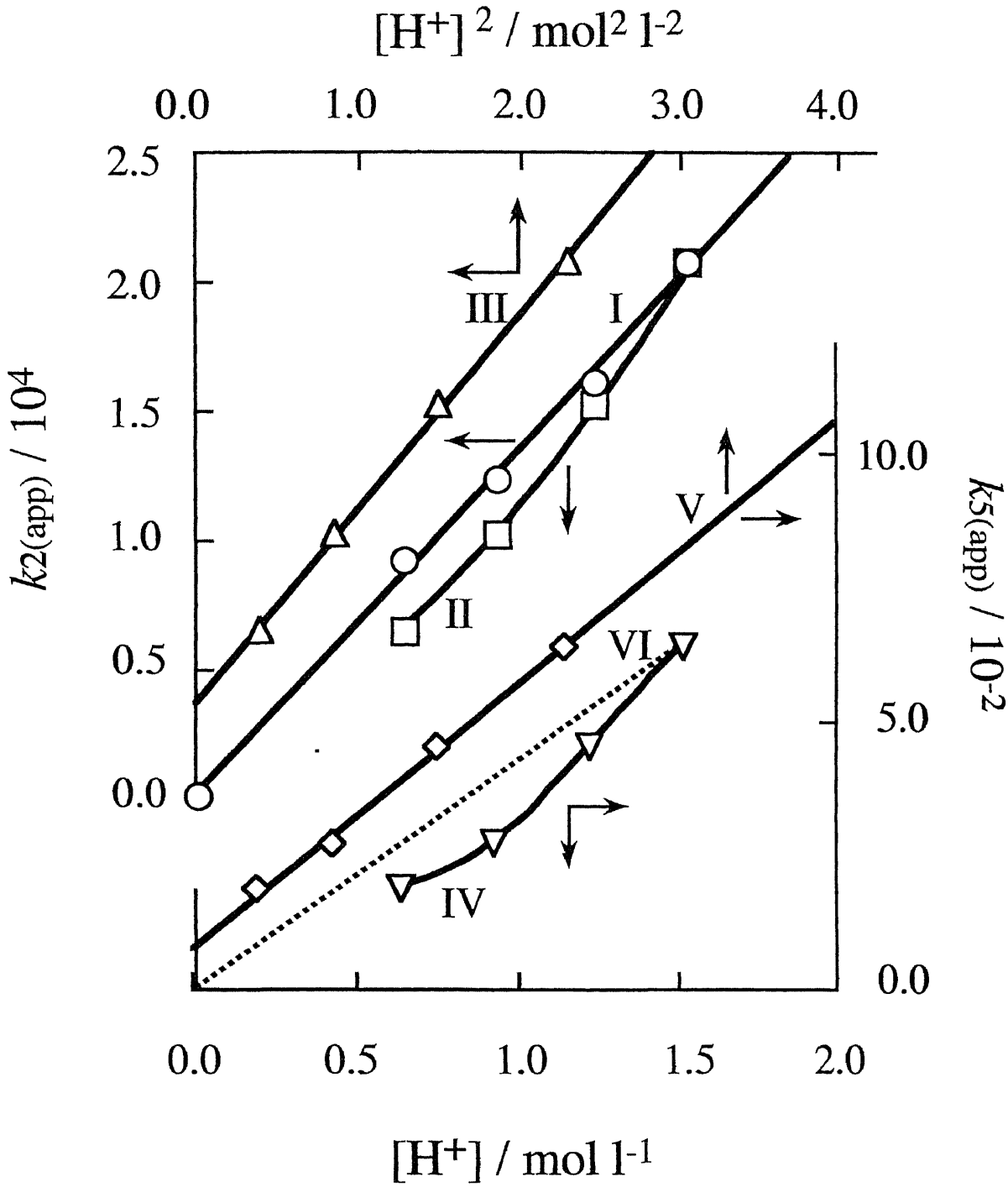

Fig. 2.9 Dependence of apparent rate constants $k_{2(app)}$ and $k_{5(app)}$ on hydrogen ion concentration. Lines I, III and curve II: iodide catalyzed reaction [conditions as in Fig. 2.8]; lines V, VI and curve IV: in the absence of iodide[conditions as in Fig. 2.11]. Line I: ionic strength maintained constant at 1.5 mol l^{-1}; lines III, V and curves II, IV: ionic strength not adjusted constant. Line VI: presumed.

Table 2.4

Dependence of initial rate of catalyzed reaction on CP concentration at 30℃ with 2.0 mol l^{-1} hydrogen peroxide and 1.5 mol l^{-1} sulfuric acid

CP ($\times 10^{-4}$mol l^{-1})	$R_{0(cat)}$ ($\times 10^{-3}$ abs.s^{-1})	
	2.4×10^{-8}mol l^{-1} I^-	4.8×10^{-8}mol l^{-1} I^-
0.50	0.83	1.65
0.83	0.91	1.62
1.00	0.84	1.72
1.50	0.86	1.66
1.67	0.89	1.73
2.00	0.91	1.70
3.33	0.90	1.76
5.00	0.84	1.68
10.00	0.86	1.68

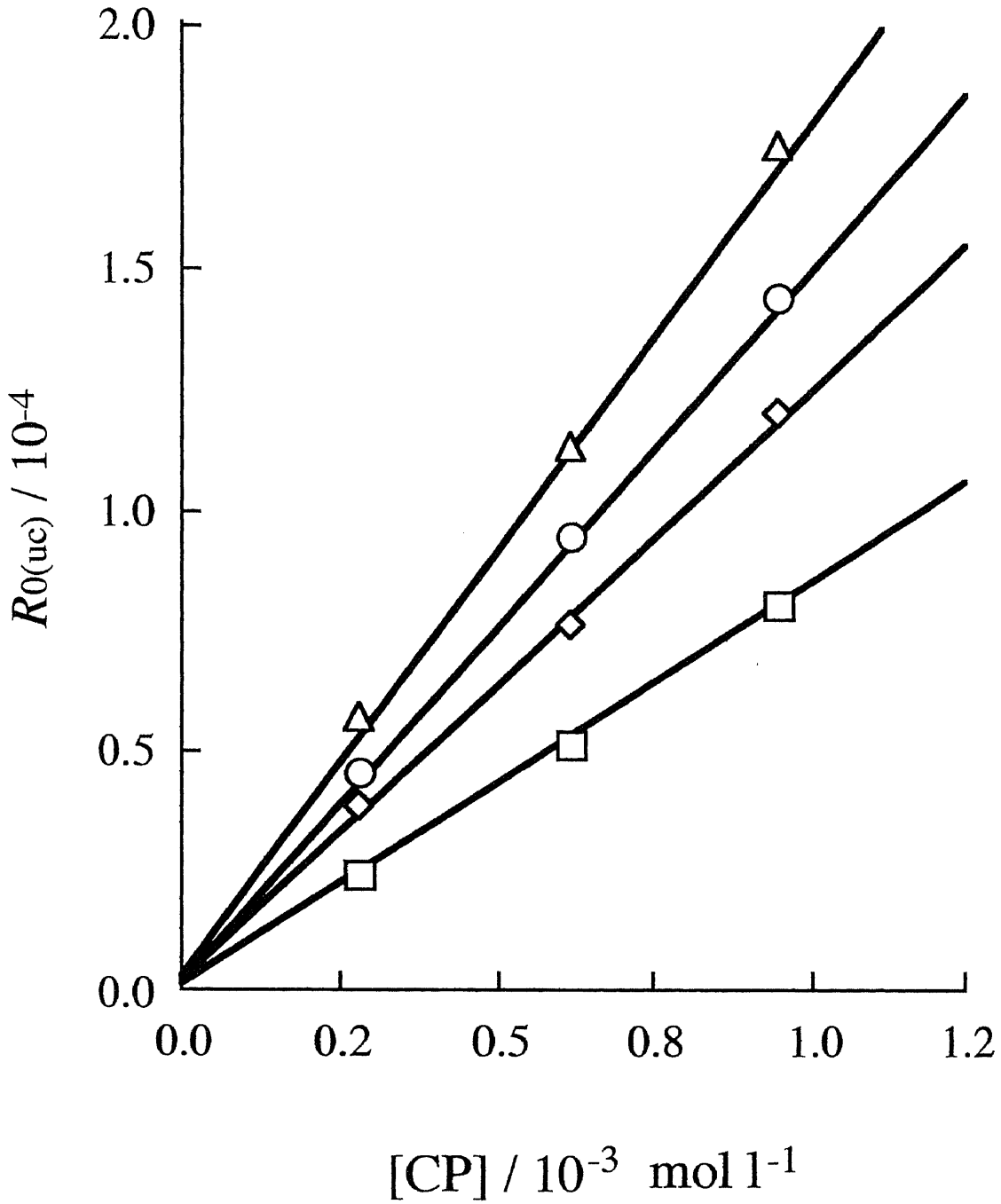

Fig. 2.10 Dependence of initial rate $R_{0(uc)}$ for the red free radical formation in the absence of iodide on CP concentration. Conditions:1.5 mol l^{-1} hydrogen ion concentration, hydrogen peroxide concentration (mol l^{-1}) [0.80 (□), 1.2 (◇), 1.6 (○), 2.0 (△)].

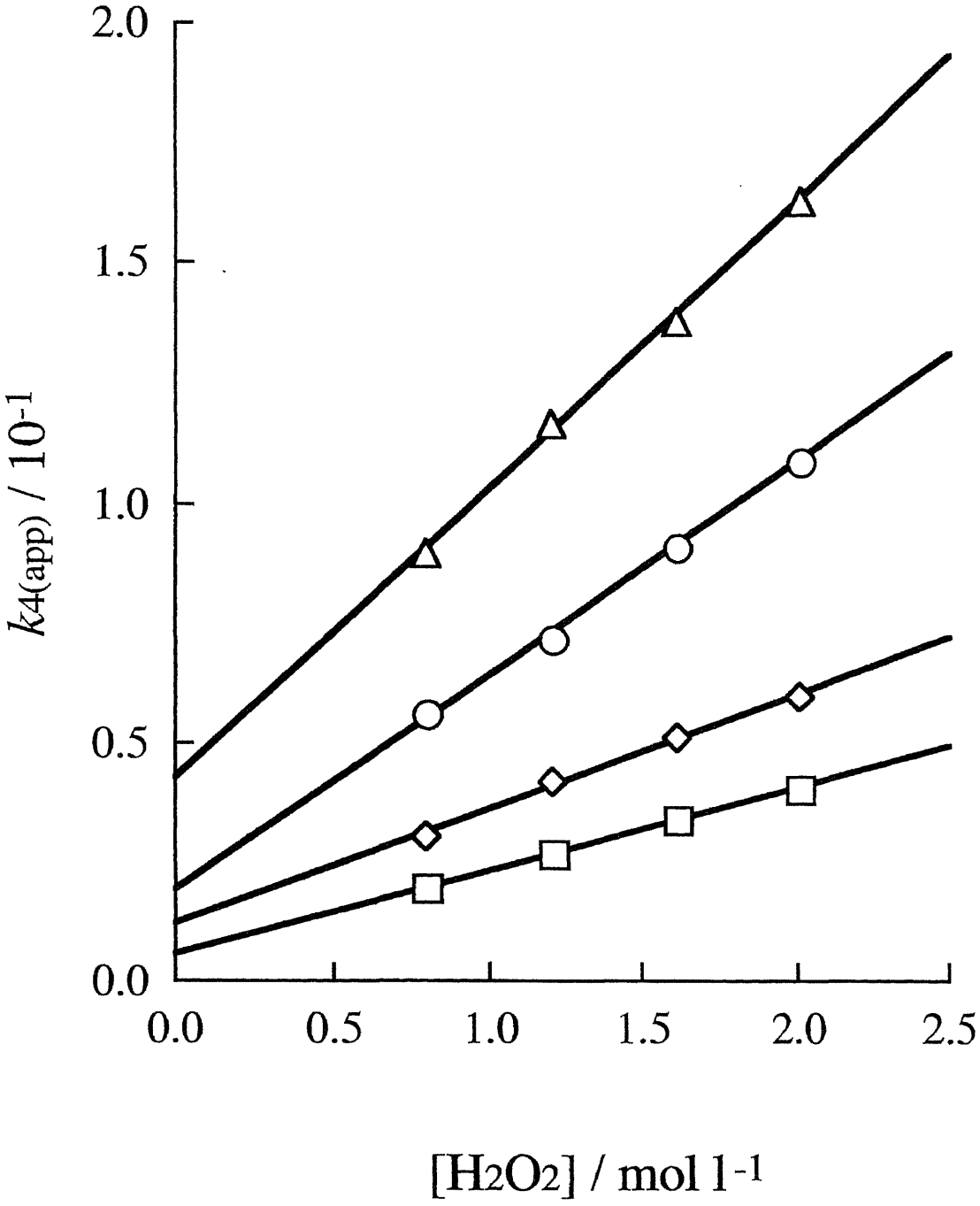

Fig. 2.11 Dependence of apparent rate constant $k_{4(app)}$ on hydrogen peroxide concentration. Conditions: hydrogen ion concentration (mol l^{-1}) [0.61 (□), 0.91 (◇), 1.2 (○), 1.5 (△)], the others as in Fig.2.10.

the rate likely to result from the effect of iodine as an impurity. If it is so, the iodide concentrations corresponding to these b values in Fig. 2.10 are evaluated as 2×10^{-10} - 7×10^{-10} mol l^{-1} (0.03 - 0.09 μg l^{-1}) from Eq. (2.7). This iodide concentration level as impurity just agrees with the contaminated from ambient air during sample collection and handling described by Yonehara, et al.[16]. The $k_{4(app)}$ values were determined at the different concentrations of hydrogen peroxide in the range 0.8 - 2.0 mol l^{-1}. The straight lines obtained by plotting $k_{4(app)}$ vs. hydrogen peroxide concentration show that the relation is given by $k_{4(app)} = k_{5(app)}[H_2O_2] + c$, where $k_{5(app)}$ is the slope of the line and c is the intercept on the ordinate. This intercept is presumably due to the other oxidants, such as dissolved oxygen (Fig. 2.11). In order to determine the dependence of $k_{5(app)}$ on the hydrogen ion concentration, $R_{0(uc)}$ was also measured in the range 0.6 - 1.5 mol l^{-1} hydrogen ion by adjusting the ionic strength of 1.5 mol l^{-1} with sodium hydrogen sulfate. However, the addition of sodium hydrogen sulfate caused a significant increase in $R_{0(uc)}$, where $R_{0(uc)}$ showed an inverse dependence on acidity. It is not clear whether this behavior resulted from the sodium ion added as sodium hydrogen sulfate or some impurity present in the reagent. Hence the dependence of the $k_{5(app)}$ on acidity could not be established at a constant ionic strength. The dependence of $k_{5(app)}$ upon hydrogen ion concentration is given in Fig. 2.9 (curve IV), where ionic strength decreases from 1.5 to 0.6 mol l^{-1} as $[H^+]$ decreases. The plot showed an apparent deviation from a linear relationship and a plot

of $k_{5(app)}$ vs. $[H^+]^2$ gave an approximately straight line. On kinetics of the iodide catalyzed reaction, $k_{2(app)}$ obtained at a constant ionic strength of 1.5 mol l^{-1} showed a first order dependence with respect to hydrogen ion (Fig. 2.9, line I), whereas, at the different ionic strength on acidity, the dependence of $k_{2(app)}$ (curve II and line III) showed a quite similar behavior as that for $k_{5(app)}$. From this fact, because of the situation that the experimental data are not obtainable, it may be valuable to assume that $k_{5(app)}$ has a first order dependence on acidity according to dashed line VI connecting the point for the ionic strength of 1.51 mol l^{-1} with the origin, as in line I; its relation is given by $k_{5(app)} = k_{6(app)}[H^+]$, where $k_{6(app)}$ is the slope of the dashed line VI. Thus, the rate equation of the uncatalyzed reaction is postulated as:

$$R_{(uc)} = k_{6(app)}[CP][H_2O_2][H^+] \qquad (2.9)$$

The rate constant $k_6(=k_{6(app)} / \varepsilon_{red})$ is $1.40 \times 10^{-6}(0.0424 / 3.03 \times 10^4)$ l^2 mol^{-2} s^{-1} (at 30℃).

2.3.2.4 Kinetics of the colorless sulfoxide formation reaction

All kinetic runs were made with hydrogen peroxide and hydrogen ions in large excess over CP by measuring the absorbance of sulfoxide at 335 nm. Typical plots are shown in Fig. 2.12 in which $\log(P\infty - P_t)$ has been plotted against time, where P_t and $P\infty$ are the absorbances at a given time and the end of the reaction, respectively. The good linearity of the plots suggests first order kinetics with respect to CP and the slope of the line corresponds to

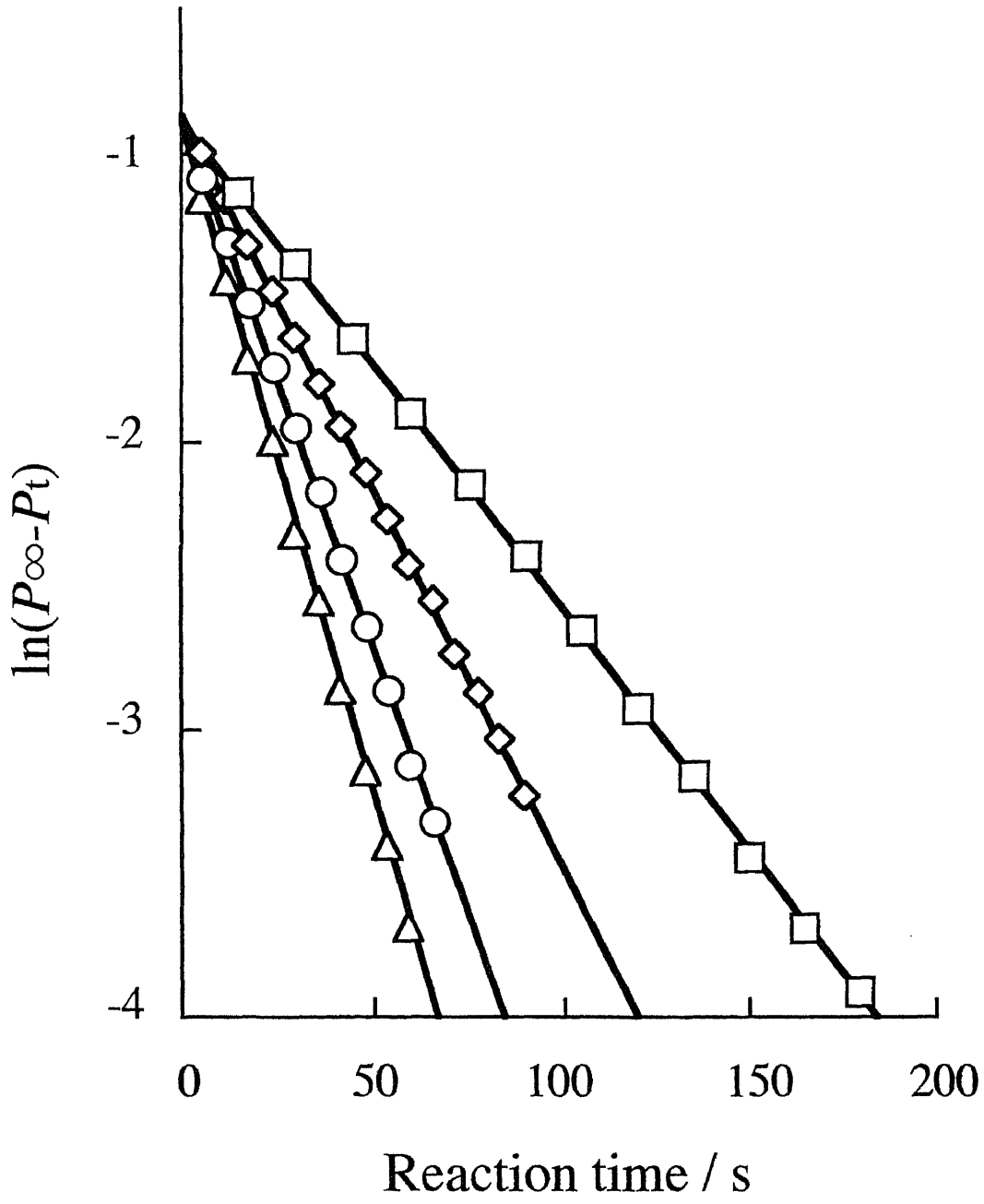

Fig. 2.12 First-order plots for the colorless sulfoxide formation. Conditions: 1.0×10^{-4} mol l^{-1} CP, 1.5 mol l^{-1} sulfuric acid, 1.5 mol l^{-1} ionic strength, 30℃, hydrogen peroxide concentration (mol l^{-1}) [0.80 (□), 1.2 (◇), 1.6 (○), 2.0 (△)].

an apparent rate constant (k_7). Variation of the hydrogen peroxide concentration enabled the reaction to be established as first order with respect to this reactant. This dependence is illustrated in Fig. 2.13a in which the slopes (k_7) from Fig. 2.12 are plotted against hydrogen peroxide concentration: $k_7=k_8[H_2O_2]$, where k_8 is the slope of the line. The k_8 values were determined at different hydrogen ion concentrations. As shown in Fig. 2.13b, the straight line obtained by plotting k_8 vs. the hydrogen ion concentration shows that the relation is given by $k_8=k_9[H^+]+k_{10}$, where k_9 is the slope of the line and k_{10} is the intercept on the ordinate. Thus, the rate of sulfoxide formation reaction ($R_{(sfo)}$) is given by:

$$R_{(sfo)} = k_9[CP][H_2O_2][H^+] + k_{10}[CP][H_2O_2] \qquad (2.10)$$

From the slope and intercept of the line in Fig. 2.13b, the rate constants k_9 and k_{10} were evaluated as 1.09×10^{-2} l^2 mol^{-2} s^{-1} and 7.15×10^{-3} l mol^{-1} s^{-1}, respectively (at 30℃). This rate law consisting of two independent terms indicates that sulfoxide formation proceeds by two independent pathways.

2.3.2.5 Mechanism of the CP-hydrogen peroxide reaction

The disappearance rate of CP is given by combining the three limiting rate laws, Eqs. (2.7), (2.9) and (2.10), derived in the preceding sections:

$$-d[CP]/dt = k_3[I^-][H_2O_2][H^+] + k_6[CP][H_2O_2][H^+] + k_9[CP][H_2O_2][H^+] + k_{10}[CP][H_2O_2] \qquad (2.11)$$

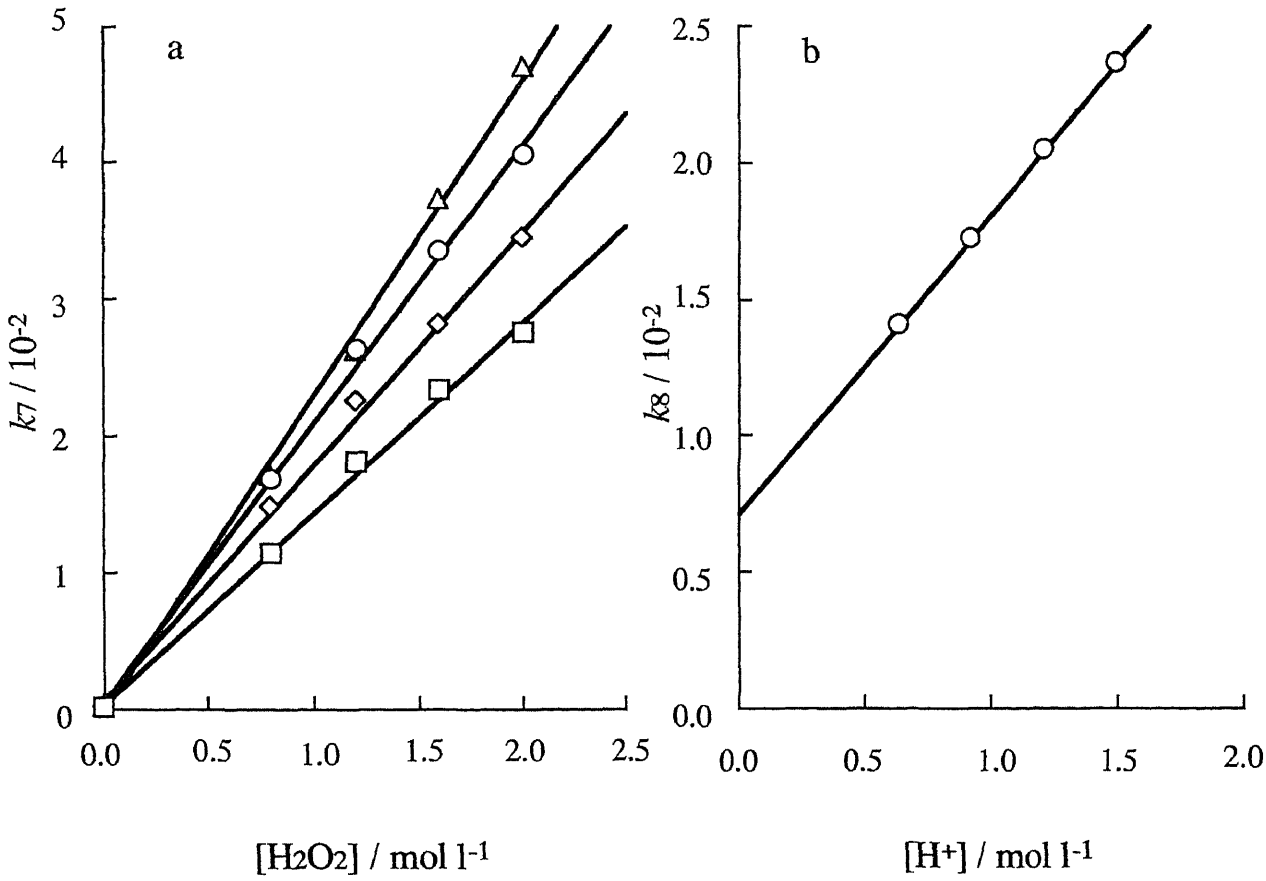

Fig. 2.13 Dependence of apparent rate constants k_7 and k_8 on hydrogen peroxide (a) and hydrogen ion (b) concentrations. Conditions: (a) sulfuric acid concentration (mol l^{-1}) [0.60 (□), 0.90 (◇), 1.2 (○), 1.5 (△)], the others as in Fig. 2.12; (b) the same as (a).

The reaction proceeds by four independent, parallel pathways.

For the iodide-catalyzed reaction two plausible mechanisms consistent with the first term in Eq. (2.11) can be proposed.

Mechanism I

$$H_2O_2 + H^+ \rightleftarrows H_3O_2^+ \quad \text{(rapid; } K_I\text{)}$$

$$I^- + H_3O_2^+ \rightarrow HOI + H_2O \quad \text{(rate-determining; } k_I\text{)}$$

$$CP + HOI \rightarrow P \quad \text{(rapid)}$$

Mechanism I'

$$H^+ + I^- \rightleftarrows HI \quad \text{(rapid; } K_I'\text{)}$$

$$HI + H_2O_2 \rightarrow HOI + H_2O \quad \text{(rate-determining; } k_I'\text{)}$$

$$CP + HOI \rightarrow P \quad \text{(rapid)}$$

where P may be an intermediate converting rapidly to the red product and I^- through several steps.

The empirical rate constant k_3 is identified according to Mechanism I as the product k_IK_I, that is, $k_3 = k_IK_I$ and the k_I value of ca.400 l mol^{-1} s^{-1} is obtained by using an evaluated value of 0.449 l^2 mol^{-2} s^{-1} for k_3 and the reported value of the order of 10^{-3} l mol^{-1} for K_I [20].

Similarly, $k_3=k_I'K_I'$ according to Mechanism I', but since HI is a strong acid ($K_I'=3.2\times 10^{-10}$ l mol^{-1} [21]), the value of k_I' becomes as improbably high as 1.4×10^9 l mol^{-1} s^{-1} which is very close to the range of values expected for diffusion-controlled reactions. This suggests that Mechanism I is more probable for the formation of HOI as an activated form of the catalyst.

The oxidation of iodide ion by hydrogen peroxide occurs via two pathways in acidic solution and its rate equation, therefore, has two terms [22]. One has the same form as the first term in Eq.

(2.11). Thus, it is considered that both reactions proceed through the same mechanism until intermediate formation in the rate-determining step and hence both rate constants have a similar value. In order to compare the rate constant k_3 with that for the iodide-hydrogen peroxide reaction, the value of the latter was spectrophotometrically determined by tracing the I_2-formation at 460 nm under the same conditions other than the iodide concentration as that for the present study ($[H_2O_2]$=0.5-2.0 mol l^{-1}, $[H^+]$=0.92-1.5 mol l^{-1}, $[I^-]=3.2\times10^{-4}$ mol l^{-1}, I=1.5 mol l^{-1}, 30℃). Then similar but lower value of 0.31 $l^2mol^{-2}s^{-1}$ was obtained as compared with the k_3 value of 0.449 $l^2mol^{-2}s^{-1}$. This result is reasonable because iodide in the I^--H_2O_2 reaction is a reactant, while iodide in the present reaction is a catalyst functioning in a cyclic manner and hence this effect is incorporated into k_3 resulting in the larger value.

It was also examined that whether HOI can oxidize rapidly CP to the red free radical. In a sulfuric acid solution CP is oxidized by iodine (I_2) to the red free radical (conditions: 1.0×10^{-3} mol l^{-1} CP, 1.5 mol l^{-1} H_2SO_4, 1.2×10^{-5} mol l^{-1} I_2, half-time for reaction $t_{1/2}$ = 3.3 s at 30℃). Iodine disproportionates in aqueous solution to HOI and I^- ion. In acidic solution, this disproportionation proceeds only a slight extent. However, the formation of HOI goes to the completion by the addition of Hg^{2+} which complexes with I^-. If HOI can rapidly oxidize CP, it is expected that the addition of Hg^{2+} ion will cause an increase in the rate of the red free radical formation. The result obtained was as expected ; the rate increased with

increasing Hg^{2+} ion concentration, and in the presence of excess Hg^{2+} over I_2, the reaction proceeded so rapidly that no absorbance-time curves could be recorded by the technique used. This fact provides further evidence for adequacy of the mechanism suggesting that the catalytic effect of iodide on the reaction arises from the formation of HOI.

The other three terms in Eq. (2.11) are the rate laws for the uncatalyzed pathways; the second term for the red free radical formation and the others for the colorless sulfoxide. Although the second term and the third one are of the same form, the contribution of the third term to the overall rate is very large, while that of the second is slight ($k_9 >> k_6$). Thus the individual terms represent contributions from different reactions, and each reaction may, therefore, occur through the respective path having its own characteristic activated complex. Two mechanisms were thus considered.

Mechanism II

$$CP + H^+ \rightleftarrows CPH^+ \quad \text{(rapid; } K_{II}\text{)}$$

$$CPH^+ + H_2O_2 \rightarrow P_{II} \quad \text{(rate-determining; } k_{II}\text{)}$$

Mechanism III

$$H_2O_2 + H^+ \rightleftarrows H_3O_2^+ \quad \text{(rapid; } K_I\text{)}$$

$$CP + H_3O_2^+ \rightarrow P_{III} \quad \text{(rate-determining; } k_{III}\text{)}$$

where P_{II} and P_{III} are intermediates converting rapidly to the red free radical or colorless sulfoxide. It is not possible to differentiate between these two on the basis of the data now available. However, it is considered that the activated complex consistent with the third term is formed with less geometrical

restrictions, since k_9 is considerably larger than k_6. Thus it is supposed that the third term corresponds to Mechanism III and accordingly the second term to Mechanism II. The rate-determining step and post steps in Mechanism III may be postulated as:

$$CP + H_3O_2^+ \rightarrow CP{\bullet}OH^+ + H_2O \quad \text{(rate-determining)}$$

$$CP{\bullet}OH^+ + H_2O_2 \rightarrow CP{=}O^{2+} + OH^- + H_2O \quad \text{(rapid)}$$

$$OH^- + H^+ \rightleftarrows H_2O \quad \text{(rapid)}$$

The path consistent with the fourth term may be interpreted by the following postulated reaction steps:

Mechanism IV

$$CP + H_2O_2 \rightarrow CP{\bullet}O_2H_2 \quad \text{(rate-determining)}$$

$$CP{\bullet}O_2H_2 \rightarrow CP{\bullet}OH^+ + OH^- \quad \text{(rapid)}$$

$$CP{\bullet}OH^+ + H_2O_2 \rightarrow CP{=}O^{2+} + OH^- + H_2O \quad \text{(rapid)}$$

$$2OH^- + 2H^+ \rightleftarrows 2H_2O \quad \text{(rapid)}$$

2.3.2.6 Rate dependence on temperature

The effect of temperature on the rate of the red free radical formation was evaluated for the conditions $[CP]_0 = 1.0 \times 10^{-3}$ mol l^{-1}, $[H_2O_2]_0 = 2.0$ mol l^{-1}, $[I^-]_0 = (0.96\text{-}4.81) \times 10^{-8}$ mol l^{-1} and $[H^+]_0 = 1.51$ mol l^{-1}. The values of $k_{1(app)}$ and $R_{0(uc)}$ were first evaluated from the slope and the intercepts of the lines obtained by plotting R_0 vs. iodide concentration in the range of 15-40℃. The values of k_3 and k_6 for each temperature were calculated by dividing the corresponding $k_{1(app)}$ value by the value of $\varepsilon_{red}[H_2O_2]_0[H^+]_0$ and the corresponding $R_{0(uc)}$ value by that of $\varepsilon_{red}[CP]_0[H_2O_2]_0[H^+]_0$, respectively.

The temperature dependence of the rate of the colorless sulfoxide formation reaction was determined under the conditions $[CP]_0=1.0\times 10^{-4}$ mol l^{-1}, $[H_2O_2]_0=2.0$ mol l^{-1}, $[H^+]_0=0.13$ - 1.51 mol l^{-1} and I=1.51 mol l^{-1} as follows. The values of k_7 were first evaluated from the slope of the pseudo-first order plots for different hydrogen ion concentrations and then the k_7 values thus obtained were plotted against hydrogen ion concentrations. These successive plots were made at different temperatures. The values of k_9 and k_{10} for each temperature were calculated by dividing the corresponding values of the slope and intercept of the straight lines obtained in the latter plots by the value of $[H_2O_2]_0$.

Arrhenius plots for these data are given in Fig. 2.14. From the plots in Fig. 2.14a, the activation energies for the iodide-catalyzed and uncatalyzed red free radical-formation reactions were calculated to be 37.4 and 65.1 kJ mol^{-1}, respectively. Activation energies for the sulfoxide formation reaction were also evaluated from the plots in Fig. 2.14b as 42.5 kJ mol^{-1} for the pathway depending upon concentration of hydrogen ion (k_9) and as 38.5 kJ mol^{-1} for the other pathway(k_{10}).

2.3.2.7 Analytical implications

Since the maximum absorbance on the absorbance-time curves increases with an increase in the iodide concentration, this value was used as a parameter for the iodide determination. It was observed that when the red coloration reached a maximum, CP had been exhausted so that the color formation had ceased (Fig. 2.1).

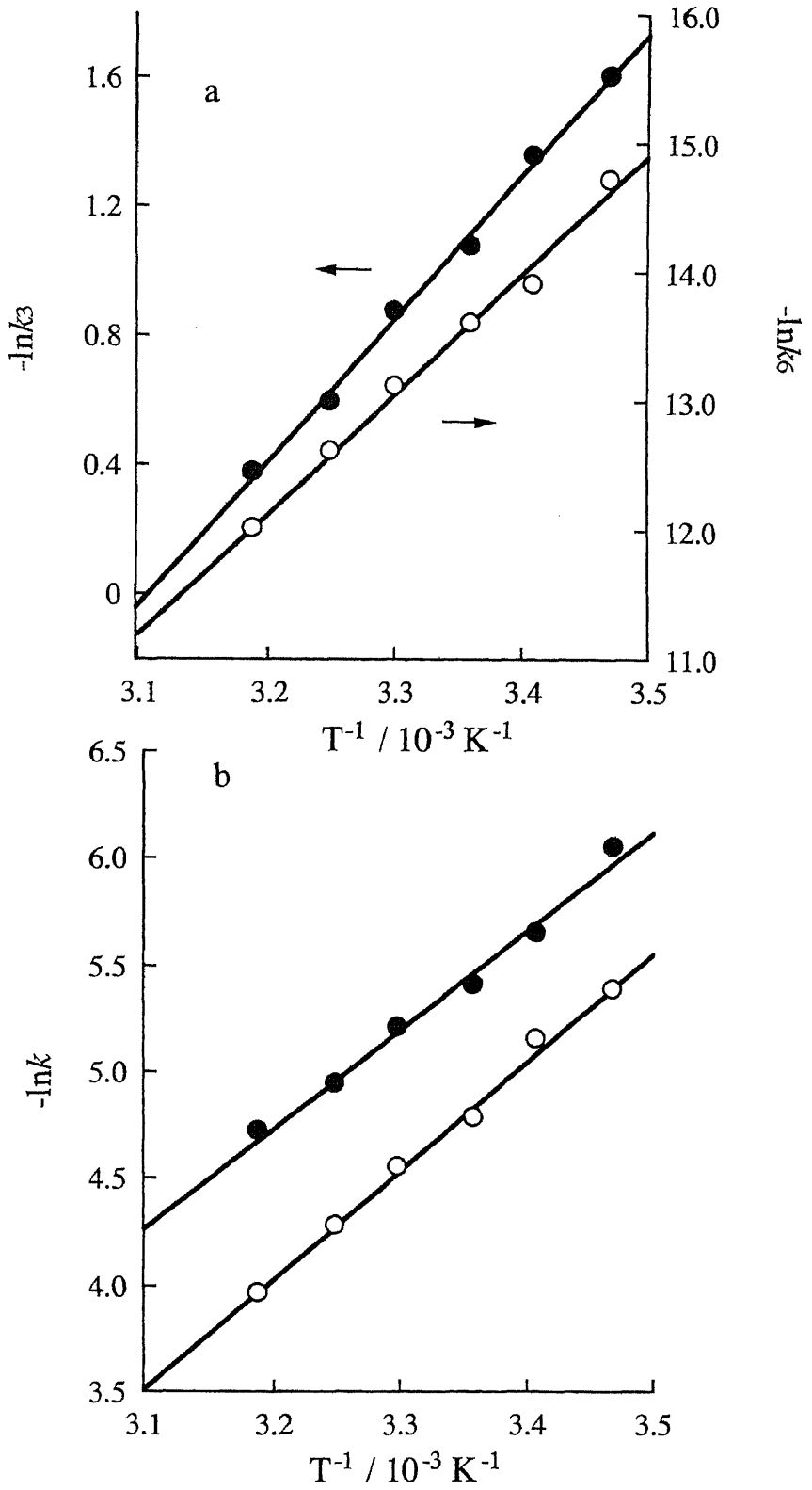

Fig. 2.14 Arrhenius plots for red free radical formation (a) and colorless sulfoxide formation (b). Conditions: (a) 1.0×10^{-3} mol l^{-1} CP, 2.0 mol l^{-1} hydrogen peroxide, 1.5 mol l^{-1} hydrogen ion, $(0.96\text{-}4.8)\times10^{-8}$ mol l^{-1} iodide, 1.5 mol l^{-1} ionic strength, [●: k_3, ○: k_6]; (b) 1.0×10^{-4} mol l^{-1} CP, 2.0 mol l^{-1} hydrogen peroxide, 0.13-1.5 mol l^{-1} hydrogen ion, 1.5 mol l^{-1} ionic strength, [○: k_9, ●: k_{10}].

Hence, the maximum values do not depend only on the catalyzed reaction rate but also greatly on the uncatalyzed one. Most of CP (> 99%) is consumed in the formation of sulfoxide under the experimental conditions for the iodide determinations and therefore the contribution of the rate of the red free radical formation to overall rate is negligible. Thus the rate equation for the disappearance of CP, Eq. (2.11), reduces to

$$-d[CP]/dt = (k_9[H^+]_0 + k_{10})[H_2O_2]_0[CP]$$

which has the integrated form

$$\ln([CP]/[CP]_0) = -(k_9[H^+]_0+k_{10})[H_2O_2]_0\ t \qquad (2.12)$$

where $(k_9[H^+]_0 + k_{10})[H_2O_2]_0$ is essentially constant, because both $[H^+]_0$ and $[H_2O_2]_0$ remain nearly constant during the course of the reaction.

Under the conditions mentioned above the rate law for the iodide-catalyzed red free radical formation, Eq. (2.7), has the integrated form

$$[CPOH\bullet^{2+}] = k_3[I^-]_0[H_2O_2]_0[H^+]_0\ t \qquad (2.13)$$

where $k_3[I^-]_0[H_2O_2]_0[H^+]_0$ is essentially constant for a given concentration of iodide.

At the time t_{max}, when the absorbance of the red free radical has just reached to the maximum value, since all CP other than that converted to colorless sulfoxide has changed to the red free radical, the concentration of CP, [CP] in Eq. (2.12) may be regarded as being equivalent to the concentration of the red free

radical. The concentration of the red free radical $[CPOH\bullet^{2+}]_{max}$ corresponds to the maximum absorbance. Then Eqs. (2.12) and (2.13) become

$$\ln([CPOH\bullet^{2+}]_{max}/[CP]_0) = -(k_9[H^+]_0+k_{10})[H_2O_2]_0\, t_{max} \qquad (2.14)$$

and

$$[CPOH\bullet^{2+}]_{max} = k_3[I^-]_0[H_2O_2]_0[H^+]_0\, t_{max} \qquad (2.15)$$

respectively. Substituting Eq. (2.15) for t_{max} into Eq. (2.14) and rearranging the resulting expression gives

$$[CPOH\bullet^{2+}]_{max} + \frac{k_3[I^-]_0[H^+]_0}{k_9[H^+]_0+k_{10}} \ln[CPOH\bullet^{2+}]_{max} = \frac{k_3[I^-]_0[H^+]_0}{k_9[H^+]_0+k_{10}} \ln[CP]_0 \qquad (2.16)$$

showing roughly the dependence of the maximum absorbance on the concentrations of the reactants.

According to Eq. (2.16), the effects of the reactants are as follows: (a) the maximum absorbance increases with increase in the CP concentration but it is independent of hydrogen peroxide concentration; (b) although there is a complicated relation between hydrogen ion concentration and the maximum absorbance, the form of the terms involving hydrogen ion concentration suggests that the maximum absorbance becomes independent of hydrogen ion at higher concentration range. Similar trends were also observed in the experimental results (Fig. 2.2).

This maximum absorbance has the advantages that reaction temperature has little influence, there is no need for control the reaction time and hydrogen peroxide and hydrogen ion concentrations have only a slight influence; however the effects of

interfering substances were complicated. Although a higher sensitivity can be achieved at higher CP concentrations, higher CP concentrations also promote the red-color formation caused by interfering species. Practically in many water samples, a coloration was observed by the addition of CP and sulfuric acid solutions prior to the addition of hydrogen peroxide and it was responsible for serious errors in the iodide determinations under the conditions of higher CP concentrations. Hence, it is practically desirable to keep the CP concentration as low as possible without greatly raising the detection limit. A species accelerating (or decelerating) the colorless sulfoxide formation also interferes the iodide determinations by decreasing (or increasing) the amount of CP available for color formation. For example, traces of W(VI), which accelerate significantly the colorless sulfoxide formation [23], cause serious negative interference.

From Eq. (2.7), it is clear that the use of the initial rate of the iodide-catalyzed red coloration as a parameter for iodide determinations gives a linear calibration graph (Fig. 2.7). The sensitivity of the method increases with increasing hydrogen peroxide concentration and also with increasing temperature. Furthermore, the rate is independent of CP concentrations and therefore the sensitivity of the initial-rate approach is not affected by decreasing the CP concentration.

Moreover, it is meaningful that this kinetic investigation has led to considerations concerning contamination during the procedure and impurities present in the reaction solution, which are

practically important problems for obtaining reliable results in trace determinations as mentioned in Section 2.3.2.3.

Chapter 3

Spectrophotometric Determination of Trace Amounts of Iron by Its Catalytic Effect on the Chlorpromazine-Hydrogen Peroxide Reaction. A Kinetic Study of the Reaction and Its Analytical Implications

3.1 Introduction

A number of catalytic methods based on different indicator reactions have been proposed for iron determination [24-30]. Some of them were applied to the determination of iron in water samples [26-29]. However, the detection limit of these methods was sub - mg l^{-1} order, and the determination of iron in water samples at $\mu g\ l^{-1}$ levels was difficult. Kawashima et al. have reported the N-(p-methoxyphenyl)-N',N'-dimethyl-p-phenylenediamine (MDP) - H_2O_2 system, which allowed the determination of $\mu g\ l^{-1}$ level of iron [30]. But the determinable range of the method, 2-14 $\mu g\ l^{-1}$ iron, was not wide enough.

In an acidic medium, CP can be oxidized to a red intermediate by the action of several oxidizing agents. When sulfuric acid and hydrogen peroxide were used, this reaction was catalyzed by iodide as described in Chapter 2 [31]. It was found that iron catalyzed the color formation reaction and that the catalytic effect of iodide in hydrochloric acid slightly decreased compared with sulfuric acid medium. Thus, a kinetic spectrophotometric method for the determination of iron based on its catalytic effect on the

CP-hydrogen peroxide reaction was developed. The proposed method is highly sensitive and reproducible: as low as 5 $\mu g\ l^{-1}$ of iron can be determined with good reproducibility. This method has been successfully applied to the determination of iron in tap and natural water samples. Kinetics of the iron-catalyzed reaction has also been studied to obtain better understanding of the reaction process and elucidate the mechanism. The proposed mechanism, which satisfies the experimental observations, was utilized to derive a rate equation. The rate equation represents the quantitative behavior of the reaction throughout the range of conditions studied. The utility of the rate equation was discussed to select the optimal conditions for the trace determination of iron by the initial-rate procedure.

3.2 Experimental

3.2.1 Apparatus and reagents

Spectrophotometer for measuring the absorbance, a circulating thermostat bath and magnetic stirrer used were the same as those described in Chapter 2.

An iron(II) stock solution (1000 mg l^{-1}) was prepared by dissolving 1.404 g of ammonium iron(II) sulfate hexahydrate in 200 ml of 0.1 mol l^{-1} hydrochloric acid. Working solutions were prepared by diluting this solution with water.

A hydrochloric acid (6.0 mol l^{-1}) solution was prepared by distilling 1:1 hydrochloric acid solution.

Other chemicals used were the same as described in Chapter 2.

3.2.2 Recommended procedure

To 10.0 ml of a sample solution in a glass-stoppered tube, 1.0 ml of 6.0 mol l^{-1} hydrochloric acid and 1.0 ml of 0.15 mol l^{-1} CP solution were added. After mixing the solution, it was kept at 30℃ in a water bath for 15 min in order to achieve the required temperature. Then a 1.8 ml aliquot was taken into a 1-cm glass cell. The cell was placed in the cell holder at 30℃ and the solution was magnetically stirred. The reaction was initiated by injecting of 0.20 ml of a 1.2 mol l^{-1} hydrogen peroxide solution (30℃). The increase in absorbance of the red intermediate at 525 nm was recorded against a pure-water reference and the tanα [=Δ(abs.)/Δ(s)] of the linear range of reaction rate curves was used as a parameter for iron determination.

3.2.3 Kinetic measurements

To a standard iron(II) solution in a glass-stoppered tube, appropriate concentrations of CP and hydrochloric acid solutions were added and the final volume was adjusted to 12 ml with water, where the ionic strength was maintained constant at 0.49 mol l^{-1} by addition of sodium chloride. This solution was kept at 30℃ in a water bath; a 1.8 ml aliquot was then taken into a 1-cm glass cell. The cell was placed in the holder at 30℃ and the solution was magnetically stirred. The reaction was initiated by injecting 0.20

ml of hydrogen peroxide (30℃); where the ionic strength was 0.44 mol l^{-1}. The increase in absorbance of the red free radical at 525 nm was recorded against a pure-water reference.

3.3 Results and Discussion

3.3.1 Kinetic determination of iron

3.3.1.1 Oxidation of CP by hydrogen peroxide and the accelerating effect of iron on the color formation

CP is oxidized by hydrogen peroxide in hydrochloric acid medium to a red free radical, which is further oxidized to a colorless compound. The color formation reaction is accelerated by trace amounts of iron. The reaction can be followed by measuring the increase in absorbance of the red intermediate at 525 nm. The absorbance increases with an increase in reaction time, and reaches a maximum value. The required time for maximum absorbance after adding the hydrogen peroxide solution decreased with increasing the iron concentration. After the absorbance reached maximum value (a few min.), the absorbance decreased gradually. Although the maximum absorbance increased with increasing iron concentration, it was not adequate as a parameter for iron determination, because of the long reaction time and high blank value. By the use of an absorbance value at a given reaction time, the time required for single determination cold be shortened and the blank value became lower. But the determinable range 0.5-20 μg l^{-1}

of the method was not wide enough [32]. Thirty seconds after the initiation of the reaction, the absorbance/time curves became linear and the linearity was kept constant for a few min. The slopes of the linear range increased with the increase in the iron concentration. The difference of the slopes between catalyzed and uncatalyzed reaction was larger, because the color formation reaction on the uncatalyzed reaction progressed slowly. The slope, tanα [=Δ(abs.)/Δ(s)], was used as a parameter for the iron determination.

3.3.1.2 Effect of reaction variables

The influence of temperature on the tanα was studied over the range 20-45℃ under the conditions as in the recommended procedure. Although higher sensitivity was obtained at higher temperature, the reproducibility of the method became poorer as the reaction rate increased. A temperature of 30℃ was chosen.

Figure 3.1 shows the effect of CP concentration represented by tanα. The blank value increased with increasing CP concentration over the concentration range examined. The sensitivity of the method increased with the increase in the CP concentration up to 0.01 mol l^{-1} and remained constant over the higher concentration range. A CP concentration of 0.011 mol l^{-1} was chosen, since it gave the highest sensitivity and lower blank. The influence of hydrogen peroxide concentration was examined in the range of 0.04-0.20 mol l^{-1}. As can be seen in Fig. 3.2, the tanα of the uncatalyzed reaction remained constant in this concentration range.

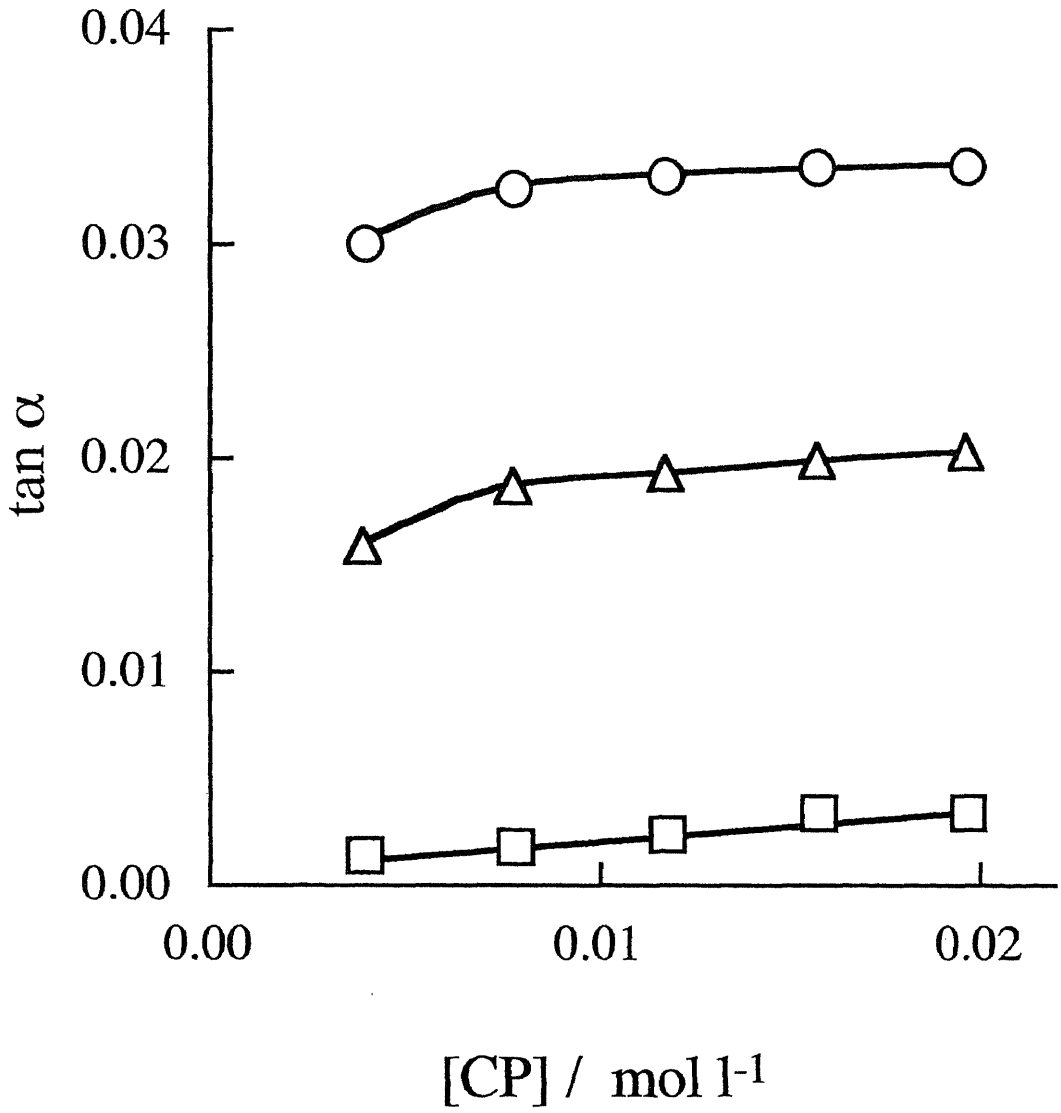

Fig. 3.1 Effect of the CP concentration on the catalytic effect of iron(II) (□ blank, △ 100 μg l^{-1} , ○ 200 μg l^{-1}). Conditions : 0.12 mol l^{-1} hydrogen peroxide, 0.43 mol l^{-1} hydrochloric acid, 30℃.

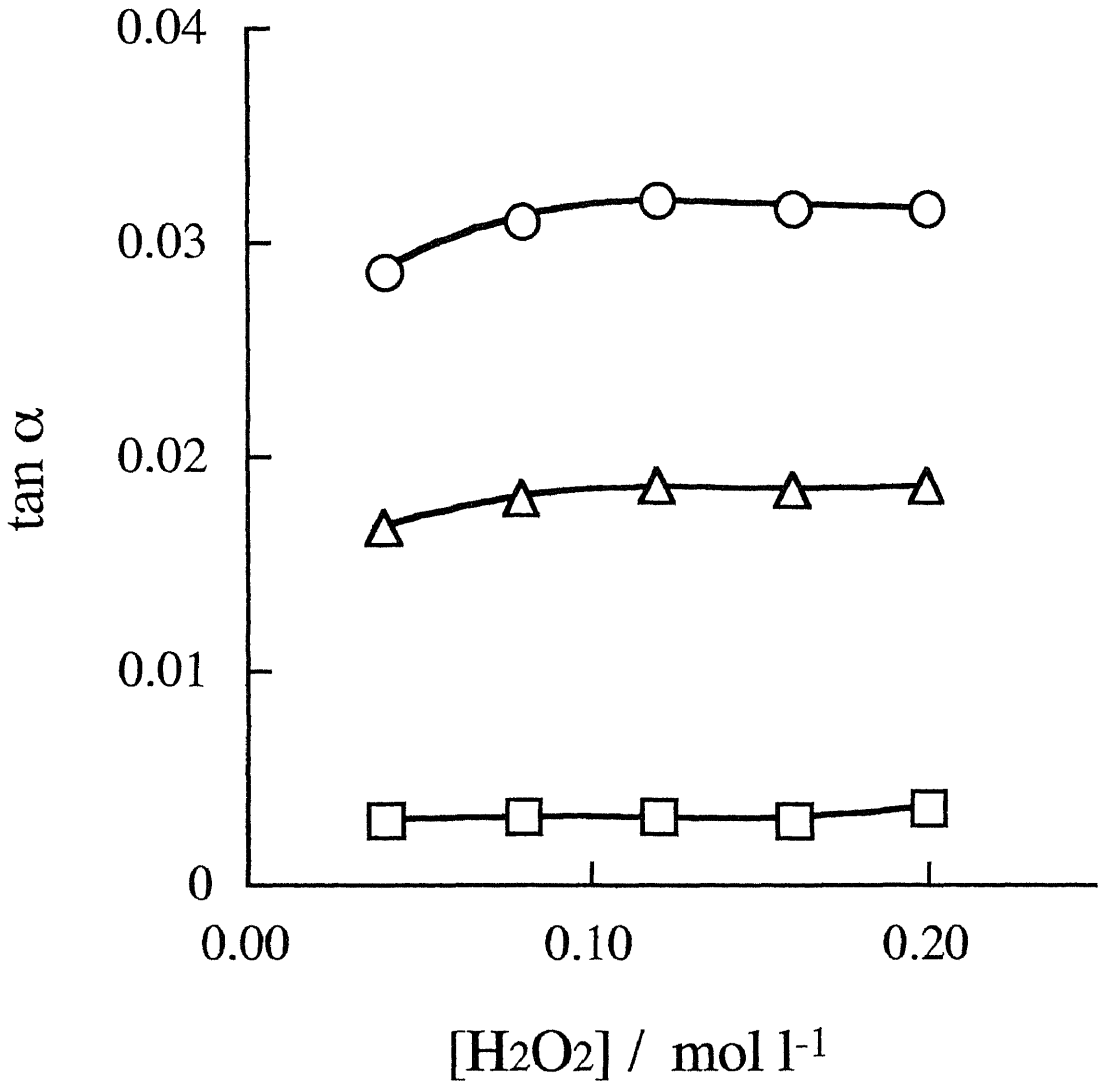

Fig. 3.2 Effect of the hydrogen peroxide concentration on the catalytic effect of iron(II) (□ blank, △ 100 μg l^{-1} , ○ 200 μg l^{-1}). Conditions: 0.011 mol l^{-1} CP, 0.43 mol l^{-1} hydrochloric acid, 30℃.

The maximum tanα on the catalyzed reaction was obtained at concentrations higher than 0.10 mol l^{-1}. A hydrogen peroxide concentration of 0.12 mol l^{-1} was chosen. The reaction rate of both catalyzed and uncatalyzed reactions increased with increasing hydrochloric acid concentration. However, the difference of the tanα between the presence and the absence of iron showed constant at higher hydrochloric acid concentration range (Fig. 3.3). A hydrochloric acid concentration of 0.43 mol l^{-1} was selected by considering the sensitivity and lower blank values.

3.3.1.3 Calibration graphs and reproducibility

A series of standard solutions of iron ranging from 0 - 200 μg l^{-1} was analyzed according to the recommended procedure. A linear calibration curve is obtained; the equation of the line is tanα = 1.40×10^{-4} [Fe] + 2.50×10^{-3}, and the correlation coefficient is r = 0.999. The relative standard deviations for 10 replicate determinations of 10, 40, 80 μg l^{-1} of iron(II) are 6.6, 2.3 and 0.8%, respectively. Detection limit is 5 μg l^{-1} with a relative standard deviation of 17.7% (n = 10).

3.3.1.4 Effect of foreign ions

The effect of various ions on the determination of 90 μg l^{-1} iron(II) was examined. The following ions showed no interference, at least at the concentrations (mg l^{-1}) shown in parentheses:Na^+ and Cl^- (2000); Ca^{2+}, K^+, SO_4^{2-} (1000); CO_3^{2-} (500); Mg^{2+}, Mn^{2+} (250); Pb^{2+}, Li^+, Cd^{2+}, Ba^{2+}, Ce^{3+}, Ni^{2+}, Sr^{2+}, As(V), As(III), NH_4^+, Br^-,

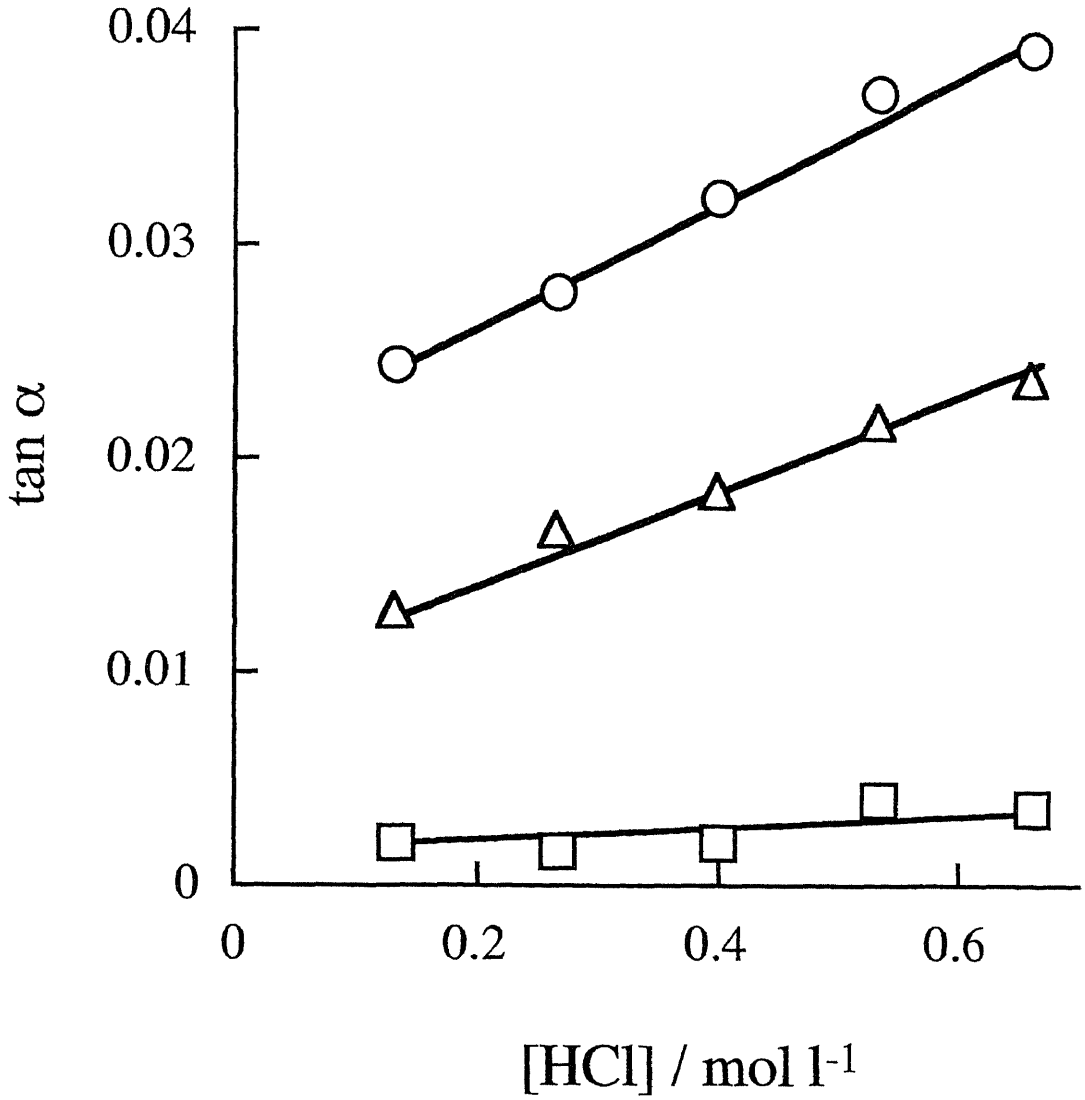

Fig. 3.3 Effect of the hydrochloric acid concentration on the catalytic effect of iron(II) (□ blank, △ 100 μg l^{-1} , ○ 200 μg l^{-1}). Conditions : 0.011 mol l^{-1} CP, 0.12 mol l^{-1} hydrogen peroxide, 30℃.

CH_3COO^-, ClO_3^-, ClO_4^- (100); Zn^{2+}, Co^{2+}, Sn(IV) (50); Ce^{4+}, Sn^{2+}, Cr^{3+}, Sb(III), PO_4^{3-} (10); Cu^{2+}, Ag^+, Mo(VI), V(V) (5). The interfering ions are listed in Table 3.1. Ions which are known to participate in redox reaction as either oxidizing or reducing agents cause serious interference. However, these ions showed no interference at concentrations one order lower than those indicated in Table 3.1.

3.3.1.5 Determination of iron in tap and natural fresh water samples

In order to test the reliability of the method, the present method was applied to the determination of iron in tap and natural fresh water samples. The determinations were made by using samples diluted at different times. The method was also checked by adding a known amount of iron to the samples. The results are shown in Table 3.2. The values corrected for dilution showed good agreement, and good recoveries of added iron were obtained ranging from 97 to 104% (mean 100%).

3.3.2. A kinetic study of the iron catalyzed CP - hydrogen peroxide reaction and its analytical implications

3.3.2.1 Kinetics of the iron-catalyzed red free radical formation reaction between CP and hydrogen peroxide

Chlorpromazine is oxidized by hydrogen peroxide to a red free radical in an acidic medium, which is further oxidized to a

Table 3.1

Effect of interfering ions on the determination of 90 $\mu g\ l^{-1}$ of iron.

Ion added	$\mu g\ l^{-1}$	Fe(II) found / $\mu g\ l^{-1}$
Cr(VI)	5000	100
SCN^-	5000	102
W(VI)	1000	71
$S_2O_3^-$	1000	85
IO_3^-	1000	96
I^-	1000	101
NO_2^-	1000	83
BrO_3^-	1000	98

Table 3.2

Determination of iron in water samples

Sample	Dilution (times)	Added / $\mu g l^{-1}$	Found / $\mu g l^{-1}$	Recovely, %	In sample $\mu g l^{-1}$
River water I	-	-	161	-	161
	2	-	83	-	166
	2	20	100	97	
	2	40	128	104	
	5	-	34	-	170
	10	-	17	-	170
					av. 167
River water II	-	-	10	-	10
	2	-	5	-	10
	2	20	25	100	
	2	40	46	102	
					av. 10
Tap water	-	-	34	-	34
	2	-	18	-	36
	2	20	37	97	
	2	40	57	98	
	5	-	7	-	35
					av. 35

colorless sulfoxide. Since CP was not only consumed by the red free radical formation reaction, but also consumed simultaneously by a reaction without any coloration competing with the former one [31], the kinetic investigation of the color formation reaction was thus carried out by the initial-rate method. The initial rate, R_0 [$=\Delta(\text{mol } l^{-1})/\ \Delta(s)$], was obtained by dividing the rate evaluated from the absorbance/time curves [$\Delta(\text{abs.})/\Delta(s)$] (Fig. 3.4) by 3.0×10^4 l mol^{-1} cm^{-1} of the molar absorption coefficient at 525 nm of the red compound [33]. All of the concentrations given in the figures are the initial analytical concentrations in the reaction mixture at the initiation of reaction. In order to determine the dependence of the R_0 upon iron concentration, a series of experiments was performed in which the iron concentration was varied while CP, hydrogen ion and hydrogen peroxide concentrations were held at constant. The plots of R_0 versus total analytical concentration of iron ($[\text{Fe(II)}]_0$) were linear in the range of $0\text{-}1.3\times 10^{-6}$ mol l^{-1} iron (Fig. 3.5). The iron catalyzed reaction was first order with respect to iron:

$$R_0 = k_{app}[\text{Fe(II)}]_0 + a \qquad (3.1)$$

where k_{app} is the apparent rate constant and a is the intercept which corresponds to the rate of an uncatalyzed reaction.

The variations in k_{app} with hydrogen peroxide, hydrogen ion and CP concentrations are shown in Figs. 3.6, 3.7 and 3.8, respectively. As can be seen in Fig. 3.9, a straight line obtained by plotting $1/k_{app}$ versus $1/[H_2O_2]$ shows that the relation is given by $k_{app}=[H_2O_2]/(b+\alpha[H_2O_2])$, where b is the slope of the line and α is

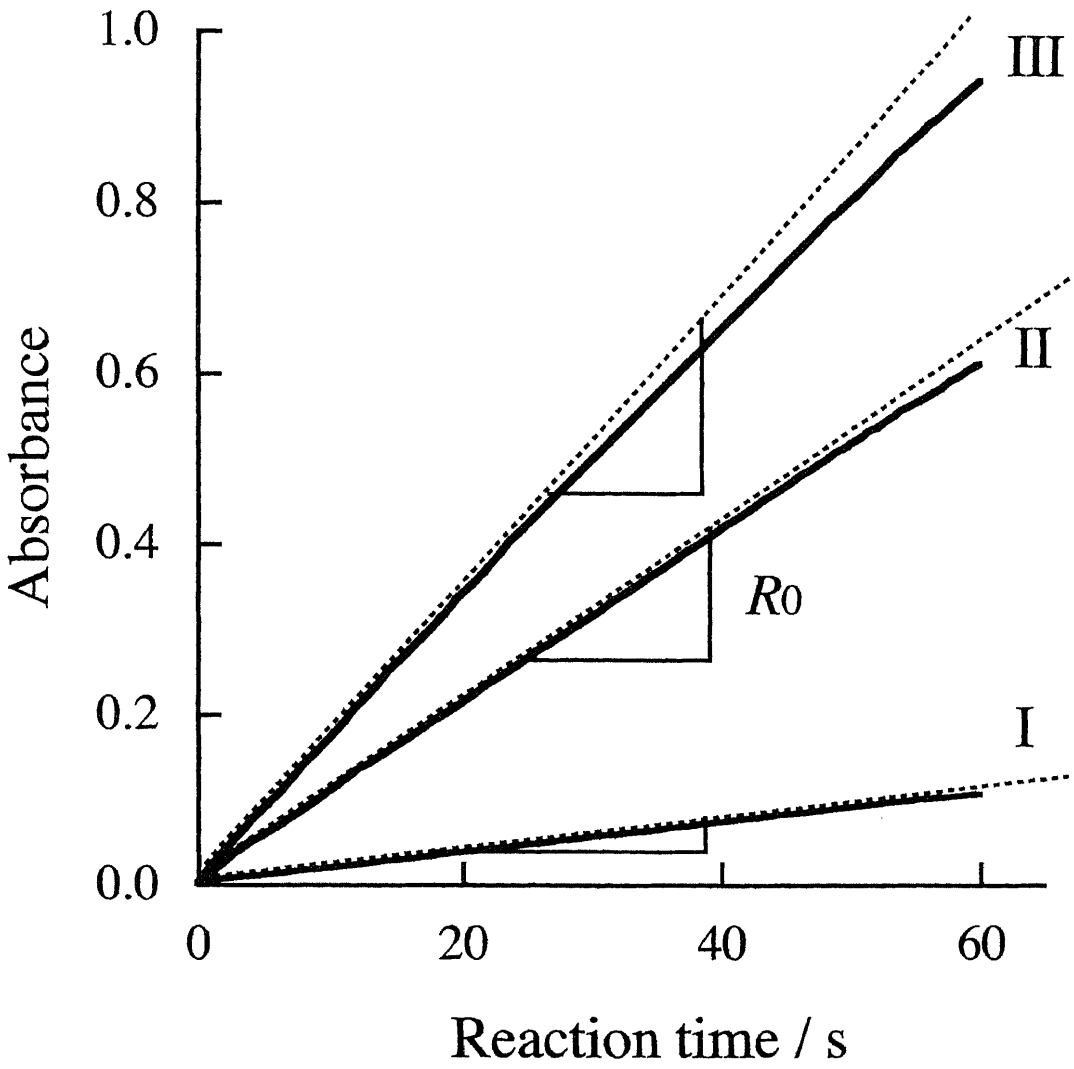

Fig.3.4 Absorbance/time curves for the CP/hydrogen peroxide reaction. Concentrations of iron ($\times 10^{-6}$ mol l^{-1}): (I) 0, (II) 0.80, (III) 1.34. Conditions: 0.011 mol l^{-1} CP, 0.43 mol l^{-1} hydrochloric acid and 0.036 mol l^{-1} hydrogen peroxide, 30℃, ionic strength 0.44 mol l^{-1}. R_0: Δ(mol l^{-1})/Δ(s) at reaction time zero was used as a measure of the initial reaction rate.

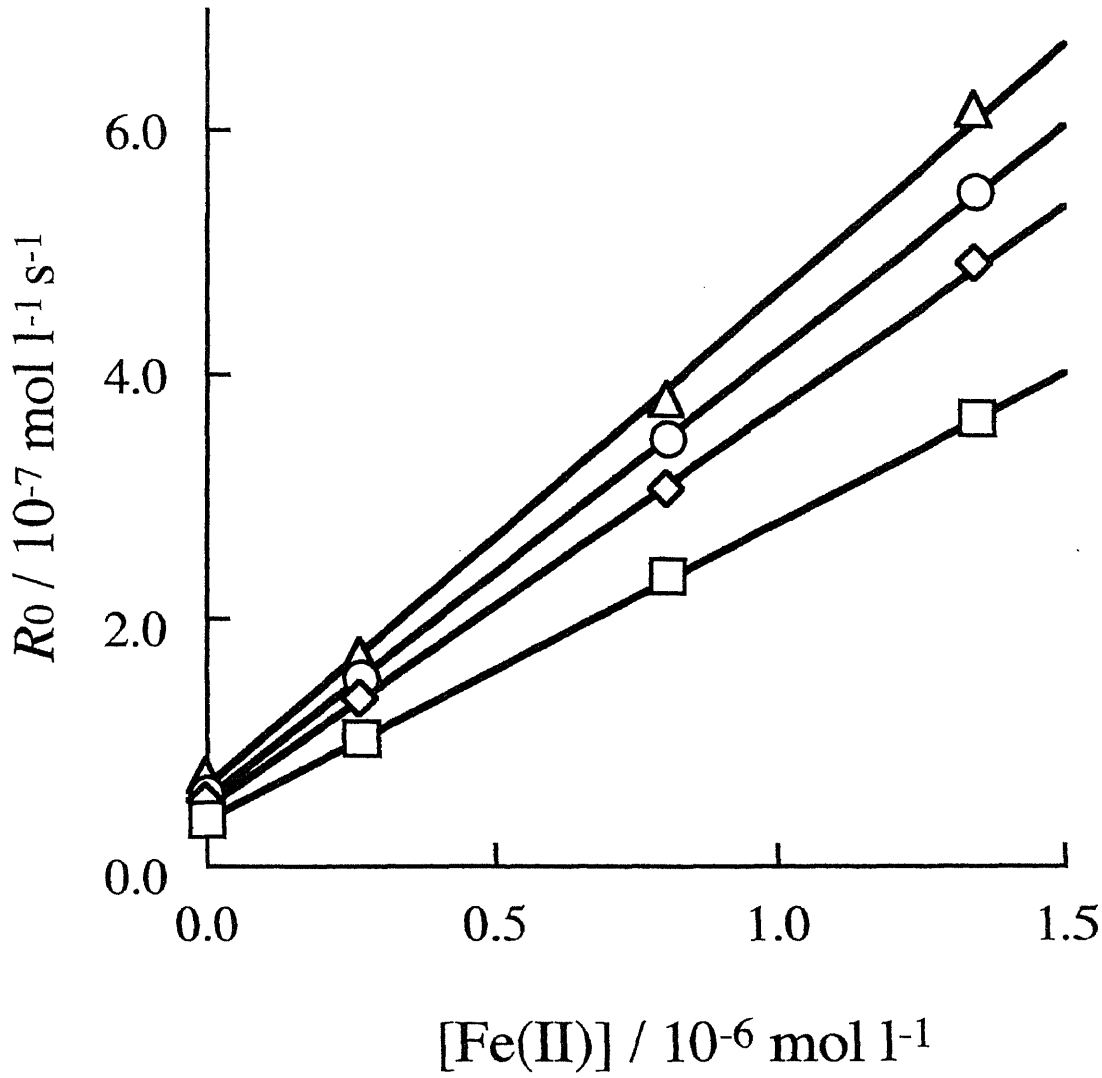

Fig. 3.5 Dependence of initial reaction rate R_0 upon iron(II) concentration. Concentrations of hydrogen peroxide ($\times 10^{-1}$ mol l^{-1}): (□) 0.12, (◇) 0.24, (○) 0.36, (△) 1.2. Conditions: 0.011 mol l^{-1} CP, 0.43 mol l^{-1} hydrochloric acid and 0.036 mol l^{-1} hydrogen peroxide, 30℃, ionic strength 0.44 mol l^{-1}.

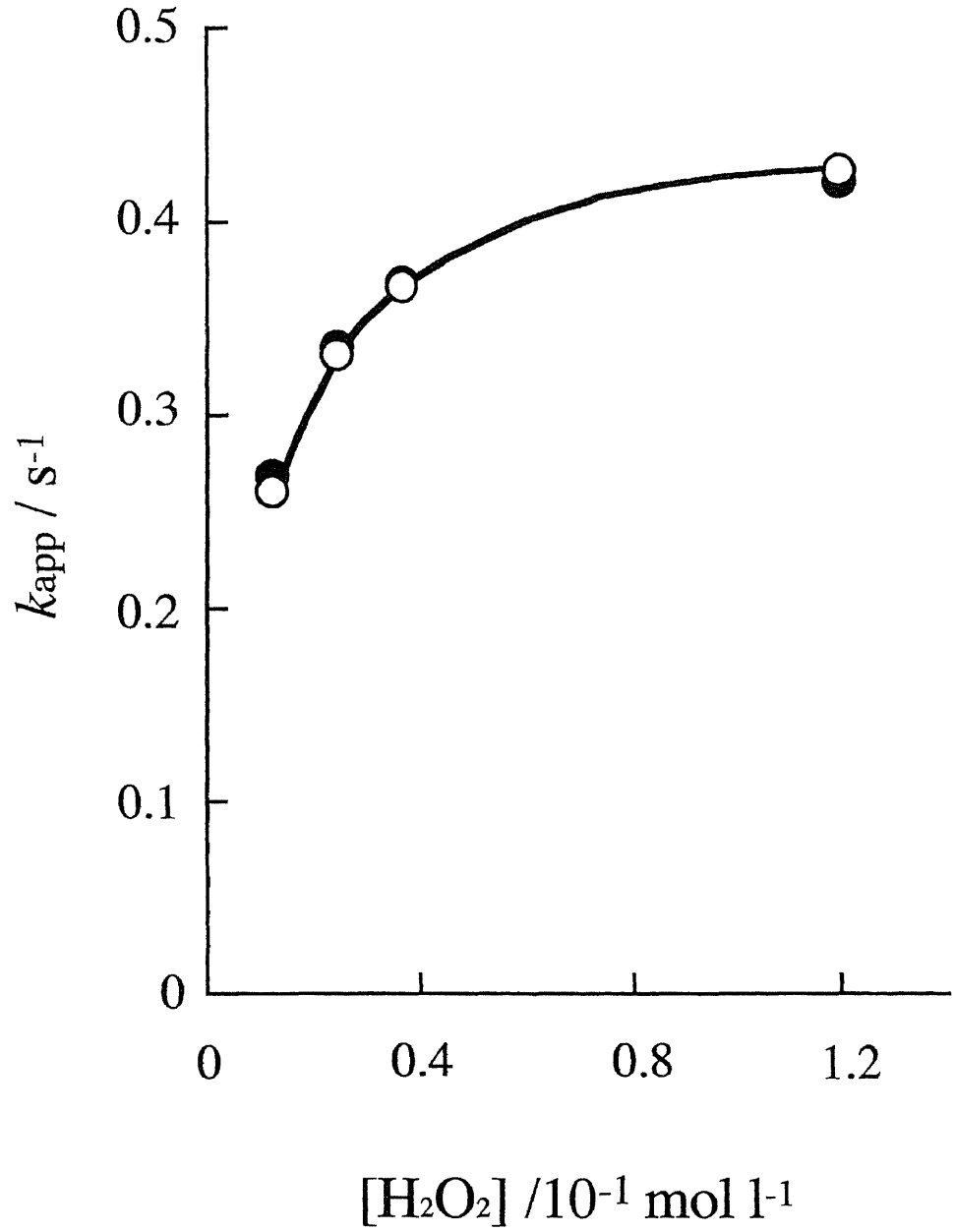

Fig. 3.6 Effect of the hydrogen peroxide concentration for apparent rate constant, k_{app} [experimental values (●), values (○) calculated by inserting the experimental conditions into the Eq.(11)']. Conditions as in Fig. 3.4, except for the hydrogen peroxide concentration.

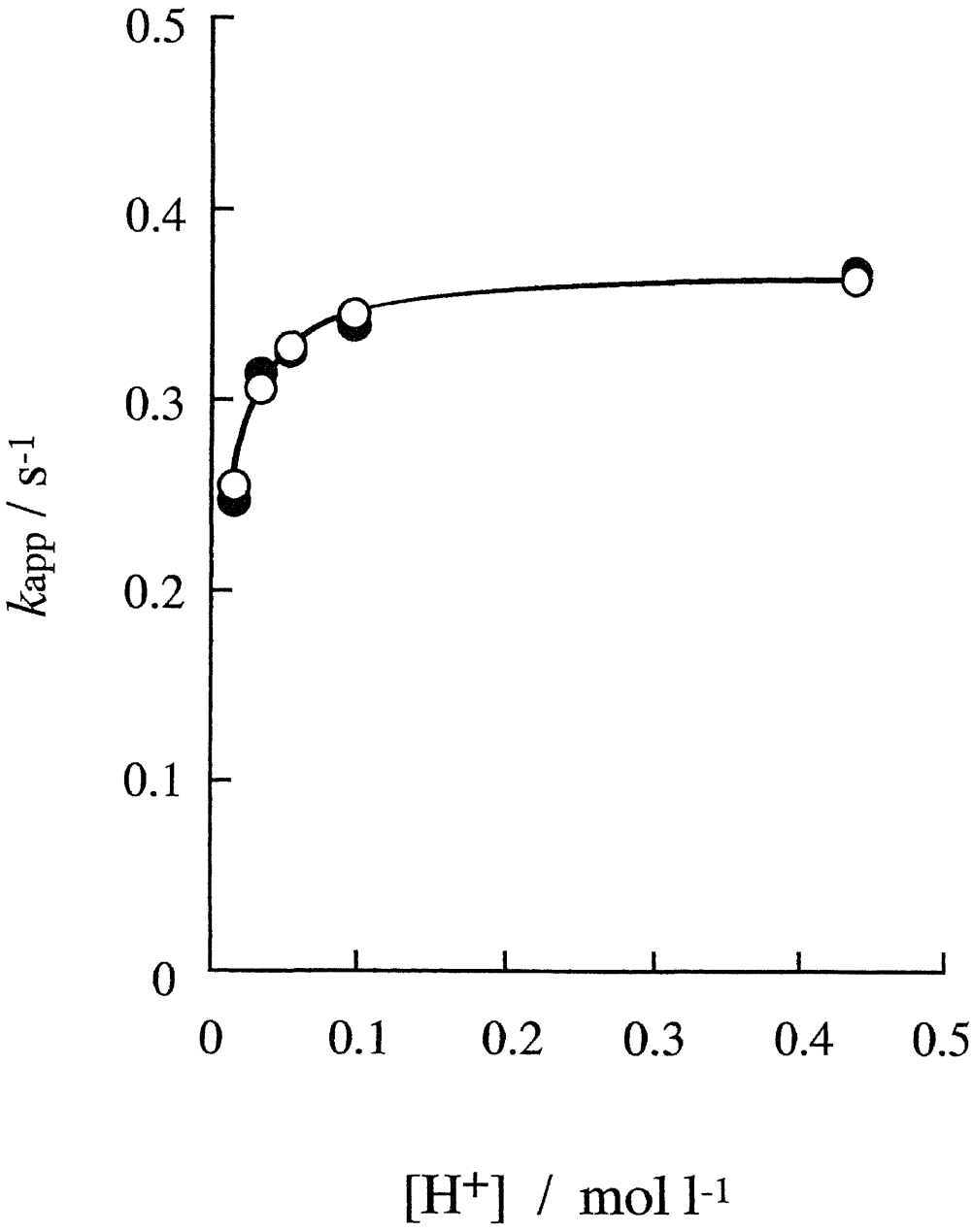

Fig. 3.7 Effect of the hydrogen ion concentration for apparent rate constant, k_{app} [experimental values (●), values (○) calculated by inserting the experimental conditions into the Eq.(11)']. Conditions as in Fig. 3.4, except for the hydrogen ion concentration.

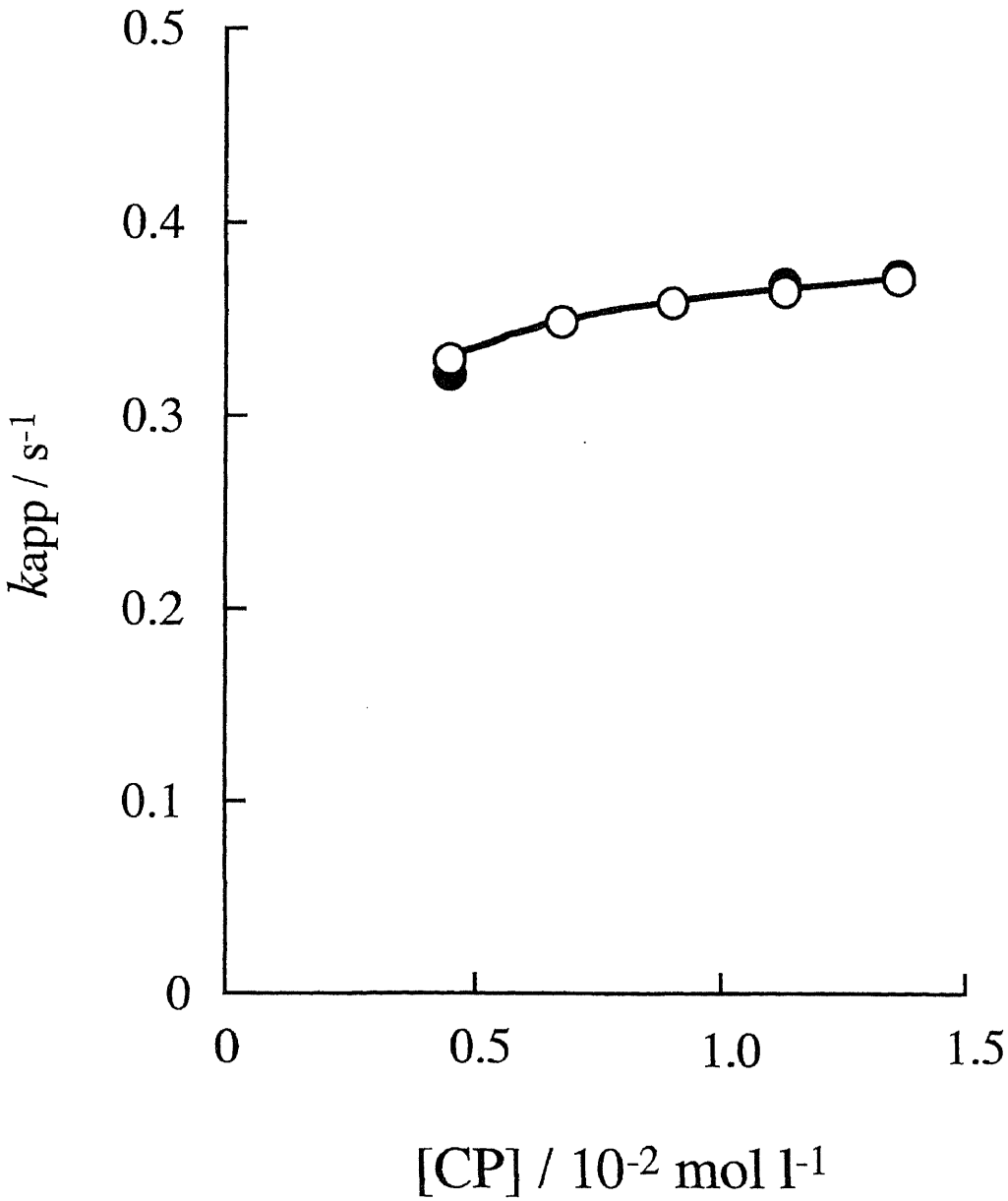

Fig. 3.8 Effect of the CP concentration for apparent rate constant, k_{app} [experimental values (●), values (○) calculated by inserting the experimental conditions into the Eq.(11)']. Conditions as in Fig. 3.4, except for the CP concentration.

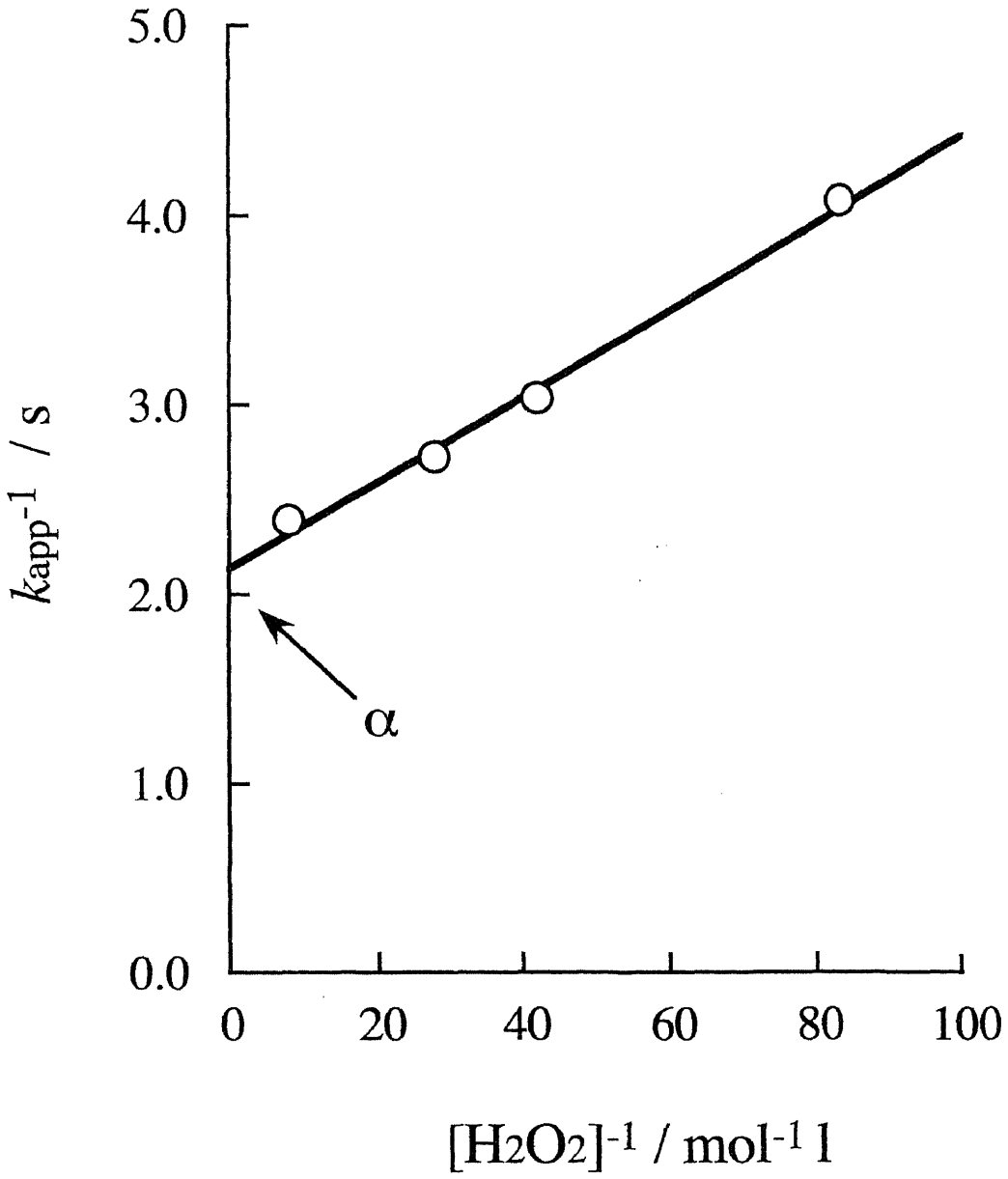

Fig. 3.9 Dependence of apparent rate constant k_{app} upon hydrogen peroxide concentration. Conditions as in Fig. 3.4, except for hydrogen peroxide concentration.

the intercept on ordinate. The dependence of b and α upon hydrogen ion concentration was examined under constant CP concentration. The slope, b, did not change significantly in the hydrogen ion concentration range of 0.016-0.44 mol l^{-1}. The plots of α versus $1/[H^+]$ were linear (Fig. 3.10a) and the relationship between α and hydrogen ion concentration was given by $\alpha = c/[H^+] + d$, where c is the slope of the line and d is the intercept on ordinate. Thus the initial rate of catalyzed reaction,

$$R_{0cat} = R_0 - a,$$

is given by:

$$R_{0cat} = \frac{[H_2O_2][H^+][Fe(II)]_0}{b[H^+] + c[H_2O_2] + d[H^+][H_2O_2]} \qquad (3.2)$$

The dependence of b and α upon CP concentration was also examined under constant hydrogen ion concentration, b did not change significantly over the CP concentration range of 0.0045-0.014 mol l^{-1}. The linearity of plots of α versus 1/[CP], as shown in Fig. 3.10b, leads to the following equation:

$$R_{0cat} = \frac{[CP][H_2O_2][Fe(II)]_0}{b[CP] + e[H_2O_2] + f[CP][H_2O_2]} \qquad (3.3)$$

where e is the slope of the line and f is the intercept on ordinate.

3.3.2.2 Mechanism of the iron-catalyzed red free radical formation reaction between CP and hydrogen peroxide

The kinetic behavior of CP, hydrogen ion and hydrogen peroxide shown by Eqs. (3.2) and (3.3) suggests the formation of a complex of iron with these reactants.

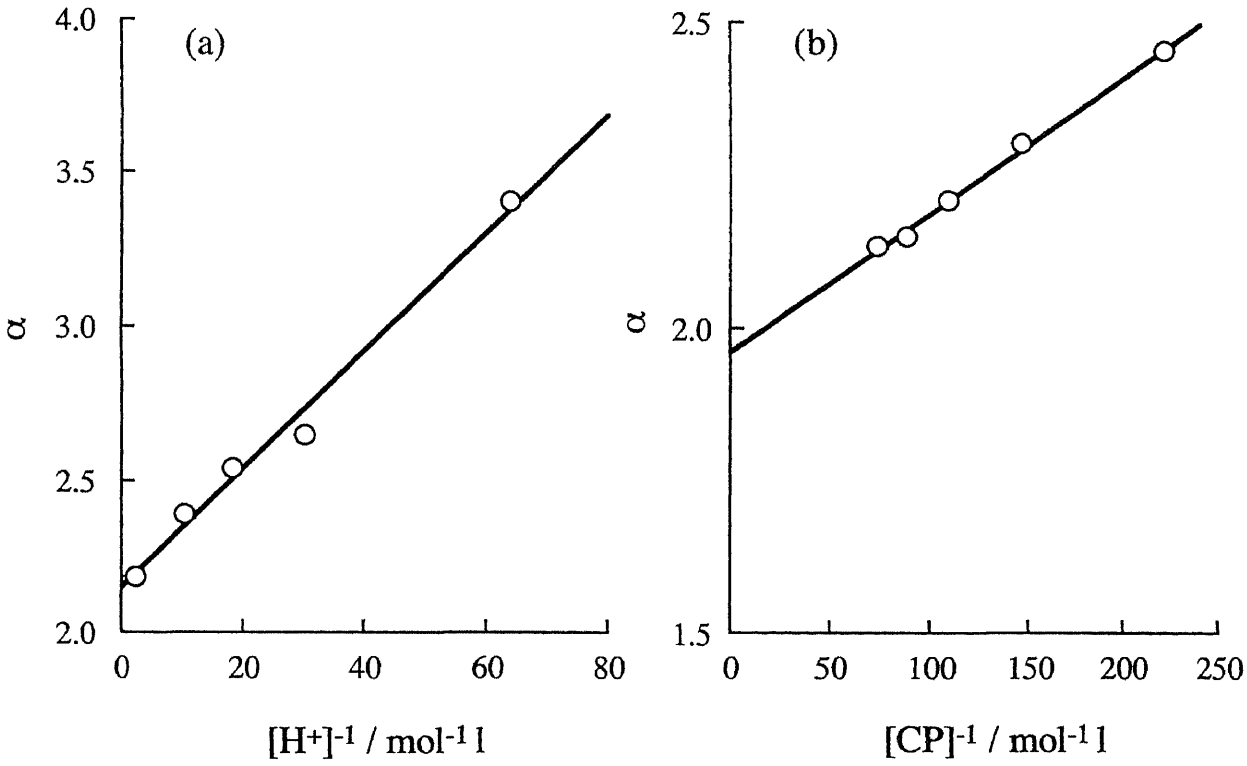

Fig. 3.10 Dependence of the intercept α upon hydrogen ion (a) and CP (b) concentrations. Conditions as in Fig. 3.4, except for hydrogen peroxide concentration and the variable indicated on abscissa.

A mechanism which is consistent with the rate measurements described above is

$$\text{I}\quad CP + H^+ \rightleftarrows (CP\text{-}H)^+ \qquad \text{(rapid, } K_1\text{)} \qquad (3.4)$$

$$Fe(II) + (CP\text{-}H)^+ \rightleftarrows (Fe\text{-}CP\text{-}H)^{3+} \qquad \text{(rapid, } K_2\text{)} \qquad (3.5)$$

$$(Fe\text{-}CP\text{-}H)^{3+} + H_2O_2 \rightleftarrows (Fe\text{-}CP\text{-}H\text{-}H_2O_2)^{3+} \qquad \text{(rapid, } K_3\text{)} \qquad (3.6)$$

$$\text{II}\quad Fe(II) + H_2O_2 \rightleftarrows (Fe\text{-}H_2O_2)^{2+} \qquad \text{(rapid, } K_4\text{)} \qquad (3.7)$$

$$H^+ + (Fe\text{-}H_2O_2)^{2+} \rightleftarrows (Fe\text{-}H_2O_2\text{-}H)^{3+} \qquad \text{(rapid, } K_5\text{)} \qquad (3.8)$$

$$(Fe\text{-}H_2O_2\text{-}H)^{3+} + CP \rightleftarrows (Fe\text{-}CP\text{-}H\text{-}H_2O_2)^{3+} \qquad \text{(rapid, } K_6\text{)} \qquad (3.9)$$

followed by

$$(Fe\text{-}CP\text{-}H\text{-}H_2O_2)^{3+} \rightarrow P \qquad \text{(rate determining; } k\text{)} \qquad (3.10)$$

where P may be an intermediate converting rapidly to the red product and Fe(II) through several steps.

The formation of the $(Fe\text{-}CP\text{-}H\text{-}H_2O_2)^{3+}$ proceeds in two parallel pathways as shown in Eqs. (3.4) ~ (3.9). The rate equation implied by this sequence, $d[Product]/dt = k[(Fe\text{-}CP\text{-}H\text{-}H_2O_2)^{3+}]$ combined with the expression for total analytical concentration of iron;

$$[Fe(II)]_0 = [Fe(II)] + [(Fe\text{-}CP\text{-}H)^{3+}] + [(Fe\text{-}H_2O_2)^{2+}] + [(Fe\text{-}H_2O_2\text{-}H)^{3+}] + [(Fe\text{-}CP\text{-}H\text{-}H_2O_2)^{3+}]$$

from which

$$[Fe(II)] = \frac{[Fe(II)]_0}{1 + K_1K_2[CP][H^+] + K_4[H_2O_2] + K_4K_5[H_2O_2][H^+] + (K_1K_2K_3 + K_4K_5K_6)[CP][H^+][H_2O_2]}$$

leads to

$$\therefore\ R_{0cat} = \frac{[Fe(II)]_0[CP][H^+][H_2O_2]}{P + Q[CP][H^+] + S[H_2O_2] + T[H_2O_2][H^+] + U[CP][H^+][H_2O_2]} \qquad (3.11)$$

where

$$P = \frac{1}{k(K_1K_2K_3 + K_4K_5K_6)} \quad , \quad Q = \frac{K_1K_2}{k(K_1K_2K_3 + K_4K_5K_6)} \quad , \quad S = \frac{K_4}{k(K_1K_2K_3 + K_4K_5K_6)} \quad ,$$

$$T = \frac{K_4K_5}{k(K_1K_2K_3 + K_4K_5K_6)}, \quad U = \frac{1}{k}.$$

If we assume that under experimental conditions

$$P << Q[CP][H^+] + S[H_2O_2] + T[H_2O_2][H^+] + U[CP][H^+][H_2O_2],$$

Eq. (3.11) becomes

$$R_{0cat} = \frac{[Fe(II)]_0[CP][H^+][H_2O_2]}{Q[CP][H^+] + S[H_2O_2] + T[H_2O_2][H^+] + U[CP][H^+][H_2O_2]} \qquad (3.11)'$$

At constant [CP], Eq. (3.11)' is of the same form as the experimentally observed Eq. (3.2) with

$$b = Q \qquad (3.12)$$

$$c = \frac{S}{[CP]} \qquad (3.13)$$

$$d = \frac{T}{[CP]} + U \qquad (3.14)$$

At constant $[H^+]$, Eq. (3.11)' is of the same form as the experimentally observed Eq. (3.3) with

$$e = \frac{S}{[H^+]} + T \qquad (3.15)$$

$$f = U \qquad (3.16)$$

Values for the Q, S, T and U calculated from the experimental values of b, c, d, e and f are 2.0×10^{-2} mol l^{-1} s, 2.2×10^{-4} mol^2 l^{-2} s, 1.8×10^{-3} mol l^{-1} s and 2.0 s, respectively. To evaluate the validity of the proposed reaction mechanism, the k_{app} values calculated by inserting these values together with each experimental

reaction condition into Eq. (3.11)' were compared with the experimental values. As shown in Figs. 3.6 - 3.8, the plots of calculated k_{app} values fall on the plots of the experimental values. R_{0cat} for 1.34×10^{-6} mol l^{-1} and 6.7×10^{-7} mol l^{-1} iron(II) were also calculated according to Eq. (3.11)'. The calculated R_{0cat} values are shown as solid lines in Figs. 3.11 - 3.13. The plots of the experimental R_{0cat} values fall on the lines. Since the calculated k_{app} and R_{0cat} values agreed closely with the experimental values over the investigated reactants concentration range, the proposed mechanism is considered to be reasonable.

3.3.2.3 The estimation of the optimum conditions for the iron determination by the initial rate method

The initial rate (R_0) is one of the parameters for the kinetic determination and has its own advantages [2]; since the measurements are performed at early stage, there is no appreciable contribution from the back reaction and complications arising from possible side-reactions. The dependence of R_0 upon iron concentration was given by

$$R_0 = k_{app}[\mathrm{Fe(II)}]_0 + a \qquad (3.1)$$

with

$$k_{app} = \frac{[CP][H^+][H_2O_2]}{2.0\times10^{-2}[CP][H^+] + 2.2\times10^{-4}[H_2O_2] + 1.8\times10^{-3}[H_2O_2][H^+] + 2.0[CP][H^+][H_2O_2]} \quad (\text{at } 30℃,\ I=0.44 \text{ mol } l^{-1}) \qquad (3.17)$$

where k_{app} is essentially constant under a given condition, because the [CP], [H_2O_2] and [H^+] remain nearly constant at the early stage

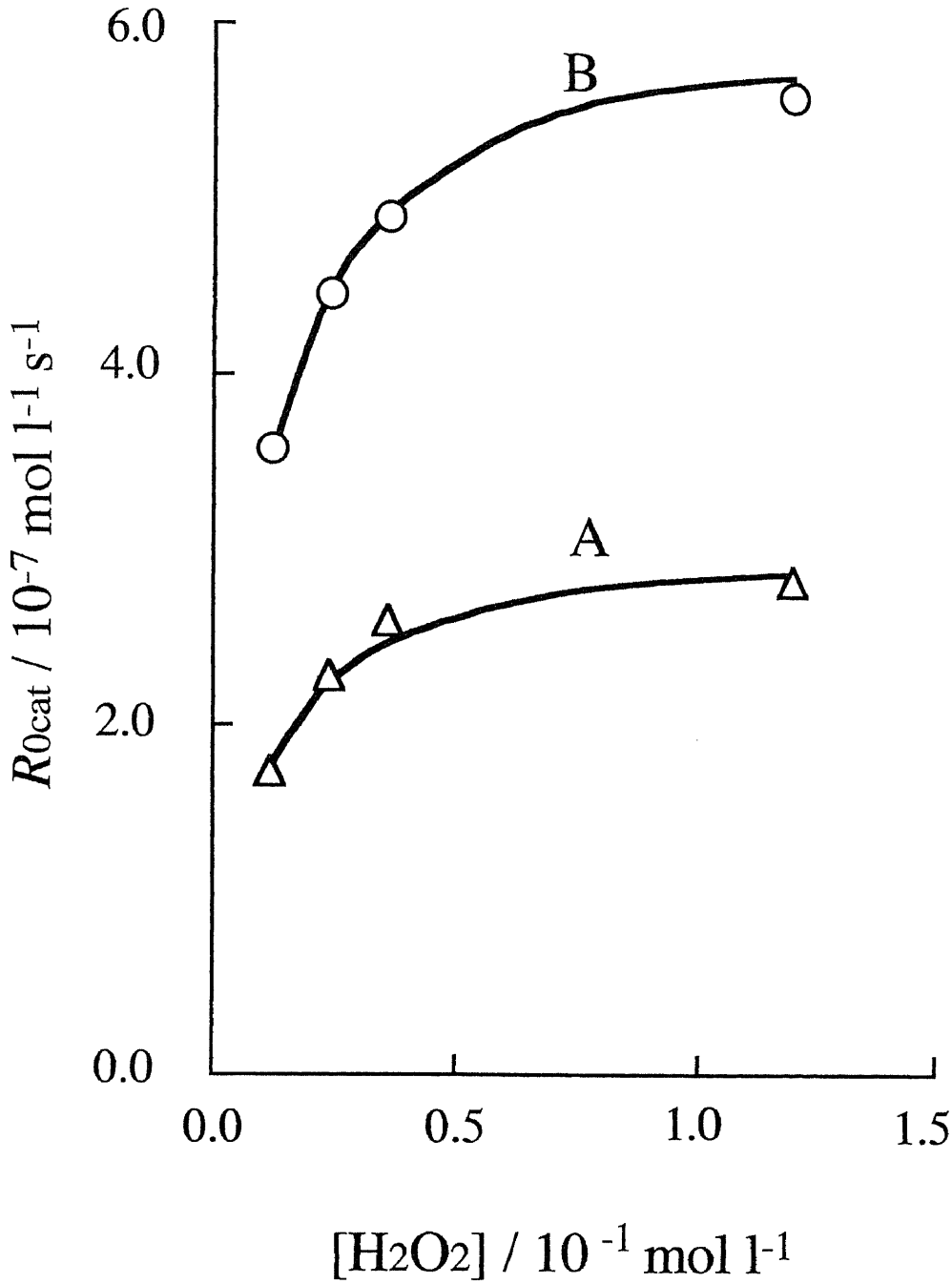

Fig. 3.11 Effect of the hydrogen peroxide concentration for initial reaction rate , R_{0cat}. The plots marked △ and ○ are the experimental R_{0cat} [6.7×10^{-7} mol l^{-1} iron(II) (△), 1.34×10^{-6} mol l^{-1} iron(II) (○)]. Conditions as in Fig. 3.4, except for the hydrogen peroxide concentration. Solid lines show the calculated initial reaction rate according to Eq. (3.11)' for (A) 6.7×10^{-7} mol l^{-1} iron(II), (B) 1.34×10^{-6} mol l^{-1} iron(II) catalyzed reaction.

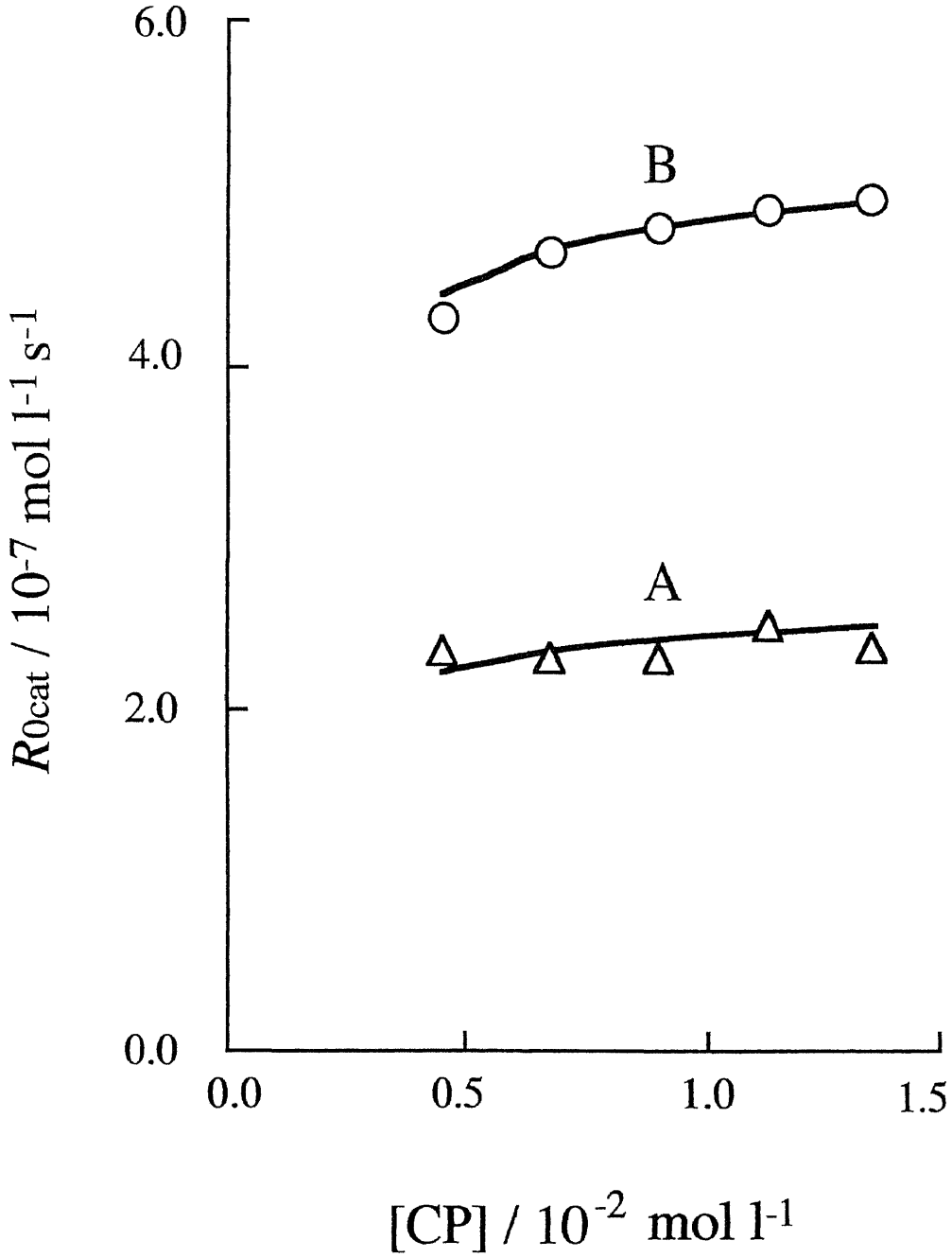

Fig. 3.12 Effect of the CP concentration for initial reaction rate , R_{0cat}. The plots marked △ and ○ are the experimental R_{0cat} [6.7×10^{-7} mol l^{-1} iron(II) (△), 1.34×10^{-6} mol l^{-1} iron(II) (○)]. Conditions as in Fig. 3.4, except for the CP concentration. Solid lines show the calculated initial reaction rate according to Eq. (3.11)' for (A) 6.7×10^{-7} mol l^{-1} iron(II), (B) 1.34×10^{-6} mol l^{-1} iron(II) catalyzed reaction.

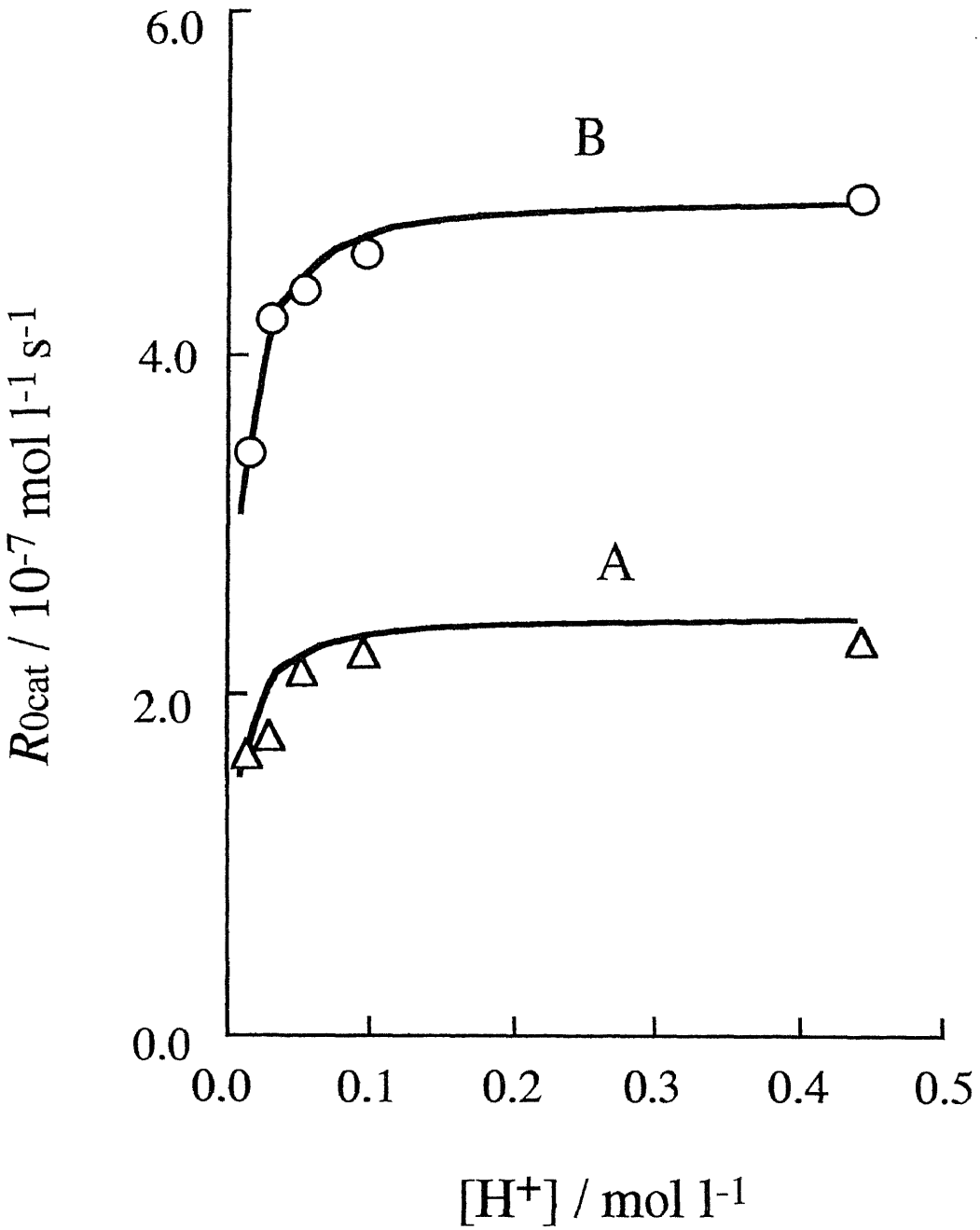

Fig. 3.13 Effect of the hydrogen ion concentration for initial reaction rate , R_{0cat}. The plots marked △ and ○ are the experimental R_{0cat} [6.7×10^{-7} mol l^{-1} iron(II) (△), 1.34×10^{-6} mol l^{-1} iron(II) (○)]. Conditions as in Fig. 3.4, except for the hydrogen ion concentration. Solid lines show the calculated initial reaction rate according to Eq. (3.11)' for (A) 6.7×10^{-7} mol l^{-1} iron(II), (B) 1.34×10^{-6} mol l^{-1} iron(II) catalyzed reaction.

of the reaction. Hence, it is clear from Eq. (3.1) that the use of the initial rate as a parameter gives the linear calibration graph with the slope of the k_{app} value and thus the larger the k_{app} value, the higher the sensitivity. This enables the sensitivity of the catalytic procedure to be optimized for the three variables CP, hydrogen peroxide and hydrogen ion concentrations on the basis of the rate equation. Figure 3.14 represents the slanting surfaces formed with the calculated plots using Eq. (3.17) of the dependence of k_{app} upon the concentrations of two reagents indicated on the abscissas for a given concentration of another one and contour lines are drawn at intervals of 0.02 s^{-1} of k_{app}. In each surface, (a), (b) and (c) in Fig. 3.14, it is observed that its slope decreases gradually to become nearly horizontal as both the reagent concentrations increase. Sets of conditions falling within this horizontal region are of the optimal conditions, because of its higher sensitivity and less influence of the reagent concentrations on the sensitivity. Thus, the range of conditions which should be investigated for the optimization can be narrowed down by this prediction. Although from this result the higher reagent concentrations are apparently suitable for realizing the higher sensitivity, the condition should be selected by considering the blank value which increases also with an increase of the reagent concentrations; too high reagent concentrations are not appropriate.

As the reaction proceeds, the rate of this iron-catalyzed reaction does not fall off normally and during the early stage of the reaction a linear range on the reaction rate curve was observed

under the conditions of higher reagent concentrations. The slope of this linear portion was conveniently used as the parameter for the iron-catalyzed determination [34]. Since the linear portion is obtained in the early stage, the slope is considered to be proportional to the initial rates. The dependence of the slope on the reaction variables also showed the similar trends to those of the calculated results discussed above. The mechanistic study is useful in optimizing an analytical condition of catalytic method, especially when its reaction has a complicated kinetic dependence on reaction variables.

Chapter 4

Kinetic Spectrophotometric Determination of Trace Amounts of Tungsten(VI) by the Catalytic Reaction of Chlorpromazine with Hydrogen Peroxide and Its Mechanistic Study

4.1 Introduction

A few methods for the catalytic determination of tungsten have been reported. Pavlova et al. [35] used reduction of triarylmethane dyes by titanium(III) as an indicator reaction, but the determinable range, 0.18 - 3.7 mg l^{-1}, is not very wide and the sensitivity is not sufficient for determining tungsten in water samples. Voevutskaya et al. [36] reported a kinetic method for the determination of tungsten by its catalytic effect on the iodide-hydrogen peroxide reaction involving the Landold effect; the detection limit is 30 μg l^{-1} and microgram amounts of tungsten had to be concentrated from 1 liter of water sample by coprecipitation on MnO_2. Thus it needs tedious preconcentration and separation procedures which require large volumes of sample.

It is known that CP is oxidized by several oxidizing agent in an acidic medium to a red free radical, which is further oxidized to a colorless sulfoxide having an absorption in an ultra violet region [7,9]. It was found that iodide, iodate and iron catalyzed the color formation reaction and catalytic photometric methods for the determination of these ions [19, 31, 32, 34] was established as described in Chapters 2 and 3. In these investigations it was

observed that CP was also oxidized directly to the colorless sulfoxide and it was found that the colorless compound formation reaction was accelerated by trace amounts of tungsten(VI): the reaction could be followed by measuring the increase in the absorbance at 344 nm. Thus, a kinetic spectrophotometric method for the determination of tungsten(VI) based on its catalytic effect on the CP-hydrogen peroxide reaction was developed. The resulting method is highly sensitive and reproducible: as little as 2 $\mu g\ l^{-1}$ of tungsten(VI) can be determined with reasonable reproducibility. This method has been applied to the determination of tungsten(VI) in hot spring water samples. This chapter also presents the results of a kinetic study of this catalyzed reaction. A mechanism is proposed which is consistent with the experimental results. The proposed mechanism was utilized to derive a rate equation which describes the quantitative behavior of the reaction throughout the range of conditions studied.

4.2 Experimental

4.2.1 Apparatus and reagents

Spectrophotometer for measuring the absorbance and absorption spectra, a circulating thermostat bath and magnetic stirrer used were the same as those described in Chapter 2.

A sulfuric acid (10.3 mol l^{-1}) solution was prepared by diluting concentrated sulfuric acid with water.

An EDTA solution (0.10 mol l^{-1}) was prepared by dissolving

3.72 g of ethylenediamine-N,N,N',N'-tetraacetic acid, disodium salt, dihydrate in water and diluting to 100 ml with water.

A commercially available tungsten(VI) standard solution (1000 mg l^{-1}) was obtained from Wako Chemical Co. Working solutions were prepared by diluting this solution with water.

Other chemicals used were the same as described in Chapter 2.

4.2.2 Recommended procedure

To 10.0 ml of a sample solution in a glass-stoppered tube, 0.5 ml of 10.3 mol l^{-1} sulfuric acid and 0.5 ml of 0.020 mol l^{-1} CP solutions were added and the solution was thoroughly mixed. This solution was then kept in a water bath at 40℃ for 15 min to achieve the required temperature. A 1.8 ml aliquot was taken into a quartz cell. The cell was placed in the holder at 40℃ and the solution was magnetically stirred. The reaction was initiated by the injection of 0.20 ml of a 0.10 mol l^{-1} hydrogen peroxide (40℃). The increase in absorbance at 344nm of the product was recorded against a CP solution reference (8.2×10^{-4} mol l^{-1} CP, 0.42 mol l^{-1} sulfuric acid) and the initial slope of reaction rate curves, R_0 [=Δ(abs.)/Δ(s)], was used as a parameter for the tungsten determination.

When a sample solution contained iron higher than 0.1 mg l^{-1}, EDTA was used to mask the interferences. After 1.0 ml of 0.10 mol l^{-1} EDTA solution was added to 9.0 ml of the sample solution, 0.5 ml of 0.020 mol l^{-1} CP and 0.5 ml of 10.3 mol l^{-1} sulfuric acid were added and the resultant solution was kept in a water bath at 40℃ for 15 min. A 1.8 ml aliquot of this solution was then taken

into 1-cm quartz cell and the absorbance/time curve was obtained as mentioned above.

4.3 Results and discussion

4.3.1 Selection of wavelength

As can be seen in Fig. 4.1, the colorless sulfoxide has absorption maxima at 298 nm and 340 nm (curve A), while CP has an absorption maximum at 300 nm and shows also significant absorption at 340 nm (curve B). Thus 344 nm was selected for the procedure taking into consideration of the sensitivity and lower absorption of CP. The absorbance at 344 nm increases with increase in reaction time as shown in Fig. 4.2. The initial slope of the reaction curves [Δ(abs.)/Δ(s)] is manually determined and then used as a measure of the initial reaction rate. Since the slope, R_0, increases with an increase in the tungsten(VI) concentration, it was used as the parameter for the tungsten(VI) determination.

4.3.2 Effect of reaction variables

The influence of temperature on R_0 was studied in the range 20-50℃ under the conditions otherwise as in the recommended procedure. Although higher sensitivity was obtained at higher temperature, at higher than 40℃ the rate of the uncatalyzed reaction became considerably higher. A temperature of 40℃ was chosen for the procedure.

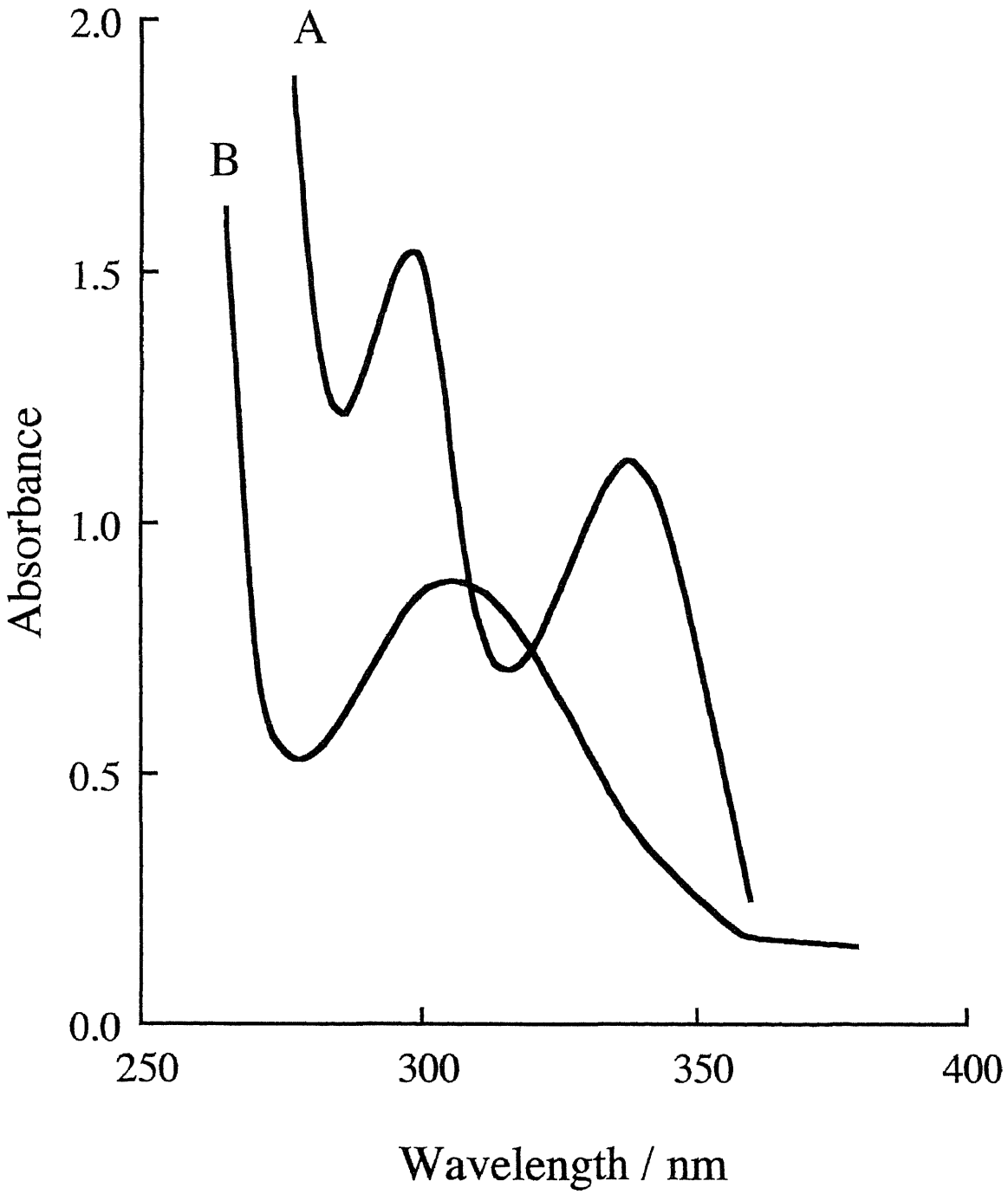

Fig. 4.1 Absorption curves of CP and its colorless oxidation product. Conditions: (A) 4.5×10^{-7} mol l^{-1} tungsten(VI), 1.6×10^{-4} mol l^{-1} CP, 0.42 mol l^{-1} sulfuric acid, 1.0×10^{-2} mol l^{-1} hydrogen peroxide, 40℃, reaction time 60 min. (B) 1.6×10^{-4} mol l^{-1} CP in 0.42 mol l^{-1} sulfuric acid solution.

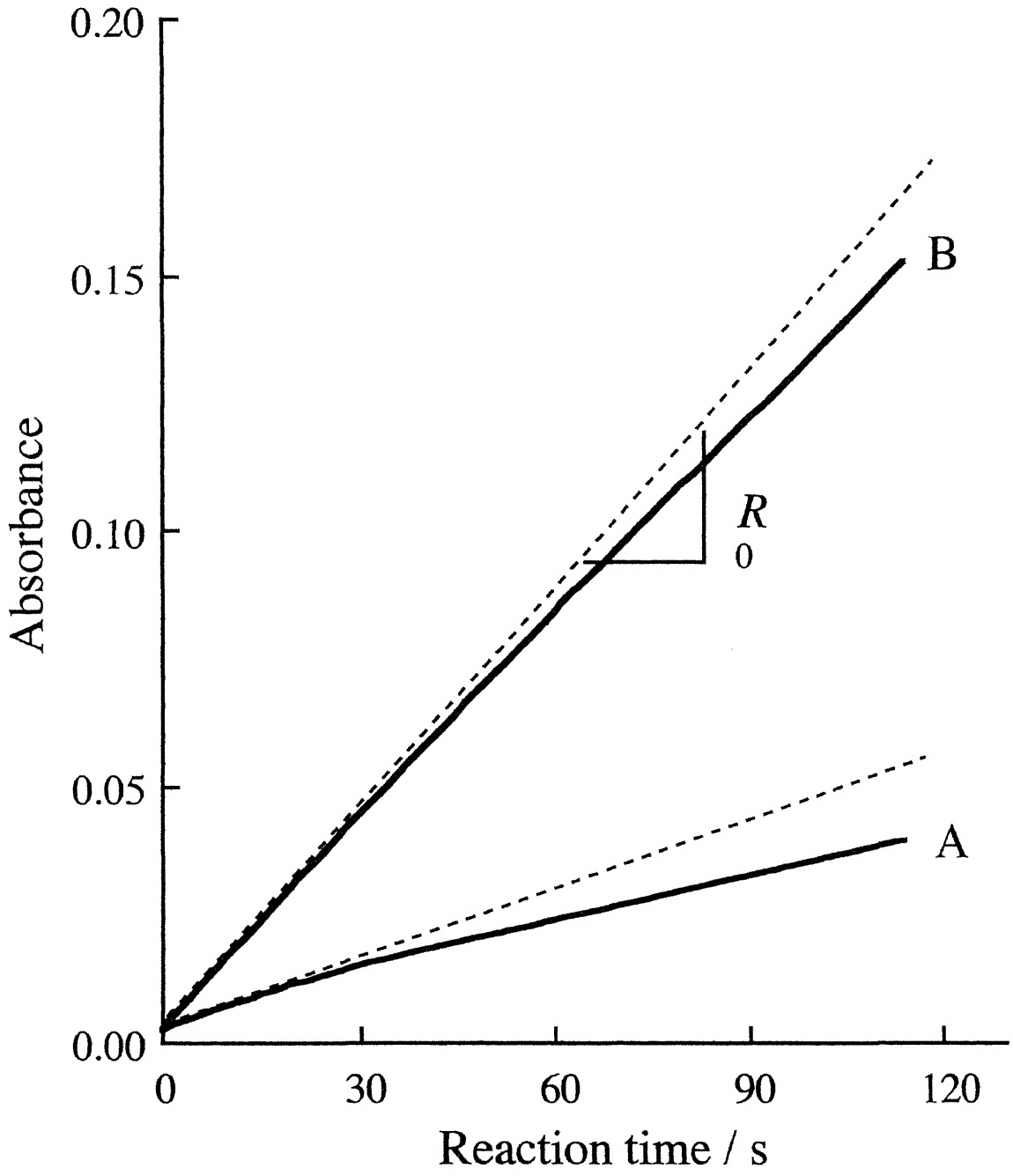

Fig. 4.2 Absorbance/time curves for the CP/hydrogen peroxide reaction. Concentrations of tungsten(VI) (μg l^{-1}): (A) 0, (B) 60. Conditions as in recommended procedure(8.2×10^{-4} mol l^{-1} CP, 0.42 mol l^{-1} sulfuric acid, 1.0×10^{-2} mol l^{-1} hydrogen peroxide, 40℃). R_0: Δ(abs.)/Δ(s) at reaction time 0 was used as a measure of the initial reaction rate.

Figure 4.3 shows the effect of CP concentration on R_0. The R_0 values increased with increasing CP concentration in the presence of tungsten(VI) and in its absence. Since the effect of CP concentration was more pronounced for the catalyzed reaction, a higher sensitivity can be realized at higher CP concentrations. However, at higher CP concentrations the absorbance was higher than 1.0 against a pure water reference before the reaction, because CP has significant absorption at 344 nm as mentioned above (Fig. 4.1). A CP concentration of 8.2×10^{-4} mol l^{-1} was chosen. At this CP concentration, the absorbance at the initiation of the reaction was about 0.75 against a pure water reference. The reaction rates in the presence and absence of tungsten(VI) increased with increasing sulfuric acid concentration (Fig. 4.4). However, the difference in these R_0 values did not change significantly in the higher sulfuric acid concentration range. A 0.42 mol l^{-1} of sulfuric acid was selected by considering the sensitivity and lower blank value as criteria. The R_0 values in the presence of tungsten(VI) and its absence increased with an increase in the hydrogen peroxide concentration (Fig. 4.5). The sensitivity of this method increased with an increase in the hydrogen peroxide concentration in the range of 2.0×10^{-3} - 1.0×10^{-2} mol l^{-1} ; above 1.0×10^{-2} mol l^{-1} the sensitivity remained constant. A hydrogen peroxide concentration of 1.0×10^{-2} mol l^{-1} was chosen because of higher sensitivity and lower blank.

4.3.3 Kinetics and mechanism of the tungsten-catalyzed sulfoxide formation reaction between CP and hydrogen

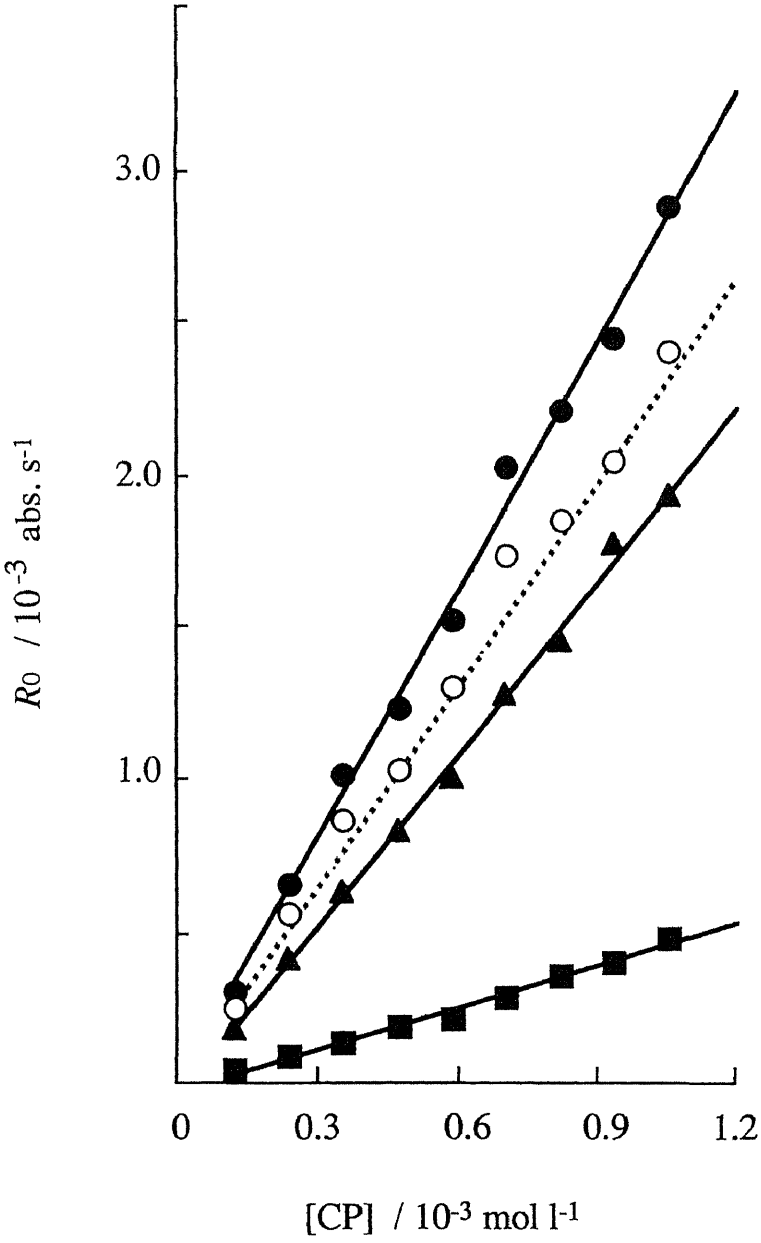

Fig. 4.3 Effect of the CP concentration on the catalytic effect of tungsten(VI) [blank (■), 60 μg l^{-1} (▲), 100 μg l^{-1} (●)]. The plot marked ○ is the difference between R_0 in presence of 100 μg l^{-1} tungsten(VI) and that in its absence. Conditions as in recommended procedure, except for the CP concentration. Dotted line shows the calculated initial reaction rate R_{0cat}' according to Eq. (4.13) for 100 μg l^{-1} tungsten(VI) catalyzed reaction.

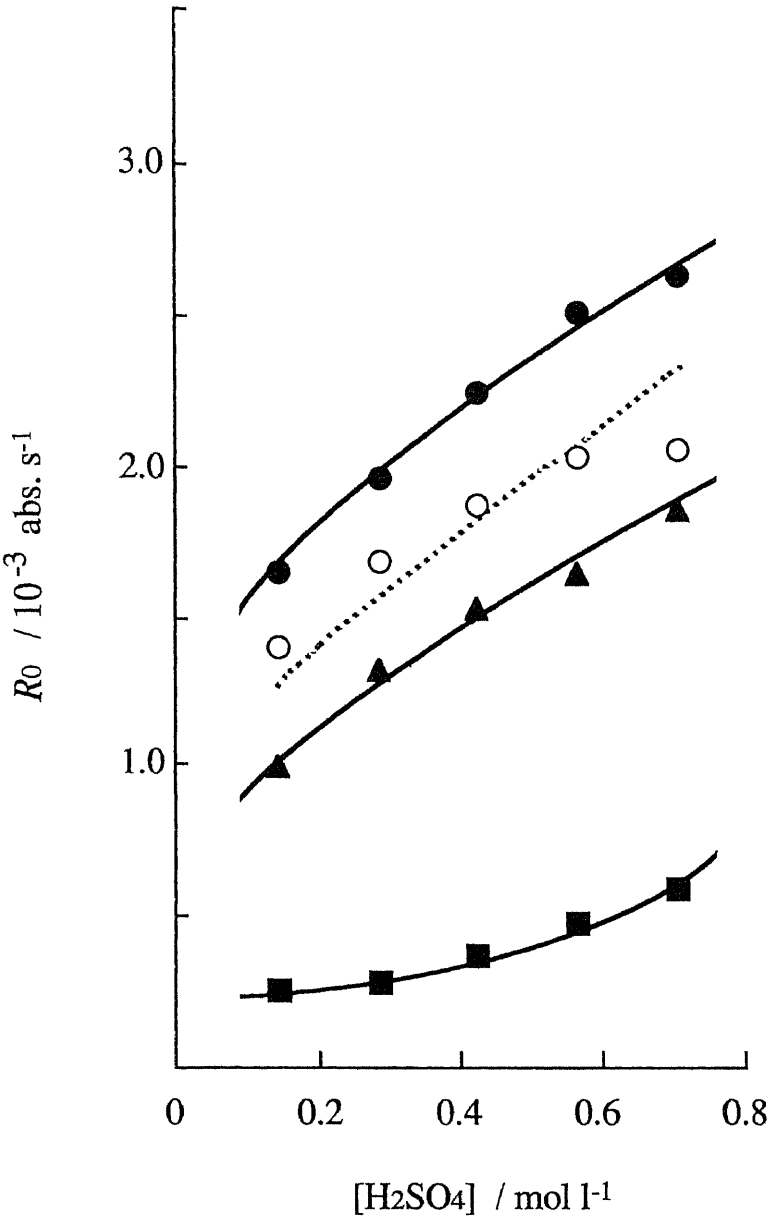

Fig. 4.4 Effect of the sulfuric acid concentration on the catalytic effect of tungsten(VI) [blank (■), 60 μg l^{-1} (▲), 100 μg l^{-1} (●)]. The plot marked ○ is the difference between R_0 in presence of 100 μg l^{-1} tungsten(VI) and that in its absence. Conditions as in recommended procedure, except for the sulfuric acid concentration. Dotted line shows the calculated initial reaction rate R_{0cat}' according to Eq. (4.13) for 100 μg l^{-1} tungsten(VI) catalyzed reaction.

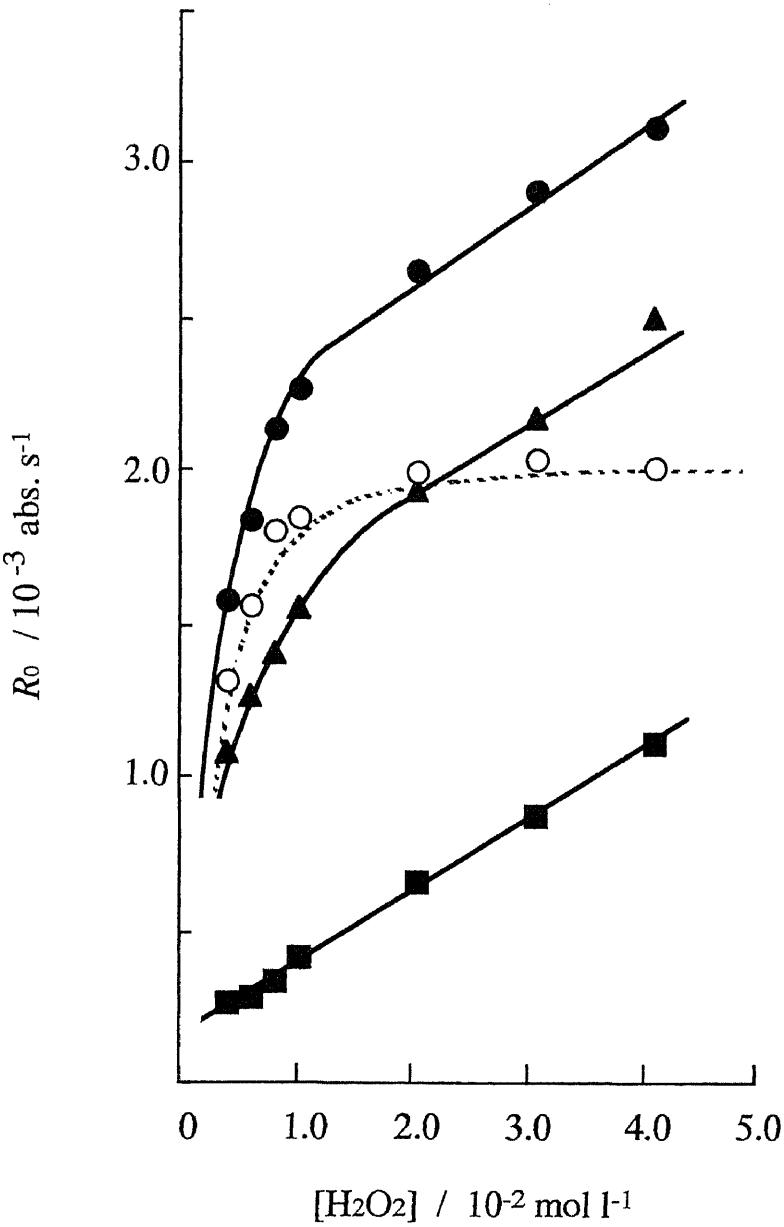

Fig. 4.5 Effect of the hydrogen peroxide concentration on the catalytic effect of tungsten(VI) [blank (■), 60 μg l^{-1} (▲), 100 μg l^{-1} (●)]. The plot marked ○ is the difference between R_0 in presence of 100 μg l^{-1} tungsten(VI) and that in its absence. Conditions as in recommended procedure, except for the hydrogen peroxide concentration. Dotted line shows the calculated initial reaction rate R_{0cat}' according to Eq. (4.13) for 100 μg l^{-1} tungsten(VI) catalyzed reaction.

peroxide

The kinetic investigation of the tungsten(VI) catalyzed sulfoxide formation reaction was carried out by the initial-rate method. The initial rate, R_0* [=Δ(mol l^{-1}) / Δ(s)], was obtained by dividing the rate evaluated from the absorbance/time curves by the molar absorptivity at 344 nm of sulfoxide. The molar absorptivity was determined as follows. When CP was oxidized by hydrogen peroxide (conditions; 3.3×10^{-5}-1.6×10^{-4} mol l^{-1} CP, 0.42 mol l^{-1} sulfuric acid, 0.010 mol l^{-1} hydrogen peroxide and 4.5×10^{-7} mol l^{-1} tungstate(VI), 40℃), the absorbance of the solution obtained by the formation of sulfoxide reached a maximum value within 2 h. The concentrations of sulfoxide ($C_{17}H_{19}ClN_2SO^{2+}$) were calculated from that of CP ($C_{17}H_{19}ClN_2S$) according to the stoichiometry given by

$$C_{17}H_{19}ClN_2S+2H_2O_2+2H^+\rightarrow C_{17}H_{19}ClN_2SO^{2+}+3H_2O$$

The molar absorptivity of sulfoxide at 344 nm was evaluated as $\varepsilon=5.6\times10^3$ l mol^{-1} cm^{-1} from the slope of the linear plots of the maximum absorbance versus sulfoxide concentration.

All concentrations given in the figures are the initial analytical concentrations in the reaction mixture at the initiation of reaction. Throughout the experiment the ionic strength was maintained constant at 0.43 mol l^{-1} by the addition of sodium hydrogen sulfate and/or sodium sulfate. In order to determine the dependence of R_0* upon the tungstate concentration, a series of experiments was performed in which the tungstate concentration was varied while

the CP, hydrogen ion and hydrogen peroxide concentrations were held constant. The plots of R_0* versus the total analytical concentration of tungstate [W(VI)] were linear in the range of 0-4.45$\times 10^{-7}$ mol l^{-1} tungstate. It was established that the tungsten catalyzed reaction was first order in tungstate:

$$R_0^* = k_{app}[W(VI)] + a \qquad (4.1)$$

where k_{app} is the apparent rate constant and a is the intercept on ordinate which corresponds to the rate of an uncatalyzed reaction. The k_{app} values were determined at different CP concentrations in the range 1.2$\times 10^{-4}$-1.1$\times 10^{-3}$ mol l^{-1}. As can be seen in Fig. 4.6, a straight line obtained by plotting k_{app} versus CP concentration shows that the relation is given by $k_{app}=u[CP]$, where u is the slope of the line. Thus the initial rate of catalyzed reaction, $R_{0cat}=R_0^* - a$, is given by:

$$R_{0cat} = u[CP][W(VI)] \qquad (4.2)$$

The dependence of k_{app} upon hydrogen peroxide concentration was also determined at constant CP and hydrogen ion concentrations (Fig. 4.7). The linearity of plots of $1/k_{app}$ versus $1/[H_2O_2]^2$, as shown in Fig. 4.8, leads to the following relation:

$$R_{0cat} = \frac{[H_2O_2]^2[W(VI)]}{v + x[H_2O_2]^2} \qquad (4.3)$$

This kinetic behavior of hydrogen peroxide suggests the formation of complex of tungstate with hydrogen peroxide.

The variation in k_{app} with hydrogen ion concentration at constant CP and hydrogen peroxide concentrations is shown in Fig.

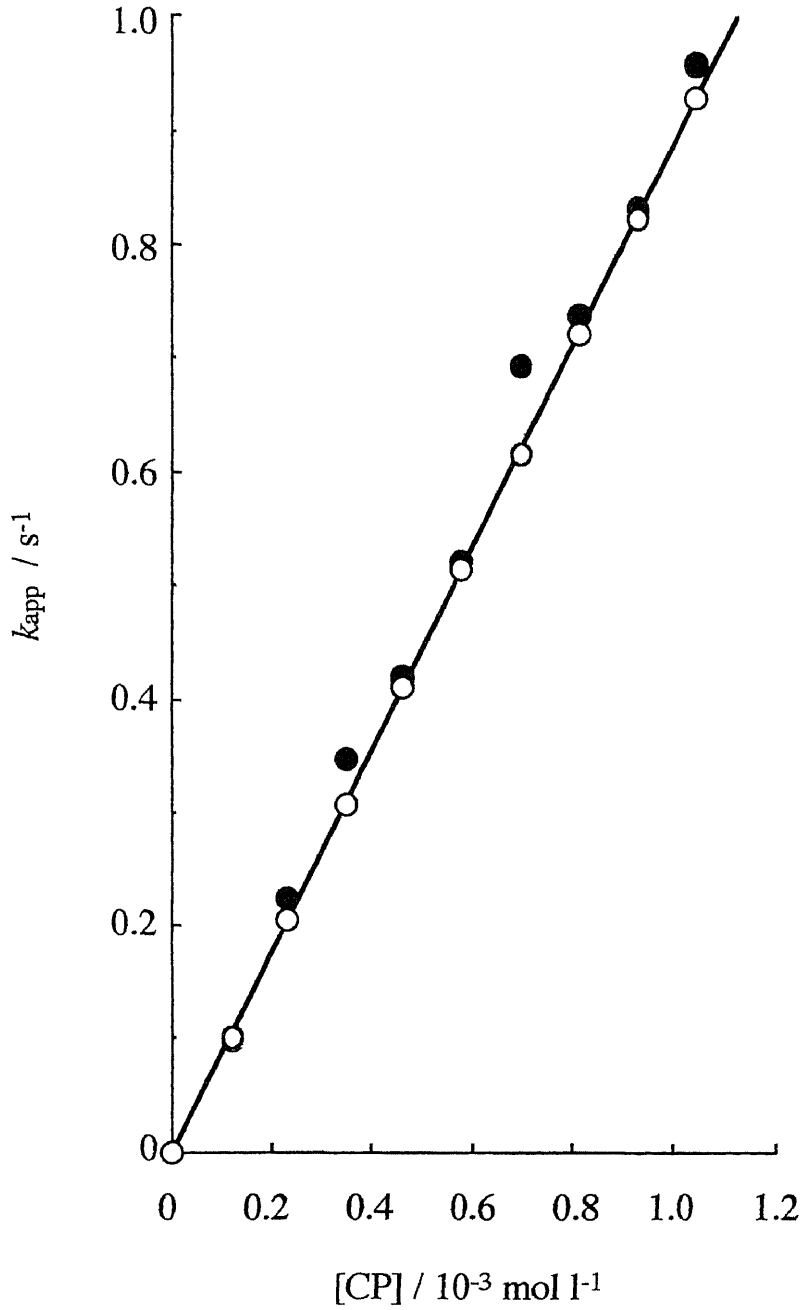

Fig. 4.6 Effect of the CP concentration for apparent rate constant, k_{app} [experimental values (●), calculated values (○) by inserting the experimental conditions into the Eq. (4.13)]. Conditions as in recommended procedure, except for the CP concentration and ionic strength of 0.43 mol l^{-1}.

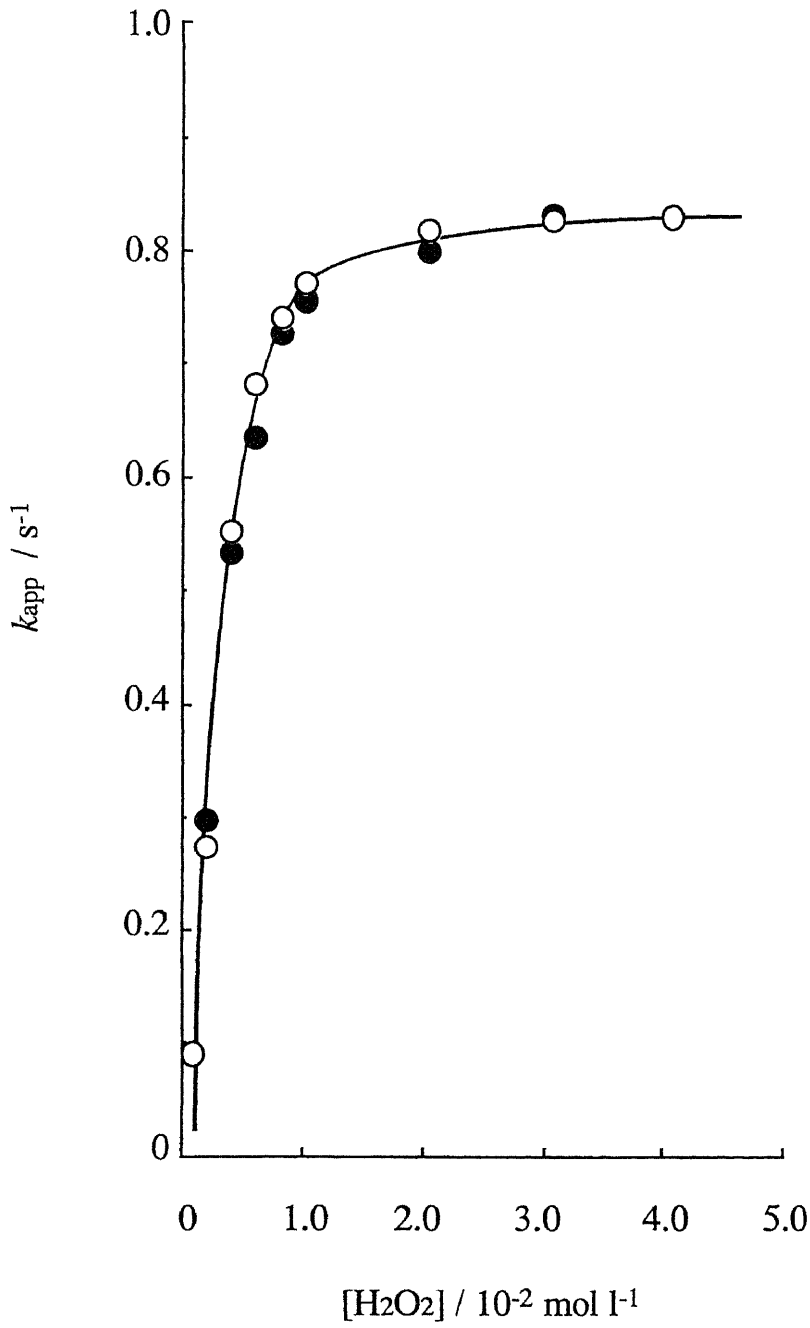

Fig. 4.7 Effect of the hydrogen peroxide concentration for apparent rate constant, k_{app} [experimental values (●), calculated values (○) by inserting the experimental conditions into the Eq. (4.13)]. Conditions as in recommended procedure, except for the hydrogen peroxide concentration and ionic strength of 0.43 mol l^{-1}.

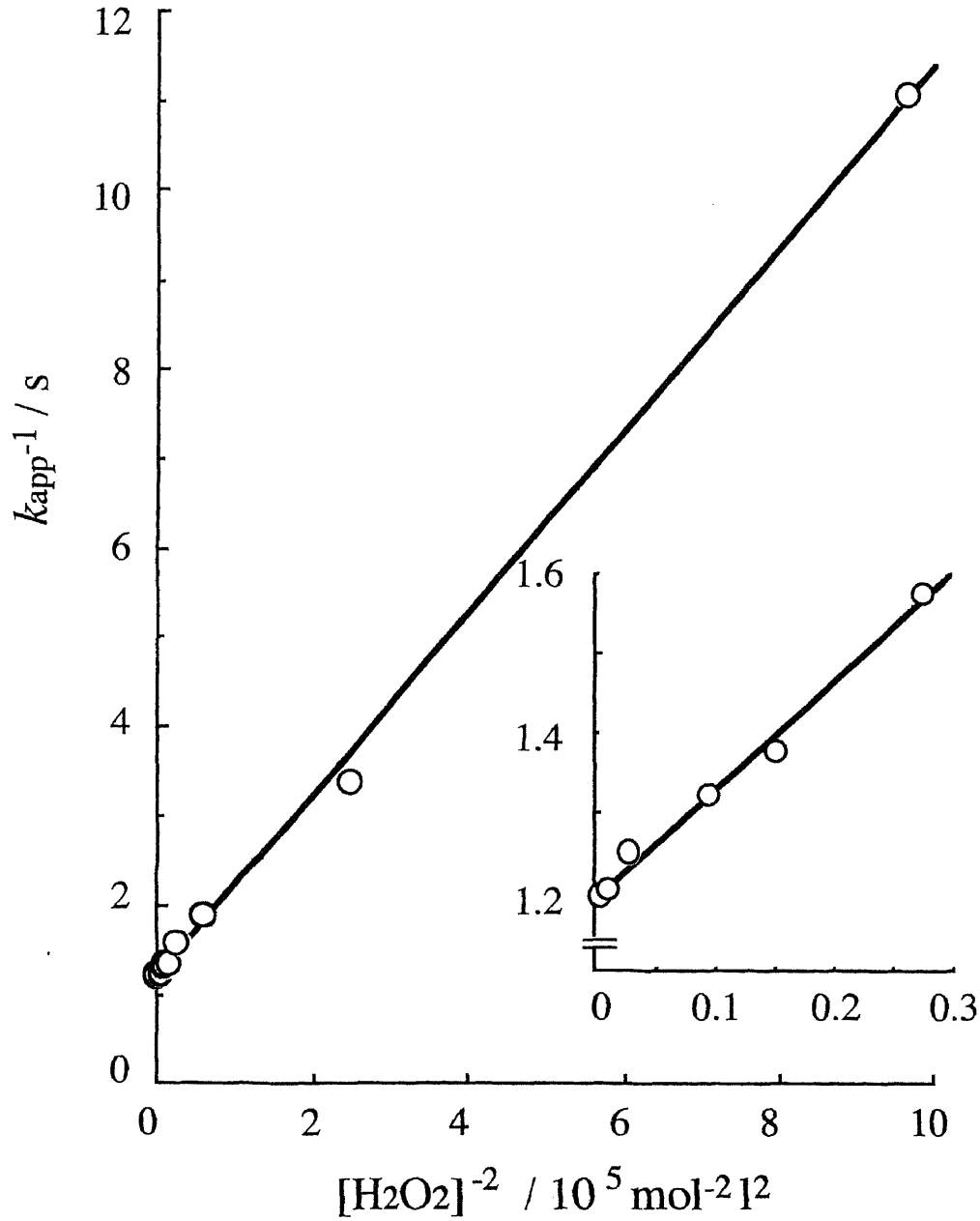

Fig. 4.8 Dependences of apparent rate constant k_{app} upon hydrogen peroxide concentration. Conditions as in Fig. 4.7. The inset provides details concerning the higher concentration range of the line.

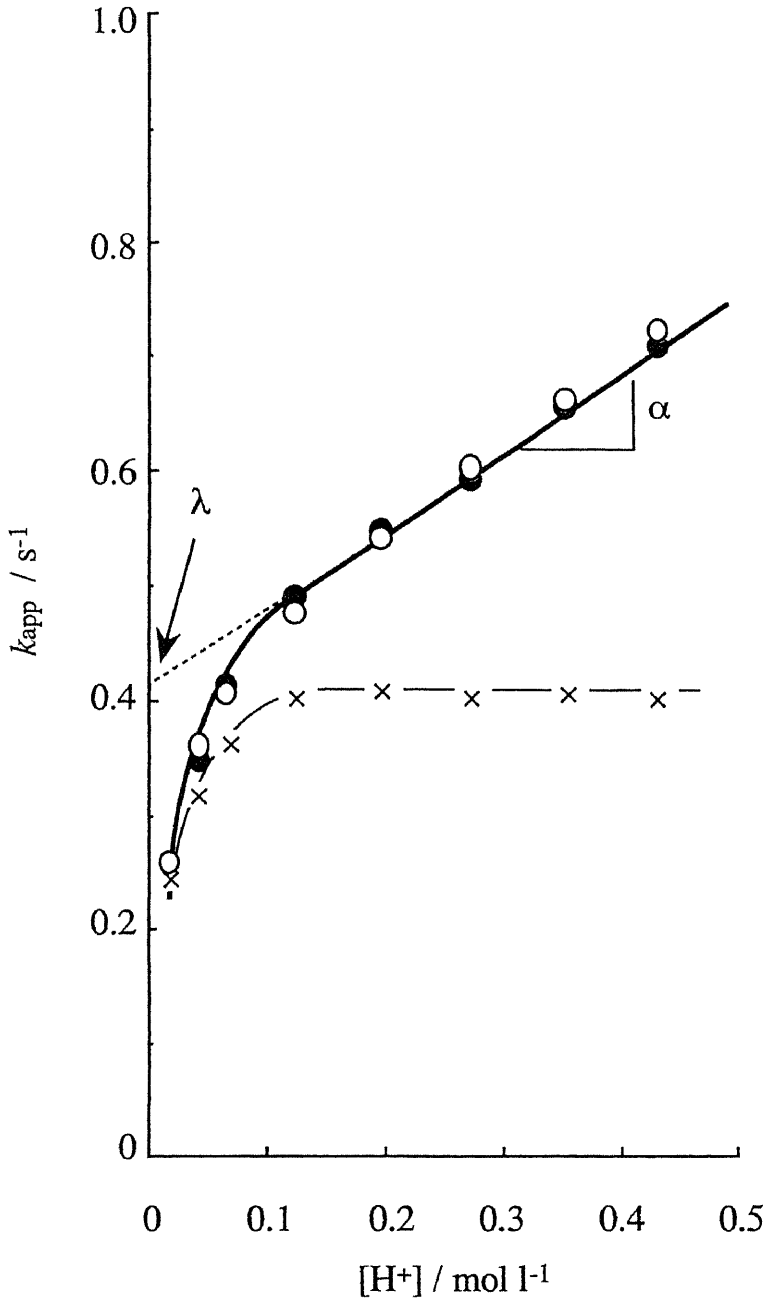

Fig. 4.9 Effect of the hydrogen ion concentration for apparent rate constant, k_{app} [experimental values (●), calculated values (○) by inserting the experimental conditions into the Eq. (4.13)]. The plots marked × are k_A and are obtained by subtracting α[H+] from k_{app}. Conditions as in recommended procedure, except for the hydrogen ion concentration and ionic strength of 0.43 mol l^{-1}.

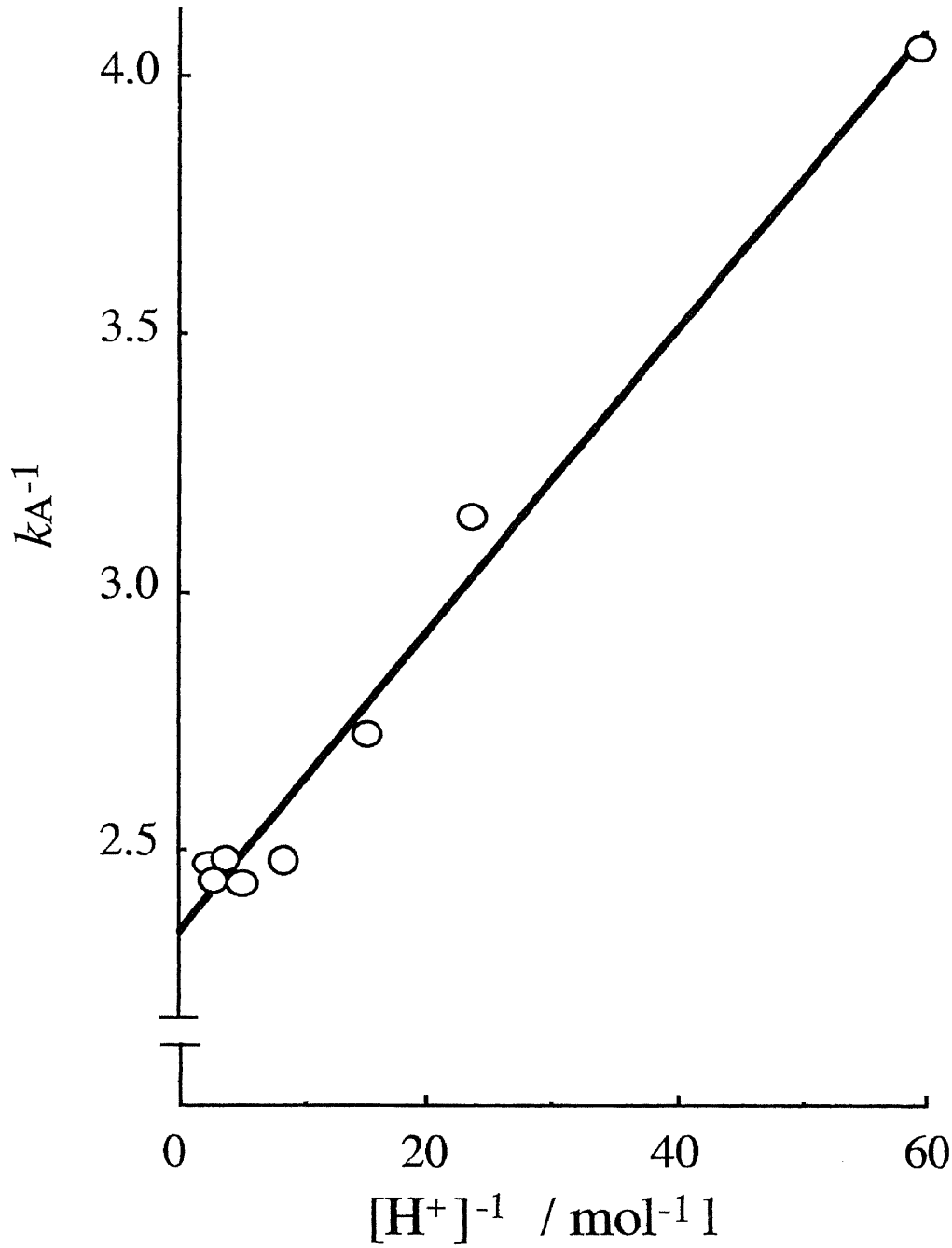

Fig. 4.10 Dependences of k_A upon hydrogen ion concentration. Conditions as in Fig. 4.9.

4.9. In the range 0.12-0.43 mol l^{-1} H^+, the k_{app} value increased linearly with an increase in the hydrogen ion concentration and the dependence of k_{app} upon hydrogen ion in this range was given by $k_{app}=\alpha[H^+]+\lambda$, where α is the slope in the linear range and λ is the intercept which is found by extrapolation of the line in the linear range (dotted line in Fig. 4.9). However, at the lower concentrations, the k_{app} value deviated negatively from the first order dependence with a decrease in the hydrogen ion concentration. These facts suggest that the k_{app} is given by the sum of two terms: $k_{app}=k_A+k_B$, where $k_B=\alpha[H^+]$. As the hydrogen ion concentration increases, k_A ($=k_{app}-k_B$) approaches gradually to a limiting value of λ as shown in Fig. 4.9. The linearity of plots of $1/k_A$ versus $1/[H^+]$ in Fig. 4.10 leads to the following relation: $k_A=[H^+]/(\beta+\gamma[H^+])$, where β is the slope of the line and γ is the intercept on ordinate. The dependence of the R_{0cat} upon hydrogen ion concentration is thus given by the following equation:

$$R_{0cat}=\left(\alpha[H^+]+\frac{[H^+]}{\beta+\gamma[H^+]}\right)[W(VI)]=\frac{(\sigma[H^+]+[H^+]^2)[W(VI)]}{y+z[H^+]} \qquad (4.4)$$

where

$$\sigma=\frac{\alpha\beta+1}{\alpha\gamma},\quad y=\frac{\beta}{\alpha\gamma}\ \text{and}\ z=\frac{1}{\alpha}.$$

The dependence of k_A and k_B upon hydrogen ion concentration suggests the evidence of formation of both protonated tungstate and protonated CP, respectively.

Before mechanism is discussed, consideration must be given to the species actually present in the reaction mixtures. It is well known that tungstate exists as mononuclear oxoanion, WO_4^{2-}, in

alkaline solution, but it condenses to polynuclear anions as pH is lowered. However in the present work the reaction was carried out in strongly acidic medium (0.43 mol l^{-1}), where the condensation of tungstate would be negligible. This is in accord with the following facts: (i) The reaction is first order with respect to tungstate. If the reaction sequence involves the formation of polynuclear species of tungstate, then a higher kinetic order or rather complex dependence upon tungstate concentration should be observed.
(ii) The tungstate concentration in the present solutions is very low ($< 4.5\times 10^{-7}$ mol l^{-1}), so that the formation of polynuclear species is less favorable. Tungstate also exists in three states, H_2WO_4, HWO_4^- and WO_4^{2-} in equilibrium with stepwise ionization constants K_{a1} and K_{a2}. Using the reported values of $K_{a1}=6.4\times 10^{-3}$ mol l^{-1} and $K_{a1}=2.0\times 10^{-4}$ mol l^{-1} [37], the ratios of $[WO_4^{2-}]/[W(VI)]$, $[HWO_4^-]/[W(VI)]$ and $[H_2WO_4]/[W(VI)]$ at 0.017 mol l^{-1} H^+ (the lowest concentration of the investigated range) were calculated to be 0.01, 0.27 and 0.72, respectively. The concentration of WO_4^{2-} may therefore be taken as negligible under the conditions of this study and the $[H_2WO_4]/[HWO_4^-]$ ratio increases gradually with an increase in hydrogen ion concentration. At higher concentration of H^+ than 0.12 mol l^{-1}, almost all the tungstate exists as H_2WO_4. In the concentration range, the plots of k_{app} in Fig. 4.9 become linear.

A mechanism is consistent with the rate measurements and represents as follows;

$$HWO_4^- + H^+ \rightleftarrows H_2WO_4 \quad \text{(rapid;}K_1\text{)} \quad (4.5)$$

$$H_2WO_4 + H_2O_2 \rightleftarrows H_2WO_4(H_2O_2) \quad \text{(rapid;}K_2\text{)} \quad (4.6)$$

$$H_2WO_4(H_2O_2) + H_2O_2 \rightleftarrows H_2WO_4(H_2O_2)_2 \quad \text{(rapid;}K_3\text{)} \quad (4.7)$$

$$H_2WO_4(H_2O_2)_2 + CP \rightarrow CP{=}O^{2+} + HWO_4^- + 2H_2O + OH^- \quad \text{(rate determining;}k_1\text{)} \quad (4.8)$$

$$OH^- + H^+ \rightleftarrows H_2O \quad \text{(rapid)} \quad (4.9)$$

$$CP + H^+ \rightleftarrows CP\text{-}H^+ \quad \text{(rapid;}K_4\text{)} \quad (4.10)$$

$$H_2WO_4(H_2O_2)_2 + CP\text{-}H^+ \rightarrow CP{=}O^{2+} + HWO_4^- + 3H_2O \quad \text{(rate determining;}k_2\text{)} \quad (4.11)$$

The formation of the sulfoxide proceeds via two parallel pathways shown by Eqs. (4.8)～(4.11). The rate equation implied by this sequence,

$$d[CP{=}O^{2+}]/dt = k_1[H_2WO_4(H_2O_2)_2][CP] + k_2[H_2WO_4(H_2O_2)_2][CP\text{-}H^+]$$

combined with the expression for total analytical concentration of tungsten;

$$[W(VI)] = [HWO_4^-] + [H_2WO_4] + [H_2WO_4(H_2O_2)] + [H_2WO_4(H_2O_2)_2]$$

from which

$$[HWO_4^-] = \frac{[W(VI)]}{1 + K_1[H^+] + K_1K_2[H^+][H_2O_2] + K_1K_2K_3[H^+][H_2O_2]^2}$$

leads to

$$R_{0cat} = \frac{[W(VI)][H^+][H_2O_2]^2[CP]}{J + L[H^+] + M[H^+][H_2O_2] + N[H^+][H_2O_2]^2} + \frac{[W(VI)][H^+]^2[H_2O_2]^2[CP]}{P + Q[H^+] + S[H^+][H_2O_2] + T[H^+][H_2O_2]^2} \quad (4.12)$$

where

$$J = \frac{1}{k_1K_1K_2K_3}, \quad L = \frac{1}{k_1K_2K_3}, \quad M = \frac{1}{k_1K_3}, \quad N = \frac{1}{k_1}, \quad P = \frac{1}{k_2K_1K_2K_3K_4} = \sigma J,$$

$$Q = \frac{1}{k_2K_2K_3K_4} = \sigma L, \quad S = \frac{1}{k_2K_3K_4} = \sigma M, \quad T = \frac{1}{k_2K_4} = \sigma N \quad (\sigma = \frac{k_1}{k_2K_4}).$$

Then Eq. (4.12) becomes

$$R_{0cat} = \frac{\sigma[W(VI)][H^+][H_2O_2]^2[CP] + [W(VI)][H^+]^2[H_2O_2]^2[CP]}{P + Q[H^+] + S[H^+][H_2O_2] + T[H^+][H_2O_2]^2} \tag{4.13}$$

At constant $[H_2O_2]$ and $[H^+]$, R_{0cat} should be proportional to [W(VI)] and [CP] as shown in the experimentally observed Eq. (4.2), with u given by

$$u = \frac{\sigma[H^+][H_2O_2]^2 + [H^+]^2[H_2O_2]^2}{P + Q[H^+] + S[H^+][H_2O_2] + T[H^+][H_2O_2]^2} \tag{4.14}$$

Assuming that under the experimental conditions $S[H^+][H_2O_2] << P + Q[H^+] + T[H^+][H_2O_2]^2$, Eq. (4.13) becomes

$$R_{0cat} = \frac{(\sigma[H^+][CP] + [H^+]^2[CP])[W(VI)][H_2O_2]^2}{P + Q[H^+] + T[H^+][H_2O_2]^2} \tag{4.13}'$$

At constant [CP] and $[H^+]$, Eq. (4.13)' is of the same form as the experimentally observed Eq. (4.3) with

$$v = \frac{P + Q[H^+]}{\sigma[H^+][CP] + [H^+]^2[CP]} \tag{4.15}$$

$$x = \frac{T}{\sigma[CP] + [H^+][CP]} \tag{4.16}$$

At constant $[H_2O_2]$ and [CP], Eq. (4.13) is of the same form as the experimentally observed Eq. (4.4) with

$$y = \frac{P}{[H_2O_2]^2[CP]} \tag{4.17}$$

$$z = \frac{Q + S[H_2O_2] + T[H_2O_2]^2}{[H_2O_2]^2[CP]} \tag{4.18}$$

Values for the P, Q, S and T calculated from the experimental values of u, v, x, y and z are 1.5×10^{-9} mol^5 l^{-5} s, 5.3×10^{-9} mol^4 l^{-4} s, 7.5×10^{-7} mol^3 l^{-3} s and 1.0×10^{-3} mol^2 l^{-2} s, respectively. In order to check the validity of the proposed reaction

mechanism, the k_{app} values calculated by inserting these values together with each experimental reaction condition into the equation (4.13) were compared with the experimental values. As shown in Figs. 4.6, 4.7 and 4.9, the plots of the calculated k_{app} values fall on the plots of the experimental values. R_{0cat} for 100 μg l^{-1} (= 4.5 × 10^{-7} mol l^{-1} in the reaction mixture) tungsten(VI) was also calculated according to Eq. (4.13). The R_{0cat} was transformed to R_{0cat}' by multiplying by ε (5.6× 10^3 l mol^{-1} cm^{-1}). The R_{0cat}' are shown as dotted lines in Figs. 4.3 - 4.5. Plots of experimental R_{0cat}, which are the difference between the initial reaction rates in the presence of tungsten(VI) and in its absence, fall on the dotted line in the CP and hydrogen peroxide concentration ranges examined (Figs. 4.3 and 4.5). Although the ionic strength varies with the variation of sulfuric acid concentration, at 0.42 mol l^{-1} sulfuric acid where the ionic strength is 0.43 mol l^{-1}, the plot of the experimental R_{0cat} value falls just on the dotted line. The kinetic investigation of the reaction system is available to estimate the optimum conditions for the determination of the trace amounts of tungsten(VI). These values of P, Q, S and T also established the validity of the assumption made earlier that $S[H^+][H_2O_2] << P+Q[H^+]+T[H^+][H_2O_2]^2$ even at 0.43 mol l^{-1} hydrogen ion and 0.0010 mol l^{-1} hydrogen peroxide (the highest and the lowest concentrations of the investigated range, respectively).

4.3.4 Calibration graphs and reproducibility

A series of standard solutions of tungsten(VI) was treated as in the recommended procedure. The calibration graphs were linear up to 10 mg l^{-1} tungsten(VI); at higher concentration than 30 mg l^{-1} a white precipitate appeared. The equation of the line is R_0 [$=\Delta$(abs.)/Δ(s)] = 2.0×10^{-5}[W(VI)] + 3.1×10^{-4} and the correlation coefficient is r = 0.999 (n=6). The relative standard deviations for 10 replicate determinations of 5, 10 and 60 μg l^{-1} of tungsten(VI) are 6.8, 6.0 and 0.8%, respectively; it is 13.9% at 2 μg l^{-1} (n = 10), which can be considered as the lower limit of the determination. Tungsten(VI) in the wide concentration range, 2 μg l^{-1} - 10 mg l^{-1}, can be determined by the proposed method with good reproducibility.

4.3.5 Effect of foreign ions

The effect of various ions on the determination of 60 μg l^{-1} tungsten(VI) was examined. The following ions showed no interference at the concentrations (mg l^{-1}) shown in parentheses: SO_4^{2-} (4000); Na^+,K^+, Cl^- (2000); Ca^{2+}, NH_4^+ (1000); Mg^{2+}, CO_3^{2-} (500); Li^+, Cd^{2+}, Ce^{3+}, Ce^{4+}, Zn^{2+}, Mn^{2+}, Cu^{2+}, Co^{2+}, Ni^{2+}, Sn(IV), Sr^{2+}, As(III), As(V), Br^-, CH_3COO^-, $S_2O_3^{2-}$, ClO_3^-, ClO_4^-, SO_3^{2-}, PO_4^{3-} (100); Pb^{2+}, Cr^{3+}, SCN^-, Sb(III) (10); Ag^+, Sn^{2+}, V(V), Cr(VI), I^-, NO_2^-, BrO_3^- (1). The interfering ions are listed in Table 4.1. Ions which are known to participate in redox reaction as either oxidizing or reducing agents cause serious interference. These ions showed no interference at concentrations one order magnitude lower than those indicated in Table 4.1.

Table 4.1

Effect of interfering ions on the determination of 60 μg l^{-1} of tungsten(VI)

Ion added	μg l^{-1}	W(VI) found/μg l^{-1}
IO_3^-	1000	87
Ba^{2+}	1000	102
Mo(VI)	100	95
Fe^{2+}	1000	66[a]
Fe^{2+}	100	71
Fe^{3+}	1000	66[a]
Fe^{3+}	100	67

a. As a masking agent, an 8.2×10^{-3} mol l^{-1} EDTA was added.

4.3.6 Elimination of the interference of iron(II) for tungsten(VI) determination

As shown in Table 4.1, iron(II) showed serious interference in the determination of tungsten(VI). In order to eliminate the interference of iron, EDTA was used as a masking agent. The influence of EDTA for this reaction system was examined in the range of 4.0×10^{-3} - 2.0×10^{-2} mol l^{-1}. The R_0 value of the uncatalyzed reaction remained constant over this concentration range. The sensitivity remained constant up to 8.2×10^{-3} mol l^{-1} EDTA and, over the higher concentration range, the sensitivity decreased with increase in the EDTA concentration. An EDTA concentration of 8.2×10^{-3} mol l^{-1} was selected. In the absence of EDTA R_0 for both catalyzed and uncatalyzed reactions increased with increasing iron(II) concentration, while in the presence of 8.2×10^{-3} mol l^{-1} EDTA, iron(II) had no effect on either the catalyzed or uncatalyzed reactions up to 0.9 mg l^{-1} iron. Any interference from iron(III) could also be avoided by the addition of EDTA.

4.3.7 Determination of tungsten(VI) in hot spring water samples

In order to test the reliability of the present method, it was applied to the determination of tungsten(VI) in hot spring water samples. The determinations were made by using samples diluted at different times. The method was also checked by adding a known amount of tungsten(VI) to the samples. The results are shown in

Table 4.2. The values corrected for dilution showed good agreement, and good recoveries of added tungsten(VI) were obtained ranging from 94 to 106% (mean 100%).

Table 4.2

Determination of tungsten(VI) in hot spring water samples

Sample	Dilution (times)	Added ($\mu g\ l^{-1}$)	Found ($\mu g\ l^{-1}$)	Recovery (%)	In sample ($\mu g\ l^{-1}$)
Hot spring	-	-	11.9	-	11.9
water I	2	-	5.9	-	11.8
	2	5	10.6	97	-
	2	10	14.9	94	-
	5	-	2.5	-	12.5
	5	5	7.6	101	-
	5	10	13.3	106	-
				ave.	12.1
Hot spring	-	-	63.9	-	63.6
water II	2	-	32.2	-	64.4
	2	5	38.4	103	-
	2	10	43.3	103	-
	5	-	13.3	-	66.5
	5	5	18.1	99	-
	5	10	23.1	99	-
				ave.	64.8

Chapter 5

Kinetic-Mechanistic Study of the Chlorpromazine-Hydrogen Peroxide Reaction Catalyzed by Molybdenum(VI) and Tungsten(VI), and Their Differential Determination

5.1 Introduction

By kinetic catalytic method, mixtures of closely related species acting as catalysts for a given reaction also could be determined differentially without prior separation, if the reaction conditions are manipulated so that the kinetic dependence on each catalyst differ significantly.

As described in Chapter 4, the author has established a kinetic- spectrophotometric method for the determination of trace amounts of tungsten(VI) based on its catalytic effect on the oxidation of CP by hydrogen peroxide in acidic solution [23]. This reaction was also catalyzed by traces of molybdenum(VI) and, hence, the presence of this species caused serious interference for the determination of tungsten(VI). The results of preliminary experiments of the molybdenum(VI)- and tungsten(VI)-catalyzed reactions revealed that there were sufficient kinetic differences between two reactions. These differences can be used to the determination of both species without a prior separation.

The aim of this work is to develop a method for the differential determination of traces of molybdenum(VI) and tungsten(VI) based on their different kinetic effects on initial

rates. Although the interdependence of reaction variables in kinetic methods is commonly rather complicated, the rate equation permits accurate prediction of the behavior of the reaction over a wide range of reaction conditions. Hence the use of rate equations is the most favorable for systematically finding optimum conditions for differential determinations. Kinetic and mechanistic investigations were made to derive the rate equations of both catalyzed reactions.

5.2 Experimental

5.2.1 Apparatus and reagents

Spectrophotometer for measuring the absorbance, a circulating thermostat bath and magnetic stirrer used were the same as those described in Chapter 2.

Commercially available molybdenum(VI) and tungsten(VI) standard solutions (1000 mg l^{-1}) were obtained from Wako Chemical Co. Working solutions were prepared by diluting these solutions with water.

A hydrochloric acid (2.85 mol l^{-1}) solution was prepared by diluting a distilled hydrochloric acid (6.0 mol l^{-1}) with water.

Other chemicals used were the same as described in Chapter 2.

5.2.2 Kinetic measurements

The kinetic investigation of the molybdenum(VI) and tungsten(VI) catalyzed sulfoxide formation reaction was carried out

as described as in Section 4.3.3. The ionic strength was maintained constant at 0.12 mol l^{-1} by the addition of sodium chloride.

5.2.3 Recommended procedure for differential determination of molybdenum(VI) and tungsten(VI)

To 10.0 ml of sample solution in a glass-stoppered tube, 0.50 ml of 2.85 mol l^{-1} hydrochloric acid and 0.50 ml of 0.019 mol l^{-1} CP were added and thoroughly mixed. This solution was kept in a water bath at 40°C. A 1.9 ml aliquot was taken into a quartz cell. The cell was placed in the holder at 40°C and the solution was magnetically stirred. The reaction was initiated by the injection of 0.10 ml of 1.92×10^{-2} mol l^{-1} hydrogen peroxide (40°C). The increase in absorbance at 344 nm of the product was recorded against a CP solution as reference (8.2×10^{-4} mol l^{-1}) and the initial slope of the reaction rate curves, R_{0S}'[=Δ(abs.)/Δ(s)], was measured. Another 1.9 ml aliquot was taken into a quartz cell from the combination prepared above. The reaction was initiated by the injection of 0.10 ml of 7.6×10^{-2} mol l^{-1} hydrogen peroxide and the initial reaction rate, R_{0D}', was measured in the same manner as described above. The two R_0' values thus obtained for a sample were used as parameters for the differential determination of molybdenum(VI) and tungsten(VI). (R_0' and k_{app}' denote the initial reaction rate and the rate constant based on absorbance change, respectively.)

5.3 Results and Discussion

5.3.1 Kinetics of molybdenum(VI) catalyzed sulfoxide formation reaction between CP and hydrogen peroxide

The kinetic investigation of the molybdenum(VI) catalyzed sulfoxide formation reaction was carried out by the initial-rate method in 0.12 mol l^{-1} hydrochloric acid. All concentrations given in the figures are the initial concentrations in the reaction mixture at the initiation of the reaction. In order to determine the dependence of R_0 upon the molybdate concentration, a series of experiments was performed in which the molybdate concentration was varied while the CP, hydrogen ion and hydrogen peroxide concentrations were held constant. The plots of R_0 versus the total analytical concentration of molybdate [Mo(VI)] were linear in the range of 0 - 1.2×10^{-6} mol l^{-1} molybdate (Fig. 5.1). It was established that the molybdate-catalyzed reaction was first order in molybdate:

$$R_0 = k_{appM}[\text{Mo(VI)}]+a \qquad (5.1)$$

where k_{appM} is the apparent rate constant and a is the intercept on the ordinate which corresponds to the rate of an uncatalyzed reaction. The k_{appM} values were determined at different CP concentrations in the range 1.6×10^{-4} - 8.2×10^{-4} mol l^{-1}. As can be seen in Fig. 5.2a, a straight line obtained by plotting k_{appM} versus CP concentration shows that the relation is given by $k_{appM} = u[\text{CP}]$, where u is the slope of the line. Thus the initial rate of the catalyzed reaction,

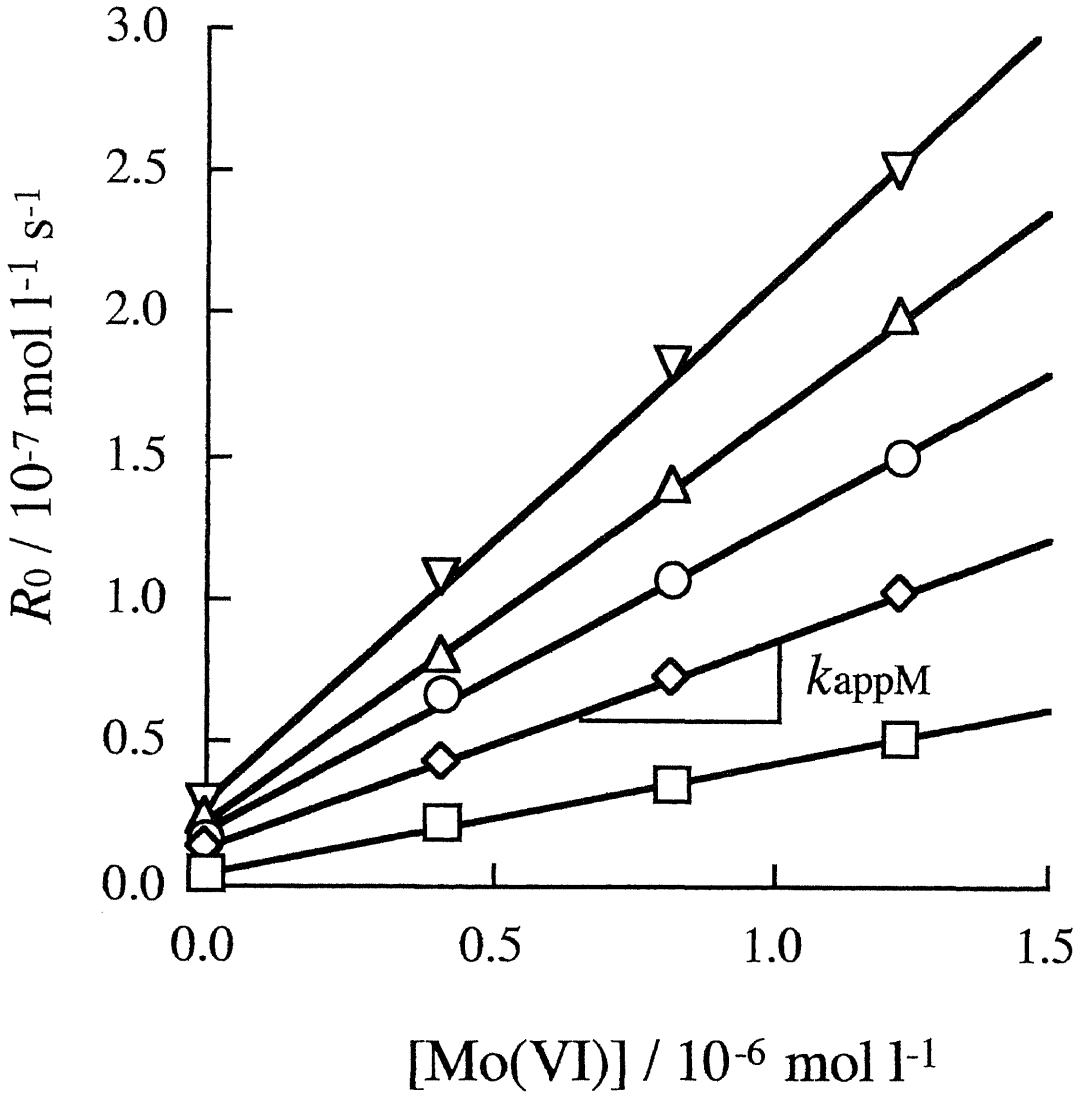

Fig. 5.1 Dependences of initial reaction rate R_0 upon molybdenum (VI) concentration . Conditions: 0.12 mol l^{-1} hydrogen ion, 2.0×10^{-3} mol l^{-1} hydrogen peroxide and CP ($\times10^{-4}$ mol l^{-1}); (□) 1.6, (◇) 3.3, (○) 4.9, (△) 6.5, (▽) 8.2. , 40℃.

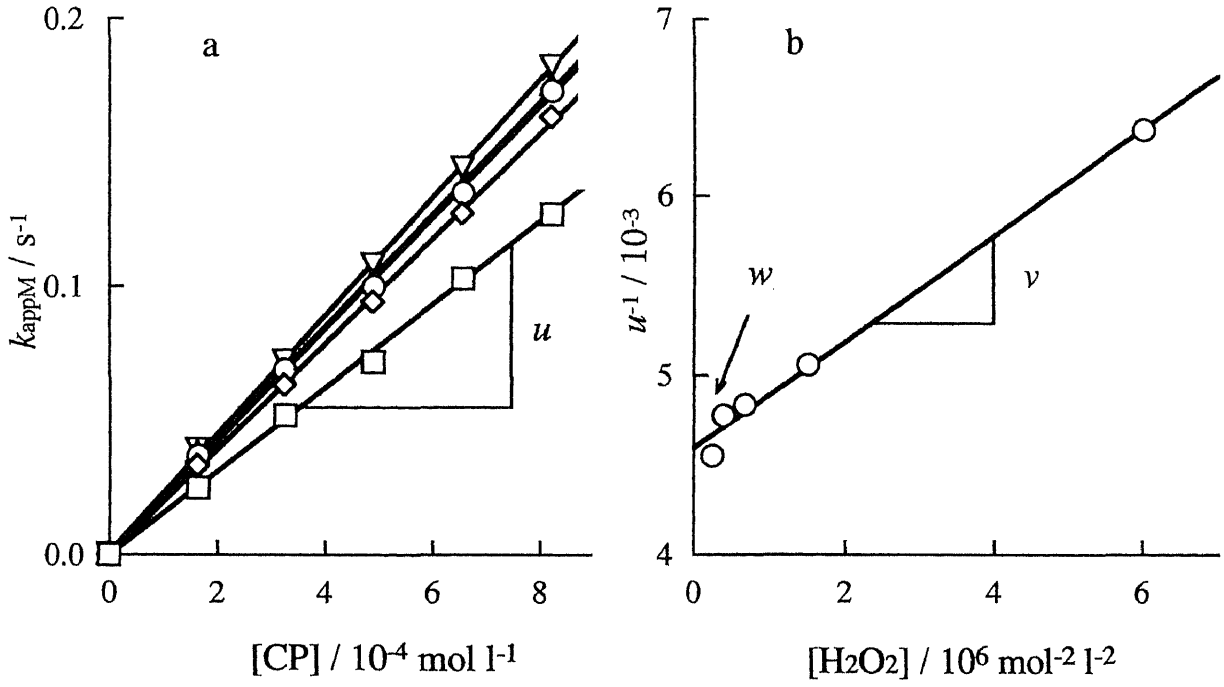

Fig. 5.2 Dependences of apparent rate constant k_{appM} upon CP concentration (a) and its slope upon hydrogen peroxide concentration (b). Conditions:(a) concentrations of hydrogen peroxide($\times 10^{-3}$ mol l^{-1}): (□) 0.4, (◇) 0.8, (○) 1.2, (△) 1.6, (▽) 2.0. Other conditions are as in Fig. 5.1.

$$R_{0catM} = R_0 - a,$$

is given by:

$$R_{0catM} = u[CP][Mo(VI)] \qquad (5.2)$$

The dependence of u upon hydrogen peroxide concentration was determined at constant hydrogen ion concentrations. The linearity of plots of $1/u$ versus $1/[H_2O_2]^2$, as shown in Fig. 5.2b, leads to the following kinetic relation:

$$R_{0catM} = \frac{[H_2O_2]^2[CP][Mo(VI)]}{v + w[H_2O_2]^2} \qquad (5.3)$$

where v is the slope of the line and w is the intercept on the ordinate, and their values are 3.35×10^{-10} $mol^3\ l^{-3} s$ and 4.59×10^{-3} $mol\ l^{-1}\ s$, respectively. This kinetic behavior of hydrogen peroxide suggests the formation of a complex of molybdate with hydrogen peroxide.

The dependence of k_{appM} upon hydrogen ion concentration was determined at constant CP and hydrogen peroxide concentrations and the results are shown in Fig. 5.3. The linearity of plots of $1/k_{appM}$ versus $1/[H^+]$ leads to the following relation:

$$R_{0catM} = \frac{[H^+][Mo(VI)]}{\beta + \alpha[H^+]} \qquad (5.4)$$

where α is the intercept on ordinate and β is the slope of the line. This kinetic behavior of hydrogen ion suggests the protonation of molybdate.

Before mechanisms are discussed, consideration must be given to the species actually present in the reaction mixtures. Although molybdate exists as the mononuclear oxoanion, MoO_4^{2-}, in alkaline

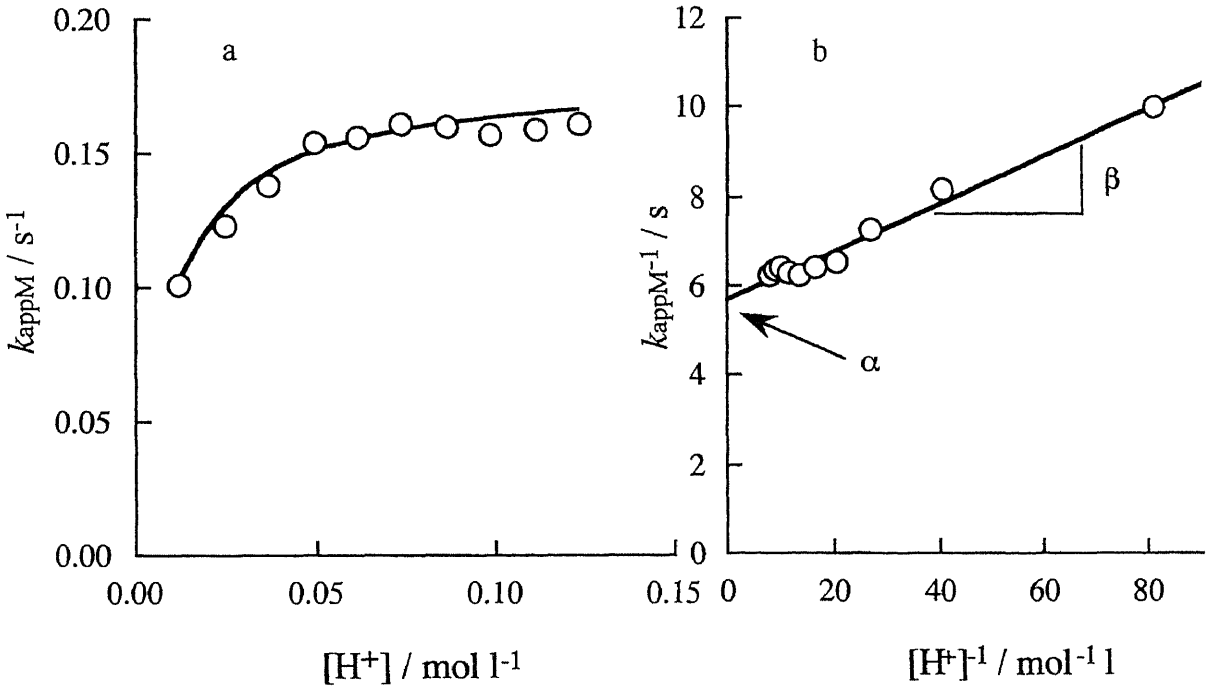

Fig. 5.3 Dependence of apparent rate constant k_{appM} upon hydrogen ion concentration. Conditions: 1.0×10^{-3} mol l^{-1} hydrogen peroxide, 8.2×10^{-4} mol l^{-1} CP, 40℃, ionic strength 0.12 mol l^{-1}.

solution, it is condensed to polynuclear complexes as pH is lowered. However, the condensation of molybdate in the present solutions can be considered to be negligible in accord with the following facts: (i) The reaction is first order with respect to molybdate. If the reaction sequence involves the formation of polynuclear species of molybdate, then a higher kinetic order or rather complex dependence upon molybdate concentration should be observed. (ii) The concentration of molybdate in the present solutions is so small ($<1\times 10^{-6}$ mol l^{-1}), that the formation of polynuclear species is less favorable; it was suggested that condensation of molybdate at low concentrations ($<1\times10^{-4}$ mol l^{-1}) was negligible even in acidic solution (0.05 mol l^{-1}) [38].

Mononuclear molybdate also exists in three states, H_2MoO_4, $HMoO_4^-$ and MoO_4^{2-} in equilibrium, with stepwise ionization constants K_{a1} and K_{a2}. Using the reported values of $K_{a1} = 2.19\times 10^{-4}$ mol l^{-1} and $K_{a2} = 2.57\times 10^{-4}$ mol l^{-1} [37], the ratios of $[HMoO_4^-]/[MoO_4^{2-}]$ and $[H_2MoO_4]/[MoO_4^{2-}]$ at 0.012 mol l^{-1} H^+ (the lowest concentration of the investigated range) were calculated to be 47.9 and 2.56×10^3, respectively. The species MoO_4^{2-} and $HMoO_4^-$ are thus negligible and almost all the molybdate exists as H_2MoO_4.

A mechanism which is consistent with the rate measurements described above is:

$$H^+ + H_2O_2 \rightleftarrows (H_2O_2\text{-}H)^+ \quad \text{(rapid, } K_1\text{)} \tag{5.5}$$

$$H_2MoO_4 + (H_2O_2\text{-}H)^+ \rightleftarrows (H_2MoO_4\text{-}H_2O_2\text{-}H)^+ \text{ (rapid, } K_2\text{)} \tag{5.6}$$

$$(H_2MoO_4\text{-}H_2O_2\text{-}H)^+ + H_2O_2 \rightleftarrows \{H_2MoO_4\text{-}(H_2O_2)_2\text{-}H\}^+$$

(rapid, K_3) (5.7)

$$\{H_2MoO_4\text{-}(H_2O_2)_2\text{-}H\}^+ + CP \rightarrow CP{=}O^{2+} + H_2MoO_4 + 2H_2O + OH^-$$

(rate determining, k) (5.8)

$$OH^- + H^+ \rightleftarrows H_2O \quad \text{(rapid)} \tag{5.9}$$

The formation of the sulfoxide proceeds through the pathway shown by Eq. (5.8). The rate equation implied by this sequence,

$$\frac{d[CP{=}O^{2+}]}{dt} = k[\{H_2MoO_4\text{-}(H_2O_2)_2\text{-}H\}^+][CP]$$

combined with the expression for total analytical concentration of molybdate:

$$[Mo(VI)]=[H_2MoO_4]+[(H_2MoO_4\text{-}H_2O_2\text{-}H)^+]+[\{H_2MoO_4\text{-}(H_2O_2)_2\text{-}H\}^+]$$

from which

$$[H_2MoO_4] = \frac{[Mo(VI)]}{1 + K_1K_2[H_2O_2][H^+] + K_1K_2K_3[H_2O_2]^2[H^+]}$$

leads to

$$R_{0catM} = \frac{kK_1K_2K_3[Mo(VI)][H^+][H_2O_2]^2[CP]}{1 + K_1K_2[H_2O_2][H^+] + K_1K_2K_3[H_2O_2]^2[H^+]} \tag{5.10}$$

Then Eq. (5.10) becomes

$$R_{0catM} = \frac{[Mo(VI)][H^+][H_2O_2]^2[CP]}{P + Q[H^+][H_2O_2] + S[H^+][H_2O_2]^2} \tag{5.11}$$

where

$$P = \frac{1}{kK_1K_2K_3}, \quad Q = \frac{1}{kK_3}, \quad S = \frac{1}{k}.$$

At constant $[H_2O_2]$ and [CP], Eq. (5.11) is of the same form as the experimentally observed Eq. (5.4), with β and α given by

$$\beta = \frac{P}{[H_2O_2]^2[CP]} \qquad (5.12)$$

and

$$\alpha = \frac{Q}{[H_2O_2][CP]} + \frac{S}{[CP]} \qquad (5.13)$$

Assuming that under the experimental conditions $Q[H_2O_2][H^+] << P + S[H_2O_2]^2[H^+]$, Eq. (5.11) becomes

$$R_{0catM} = \frac{[Mo(VI)][H^+][H_2O_2]^2[CP]}{P + S[H^+][H_2O_2]^2} \qquad (5.14)$$

At constant $[H^+]$, Eq. (5.14) is of the same form as the experimentally observed Eq. (5.3) with

$$v = \frac{P}{[H^+]} \qquad (5.15)$$

and

$$w = S \qquad (5.16)$$

Values for the P, Q and S obtained from experimental values of α, β, v and w are 4.12×10^{-11} mol^4 l^{-4} s, 6.24×10^{-8} mol^2 l^{-2} s and 4.59×10^{-3} mol l^{-1} s, respectively. These values of P, Q and S also established the validity of the assumption made earlier that $Q[H_2O_2][H^+] << P + S[H_2O_2]^2[H^+]$ even at 0.12 mol l^{-1} hydrogen ion and 4.1×10^{-4} mol l^{-1} hydrogen peroxide (the highest and the lowest concentrations in the investigated range, respectively). The calculated k_{appM} values are shown as solid line in Fig. 5.3a. The plots of the experimental k_{appM} values marked ○ fell just on the line. Since the calculated k_{appM} values agreed closely with the experimental values over the investigated reactant concentration range, the proposed mechanism is considered to be favorable.

5.3.2 Kinetics of the tungsten(VI)-catalyzed sulfoxide formation reaction

The kinetic behavior of the tungsten catalyzed reaction has been examined in sulfuric acid medium in detail in Chapter 4 [22]. In this study, a mechanism has been proposed which satisfies the experimental observations. The following rate equation was derived from the proposed mechanism:

$$R_{0catT} = \frac{(\sigma[H^+] + [H^+]^2)[CP][W(VI)][H_2O_2]^2}{P + Q[H^+] + S[H^+][H_2O_2] + T[H^+][H_2O_2]^2} \qquad (5.17)$$

Since the third term in the denominator in Eq. (5.17), $S[H^+][H_2O_2]$, is very small compared to the other terms even at relatively high hydrogen ion and low hydrogen peroxide concentrations, this term can be negligible from the equation. Thus, at constant $[H^+]$, Eq. (5.17) reduced to:

$$R_{0catT} = \frac{[CP][H_2O_2]^2[W(VI)]}{y + z[H_2O_2]^2} \qquad (5.18)$$

with

$$y = \frac{P + Q[H^+]}{\sigma[H^+] + [H^+]^2} \text{ and } z = \frac{T[H^+]}{\sigma[H^+] + [H^+]^2}.$$

At the constant CP and hydrogen peroxide concentrations, Eq. (5.18) reduces further to:

$$R_{0catT} = k_{appT}[W(VI)] \qquad (5.19)$$

where

$$k_{appT} = \frac{[CP][H_2O_2]^2}{y + z[H_2O_2]^2} \qquad (5.20)$$

In order to systematically determine the optimum conditions for the differential determination by using the rate equations, the

kinetics of tungsten-catalyzed reaction were reinvestigated at a constant hydrochloric acid concentration of 0.12 mol l^{-1} for the same reactant concentration ranges and in the same manner as those for molybdenum(VI). The same rate equation as the simplified equation, Eq. (5.18) was thus obtained and the experimental values of y and z were 2.74×10^{-9} mol^3 l^{-3} s and 1.99×10^{-3} mol l^{-1} s, respectively.

5.3.3 Selection of reaction conditions for the differential determination of molybdenum(VI) and tungsten(VI)

It is expected from the results of kinetic studies that k_{appT} increases with an increase in hydrogen ion concentration [23], whereas the k_{appM} does not change significantly at the higher hydrogen ion concentration range. Thus at higher hydrogen ion concentrations the difference between k_{appM} and k_{appT} would become larger, which may be favorable for the differential determination. However, the higher the concentration of hydrogen ion the faster the uncatalyzed reaction. Moreover, a fixed hydrogen ion concentration is practically favorable since the kinetic parameters for the differential determination, R_0's and $R_{0'D}$, can be obtained from a single reaction combination (the mixture of sample, CP and hydrochloric acid) simply by changing the concentration of hydrogen peroxide as a initiator of the reaction. A hydrogen ion concentration of 0.12 mol l^{-1} was, thus selected for the further investigation.

The dependence of R_0 upon molybdenum(VI) and tungsten(VI)

concentrations at 0.12 mol l^{-1} hydrochloric acid were given by

$$R_0 = k_{appM}[Mo(VI)]+a \quad (5.1)$$

with

$$k_{appM} = \frac{[H_2O_2]^2[CP]}{3.35\times10^{-10}+4.59\times10^{-3}[H_2O_2]^2} \quad (5.21)$$

and

$$R_0 = k_{appT}[W(VI)]+a \quad (5.19)$$

with

$$k_{appT} = \frac{[H_2O_2]^2[CP]}{2.74\times10^{-9}+1.99\times10^{-3}[H_2O_2]^2} \quad (5.22)$$

(at 40℃ and I = 0.12 mol l^{-1}) where k_{appM} and k_{appT} are essentially constant under the given conditions, because $[H_2O_2]$ and [CP] remain almost constant in the early stage of the reaction. Hence, it is clear from Eqs. (5.21) and (5.22) that the use of the initial reaction rate as a parameter gives linear calibration graphs with the slope of the k_{appM} and k_{appT} values. Thus the total concentration of tungsten(VI) and molybdenum(VI) can be determined under the conditions in which $k_{appM} = k_{appT}$. Figure 5.4 shows the variation in the calculated k_{appM} and k_{appT} values according to Eqs. (5.21) and (5.22), respectively, by changing the concentrations of CP and hydrogen peroxide, with contour lines drawn at intervals of 0.05 s^{-1} of k_{app}. The k_{appT} values increase with an increase in hydrogen peroxide concentration, whereas k_{appM} shows no significant change over the concentration range used for the calculation. Both k_{appM} and k_{appT} increase with an increase in CP concentration and therefore the higher the CP concentration, the higher the sensitivity. However, the higher CP concentrations are not very

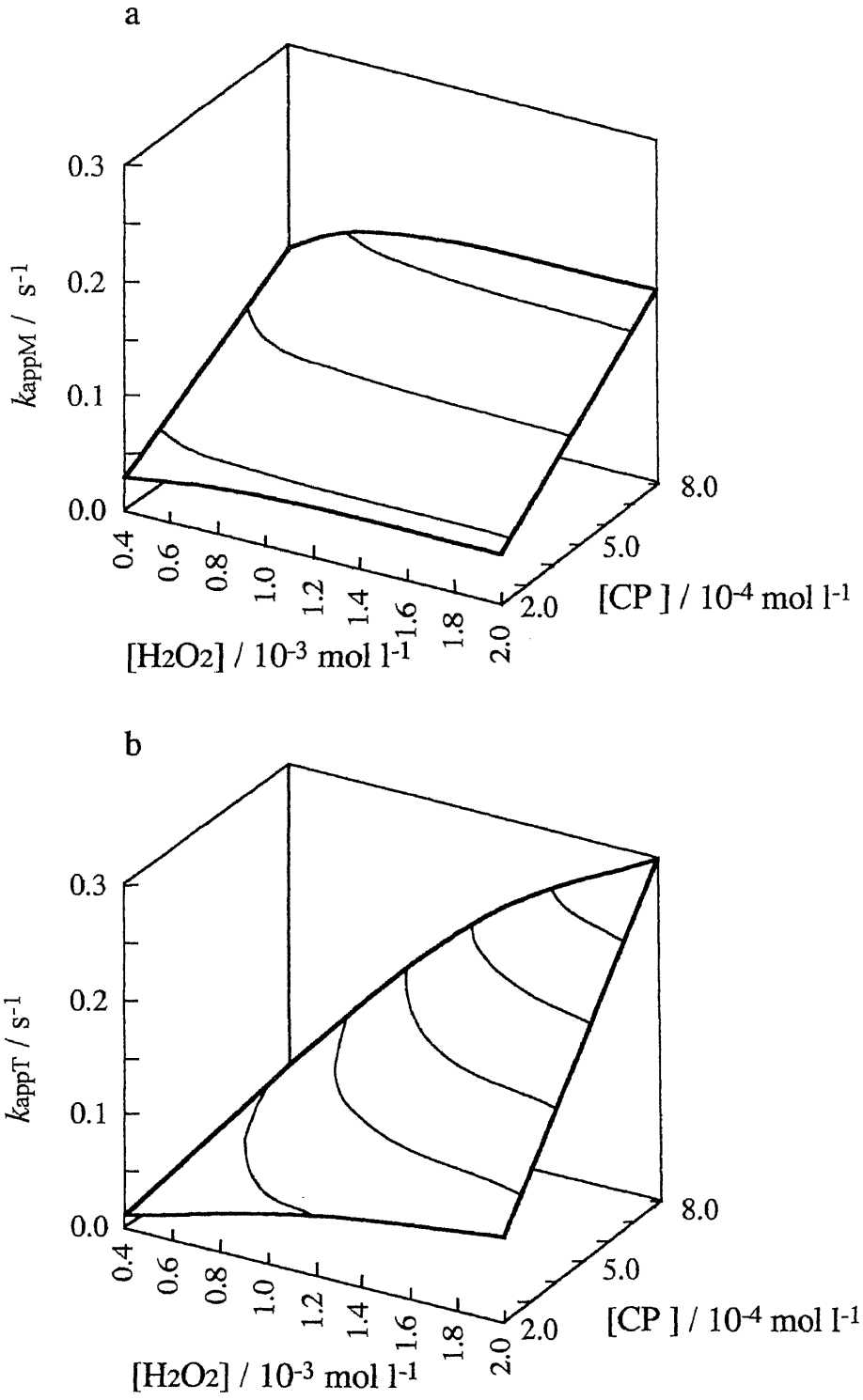

Fig. 5.4 Variation in the calculated k_{appM} (a) and k_{appT} (b) values according to Eqs. (5.21) and (5.22), respectively, by changing the concentrations of CP and hydrogen peroxide.

favorable because CP has significant absorption at 344 nm [23]. A CP concentration of 8.2×10^{-4} mol l^{-1} was selected.

The dependence of k_{appM} (curve I) and k_{appT} (curve II) on hydrogen peroxide concentration at 8.2×10^{-4} mol l^{-1} CP is shown in Fig. 5.5. At higher hydrogen peroxide concentrations, tungsten(VI) acts as an effective catalyst than molybdenum(VI), while the molybdenum(VI) acts as an effective catalyst at lower hydrogen peroxide concentrations. Based on this kinetic difference, mixtures of molybdenum(VI) and tungsten(VI) can be analyzed by two rate equations, one for the conditions under which the reaction catalyzed by tungsten(VI) takes place preferentially and the other corresponding to the conditions favoring the catalytic effect of molybdenum(VI). Although the difference between the rate of their catalyzed reactions increased with an increase in hydrogen peroxide concentration, higher concentrations were not very favorable, because the reaction rate of the uncatalyzed reaction becomes progressively higher as the hydrogen peroxide concentration is raised. Thus a hydrogen peroxide concentration of 3.8×10^{-3} mol l^{-1} was selected, since the k_{appM} / k_{appT} values do not change significantly above 3.0×10^{-3} mol l^{-1}. Provided that the reaction rates for the two catalysts are independent of each other, the overall initial rate under this condition for the mixture (R_{0D}) is given by:

$$R_{0D} = k_{appM}[\mathrm{Mo(VI)}] + k_{appT}[\mathrm{W(VI)}] + a_D, \qquad (5.23)$$

where a_D is the uncatalyzed reaction rate at 3.8×10^{-3} mol l^{-1} hydrogen peroxide.

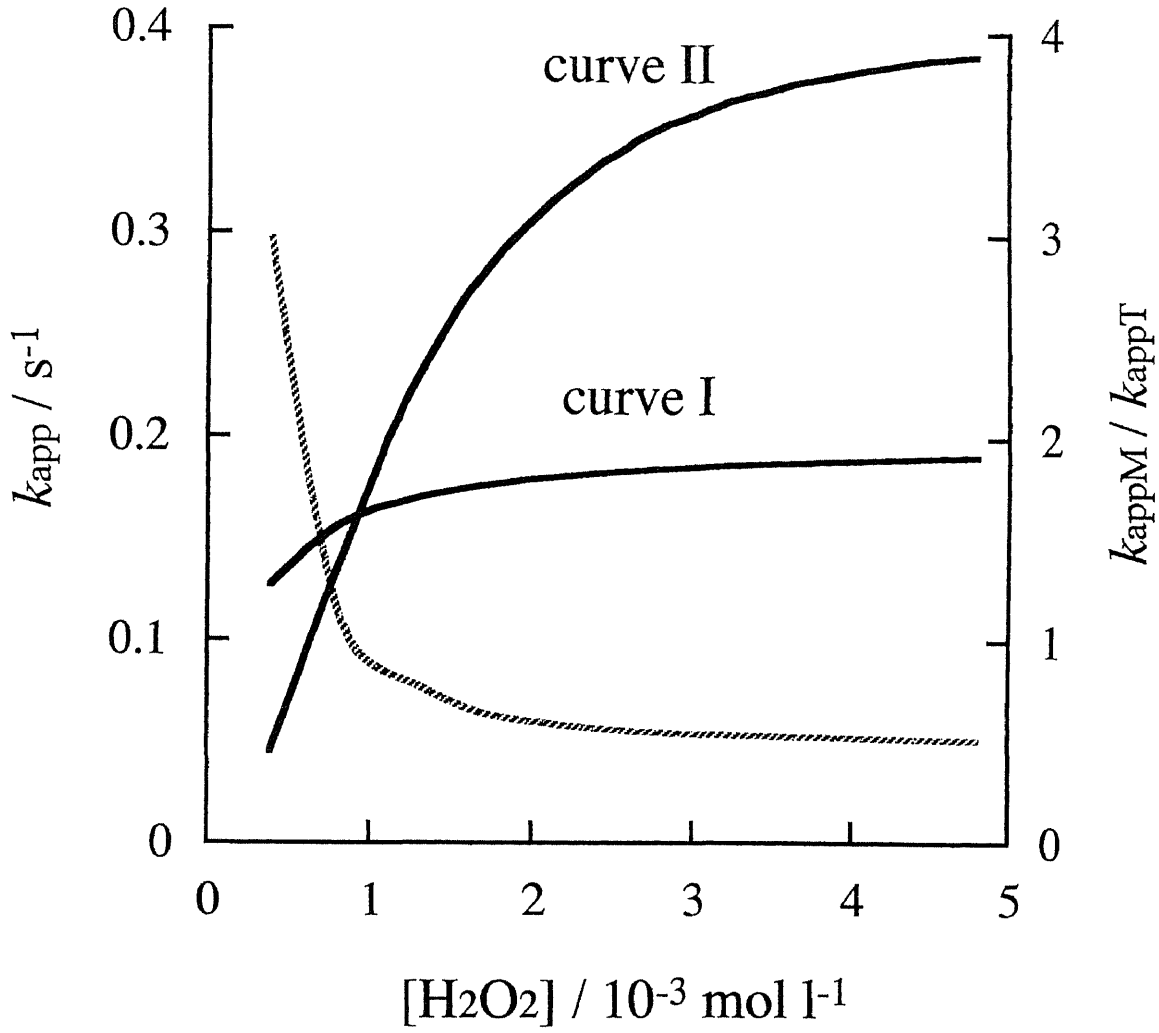

Fig. 5.5 Variation in the calculated k_{appM} (curve I) and k_{appT} (curve II) values according to Eqs. (5.21) and (5.22), respectively, by changing the concentration of hydrogen peroxide. The dotted line shows k_{appM} / k_{appT}.

It is also desirable to select a condition favorable for the catalytic effect of molybdenum(VI), but under such conditions both k_{app} values are rather small so that the selection of such a condition made it difficult to carry out an accurate measurement of the reaction rate. As can be seen in Fig. 5.5, the curves of k_{appM} and k_{appT} intersect at 9.6×10^{-4} mol l^{-1} hydrogen peroxide, where molybdenum(VI) and tungsten(VI) would have the same catalytic effect, and hence the sum of the concentrations of both catalysts are determinable. Thus a hydrogen peroxide concentration of 9.6×10^{-4} mol l^{-1} was selected, at which the initial rate for the mixture (R_{0S}) is given by:

$$R_{0S} = k_s([\mathrm{Mo(VI)}]+[\mathrm{W(VI)}]) + a_S \qquad (5.24)$$

where $k_s = k_{appM} = k_{appT}$ and a_S is the uncatalyzed reaction rate for 9.6×10^{-4} mol l^{-1} hydrogen peroxide.

Solving Eqs. (5.23) and (5.24) gives [Mo(VI)] and [W(VI)], that is,

$$[\mathrm{Mo(VI)}] = \frac{k_S(R_{0D} - a_D) - k_{appT}(R_{0S} - a_S)}{k_S(k_{appM} - k_{appT})} \qquad (5.25)$$

$$[\mathrm{W(VI)}] = \frac{k_{appM}(R_{0S} - a_S) - k_S(R_{0D} - a_D)}{k_S(k_{appM} - k_{appT})} \qquad (5.26)$$

In order to determine the k_{appM}', k_{appT}', k_s', a_S' and a_D' values, a series of standard solutions of molybdenum(VI) and tungsten(VI) was treated independently by the recommended procedure. At 3.8×10^{-3} mol l^{-1} hydrogen peroxide, the plots of the initial rates (R_{0D}') versus the molybdenum(VI) and tungsten(VI) concentrations gave separate straight lines with the same intercept for each of two species. From the slope a k_{appM}' value of 8.23×10^{2}

abs.s^{-1} mol^{-1} l and $k_{appT'}$ value of 1.80×10^{3} abs.s^{-1} mol^{-1} l were evaluated and from the intercept the value of $a_{D'}$ was found to be 1.64×10^{-4} abs.s^{-1}. At 9.6×10^{-4} mol l^{-1} hydrogen peroxide concentration, both the plots of the initial rates ($R_{0S'}$) versus the molybdenum(VI) or tungsten(VI) concentrations agreed well with each other. From the slope and intercept a $k_{s'}$ value of 7.25×10^{2} abs.s^{-1} mol^{-1} l and $a_{S'}$ value of 1.56×10^{-4} abs.s^{-1}, respectively, were obtained. Insertion of these values into Eqs. (5.25) and (5.26) the following equations are given:

$$[Mo(VI)] = 2.54\times 10^{-3}\, R_{0S'} - 1.02\times 10^{-3}\, R_{0D'} - 2.28\times 10^{-7} \quad (5.27)$$

$$[W(VI)] = 1.02\times 10^{-3}\, R_{0D'} - 1.16\times 10^{-3}\, R_{0S'} + 1.34\times 10^{-8} \quad (5.28)$$

By using these equations the concentrations of molybdenum(VI) and tungsten(VI) in mixtures can be calculated.

5.3.4 Differential determination of molybdenum(VI) and tungsten(VI)

Molybdenum(VI) and tungsten(VI) were determined by using mixed solutions containing known amounts of molybdenum(VI) and tungsten(VI). Their concentrations in the mixture were calculated from Eqs. (5.27) and (5.28). The results shown in Table 5.1 indicate that most of the mixtures can be analyzed within an error of 10%. The higher error was observed in the determination of 1.0×10^{-7} mol l^{-1} of tungstate (+20%), 2.0×10^{-7} mol l^{-1} of molybdate (-16.5%) and 2.0×10^{-7} mol l^{-1} of tungstate (+15%) in Mo(VI)/W(VI) mixtures in 1:1, 1:4 and 4:1 ratios, respectively.

Table 5.1

Recovery of molybdenum(VI) and tungsten(VI) in synthetic mixture

Mixture taken/10^{-7} mol l^{-1}		Found / 10^{-7} mol l^{-1}	
Mo(VI)	W(VI)	Mo(VI)	W(VI)
1.0	1.0	0.91 (-9.0)	1.20 (+20.0)
1.0	3.0	1.06 (+6.0)	2.98 (-0.7)
2.0	2.0	2.03 (+1.5)	2.00 (±0.0)
3.0	1.0	3.15 (+5.0)	0.96 (-4.0)
2.0	4.0	1.99 (-0.5)	4.14 (+3.5)
3.0	3.0	2.93 (-2.3)	3.07 (+2.3)
4.0	2.0	4.19 (+4.8)	1.90 (-5.0)
2.0	6.0	2.22 (+11.0)	5.87 (-2.2)
4.0	4.0	3.89 (-2.8)	4.23 (+5.8)
6.0	2.0	6.21 (+3.5)	1.97 (-1.5)
2.0	8.0	1.67 (-16.5)	8.30 (+3.8)
5.0	5.0	4.84 (-3.2)	5.30 (+6.0)
8.0	2.0	7.70 (-3.8)	2.30 (+15.0)

The values in the parentheses indicate error (%).

This method permits the resolution of Mo(VI)/W(VI) mixtures in ratios from 1:3 to 3:1 at the 10^{-7} mol l^{-1} level with acceptable precision.

The plots of the R_{0s}' values for mixtures versus the sums of the concentrations of molybdenum(VI) and tungsten(VI) fell just on the line with a slope of k_s' and the intercept of a_s' described in the preceding section. This fact indicates that the presence of one catalyst has no effect on the kinetic behavior of another. This may also be considered proper from the results and the previous mechanistic studies (Chapter 4). These catalyzed reactions proceed through the formations of complexes of catalyst with hydrogen peroxide and hydrogen ion, H_2MoO_4-$(H_2O_2)_2$-H^+ and H_2WO_4-$(H_2O_2)_2$, as the catalytically active species in fast equilibrium steps prior to the rate determining step. The former species reacts with CP and the latter species reacts with CP and CP-H^+ in the rate determining step, respectively. Since hydrogen ion is in a large excess over the other reagents and catalysts, and hydrogen peroxide and CP are also in a large excess over both the catalysts, it can be expected that the complex formation of one catalyst and its subsequent reaction has no effect on those of another.

5.3.5 Effect of foreign ions

The effect of various ions on the determination of 4.5×10^{-7} mol l^{-1} molybdenum(VI) and 4.5×10^{-7} mol l^{-1} tungsten(VI) in a mixture was examined. The following ions showed no interference

at the concentrations (mol l^{-1}) shown in parentheses: Na^+,K^+, Li^+, Mn^{2+}, Ca^{2+}, Cl^-, SO_4^{2-}, NO_3^-, CO_3^{2-} (10^{-2}); Mg^{2+}, Co^{2+}, Ni^{2+}, Sr^{2+}, Cd^{2+}, NH_4^+, Br^-, ClO_3^-, ClO_4^-, $S_2O_3^{2-}$, SO_3^{2-} (10^{-3}); Pb^{2+}, Cr^{3+}, SCN^- (10^{-4}); V(V), Hg^{2+}, Ag^+, Sn^{2+}, I^-, BrO_3^- (10^{-5}); Cr(VI), Fe^{3+}, IO_3^- (10^{-6}); NO_2^-, Fe^{2+} (10^{-7}). Ions which are known to participate in redox reaction as either oxidizing or reducing agents cause serious interference.

5.3.6 Differential determination of molybdenum(VI) and tungsten(VI) in a hot spring water sample

In order to test the reliability of the present method, it was applied to the differential determination of molybdenum(VI) and tungsten(VI) in hot spring water. The determinations were made by using samples diluted at different times. The method was also checked by adding a known amount of molybdenum(VI) and tungsten(VI) to the samples. The results are shown in Table 5.2. The values corrected for dilution showed good agreement, and good recoveries of added molybdenum(VI) and tungsten(VI) were obtained ranging from 93% to 107% (mean 101%). The concentration of tungsten(VI) was also determined by other methods and the results of 3.3×10^{-7} mol l^{-1} [23] and 3.1×10^{-7} mol l^{-1} [39] agreed very closely with that obtained by the proposed method [40].

Table 5.2

Differential determination of molybdenum(VI) and tungsten(VI) in a hot spring water.

Dilution / times	Added / 10^{-7} mol l^{-1}		Found /10^{-7} mol l^{-1}		In sample / 10^{-7} mol l^{-1}		Recovery, %	
	Mo(VI)	W(VI)	Mo(VI)	W(VI)	Mo(VI)	W(VI)	Mo(VI)	W(VI)
1	-	-	(0.27)[a]	2.93	N.D.[b]	2.9	-	-
2	-	-	(0.07)[a]	1.76	N.D.	3.5	-	-
2	2.0	-	2.11	1.92	-	-	102	-
2	-	2.0	(0.33)[a]	3.51	-	-	-	93
2	2.0	2.0	2.08	4.07	-	-	101	107
4	-	-	(0.32)[a]	0.75	N.D.	3.0	-	-
					av. N.D.	3.1	av. 101	100

a. Analytical results which are lower than 0.5×10^{-7} mol l^{-1}, are not reliable.

b. No detectable.

Chapter 6

Conclusion

Catalytic effect of some trace elements on the CP-hydrogen peroxide reaction was studied analytically and kinetically. The oxidation of CP by hydrogen peroxide proceeds by two independent and parallel reactions, one of which proceeds through the red intermediate, another is the reaction directly to the colorless product, and the author found that iodide and iron(II, III) catalyzed the red intermediate formation and tungsten(VI) and molybdenum(VI) catalyzed the direct sulfoxide formation.

A catalytic photometric method for the determination of trace amounts of iodide was proposed. In the presence of iodide, CP is oxidized by hydrogen peroxide in a sulfuric acid solution to a red intermediate, which is further oxidized to a colorless compound. The reaction is followed by measuring the increase in the absorbance at 525 nm ; the maximum absorbance is obtained on an absorbance/time curve at a given reaction time. Since the maximum value of the absorbance increases with an increase in the iodide concentration, this value is used as a parameter for the iodide determination. Under the optimum experimental conditions (1.0×10^{-3} mol l^{-1} CP, 1.5 mol l^{-1} sulfuric acid, 2.0 mol l^{-1} hydrogen peroxide, 30℃), iodide in the range 0.2 - 10 μg l^{-1} can be determined. The relative standard deviations are 0.8, 2.6 and 4.2% for 6.0, 2.0 and 0.6 μg l^{-1} iodide, respectively. Although iodate shows the same catalytic effect as iodide at the same concentration

level of iodine, free iodine shows a somewhat lower catalytic effect. The procedure has been successfully applied to the determination of iodide in natural water samples.

Extensive kinetic studies were also performed to investigate the mechanism of the CP-hydrogen peroxide reaction. The kinetic investigations were carried out by the initial rate method on both iodide catalyzed and uncatalyzed color formation reactions. For direct sulfoxide formation reaction, the integration method was applied. The reaction was followed by measuring the increase in the absorbance at 335 nm. The disappearance rate of CP is given by

$$-d[CP]/dt = k_3[I^-][H_2O_2][H^+] + k_6[CP][H_2O_2][H^+] + k_9[CP][H_2O_2][H^+] + k_{10}[CP][H_2O_2],$$

where the first and the second terms correspond to the coloration reaction and the third and the fourth to the colorless sulfoxide formation. The mechanisms consistent with each term were proposed. The dependence of maximum absorbance upon reagents concentrations in sulfuric acid medium could be explained by the kinetic-mechanistic study. Moreover, the kinetic investigation has led to considerations concerning contamination during the course of the reaction and impurities initially present in the reaction solution, which are practically important problems for obtaining reliable results in trace determinations.

It was found that iron(II, III) catalyzed the red intermediate formation and the catalytic effect of iodide decreased in hydrochloric acid solution. Thus, a catalytic photometric method for the determination of trace amounts of iron was developed. As

the reaction proceeds, the rate of this iron-catalyzed reaction did not fall off normally and during the early stage of the reaction a linear range on the reaction rate curve was observed under the conditions of higher reagent concentrations. Since the slope of the linear range increased with the increase in the iron concentration, tanα [=Δ(abs.)/Δ(s)] was used as a parameter for the iron determination. Under the optimum experimental conditions (0.011 mol l^{-1} CP, 0.43 mol l^{-1} hydrochloric acid, 0.12 mol l^{-1} hydrogen peroxide, 30℃), iron could be determined in the range 5 - 200 μg l^{-1}. The relative standard deviations were 6.6, 2.3 and 0.8% for 10, 40 and 80 μg l^{-1}, respectively. The procedure had been applied to the determination of iron in tap and natural fresh water samples.

The iron(II) catalyzed red intermediate formation reaction was studied kinetically by an initial-rate method. All reactions were run at constant ionic strength of 0.44 mol l^{-1} and 30℃. According to the results of a kinetic study of the iron(II) catalyzed reaction, a mechanism was proposed which led to the following rate equation:

$$R_{0cat} = \frac{[Fe(II)][CP][H^+][H_2O_2]}{2.0\times10^{-2}[CP][H^+] + 2.2\times10^{-4}[H_2O_2] + 1.8\times10^{-3}[H_2O_2][H^+] + 2.0[CP][H^+][H_2O_2]}.$$

Since the linear-portion of the absorbance/time curves used as a parameter for iron determination is still in the early stage, its slope, tan α, may be roughly comparable to the initial rates. The dependence of the slope on the reaction variables also showed the similar trends to that of the calculated results. The mechanistic study is useful in optimizing an analytical condition of catalytic method, especially when its reaction has a complicated kinetic dependence on reaction variables.

Tungsten(VI) showed the inhibitory effect for both the iodide and the iron catalyzed red intermediate formation reactions. Thus the acceleration effect of tungsten(VI) for colorless sulfoxide formation reaction was found. The reaction was followed by measuring the absorbance change at 344 nm of the sulfoxide for tungsten(VI) determination. Since the initial slopes of the absorbance/time curves, R_0 [$=\Delta(\text{abs.})/\Delta(s)$], increase with an increase in the tungsten(VI) concentration, R_0 was used as a parameter for the tungsten(VI) determination. Under the optimum experimental conditions (8.2×10^{-4} mol l^{-1} CP, 0.42 mol l^{-1} sulfuric acid, 0.010 mol l^{-1} hydrogen peroxide, 40℃), tungsten(VI) can be determined in the range 2 μg l^{-1} - 10 mg l^{-1}. By the use of initial rate as a parameter, such a wide determinable range was achieved. The relative standard deviations are 6.8, 6.0, 0.8% for 5, 10 and 60 μg l^{-1}, respectively. This method was successfully applied to a determination of tungsten(VI) in hot spring water samples. According to the results of a kinetic study of the catalyzed reaction, a mechanism is proposed which derives the following rate equation:

$$R_{0\text{cat}} = \frac{\sigma[\text{W(VI)}][\text{H}^+][\text{H}_2\text{O}_2]^2[\text{CP}] + [\text{W(VI)}][\text{H}^+]^2[\text{H}_2\text{O}_2]^2[\text{CP}]}{P + Q[\text{H}^+] + S[\text{H}^+][\text{H}_2\text{O}_2] + T[\text{H}^+][\text{H}_2\text{O}_2]^2}.$$

It was observed that the direct sulfoxide formation reaction was catalyzed not only by tungsten(VI) but also by molybdenum(VI), thus a simple and sensitive kinetic-catalytic method was developed for differential determination of these species. The molybdenum(VI) and tungsten(VI) catalyzed sulfoxide formation reactions were studied kinetically by an initial-rate

method in 0.12 mol l^{-1} hydrochloric acid solution (40℃). The rate equations of each reaction showed that the kinetic contributions to the total rate of these catalysts changed with reaction conditions; the reaction was first-order with respect to each of the two catalysts and the ratio of the apparent rate constant for molybdenum(VI) to that for tungsten(VI) decreased with an increase in the hydrogen peroxide concentration as shown in following equations (at 40°C and I = 0.12 mol l^{-1}):

$$k_{appM} = \frac{[H_2O_2]^2[CP]}{3.35\times10^{-10} + 4.59\times10^{-3}[H_2O_2]^2}$$

$$k_{appT} = \frac{[H_2O_2]^2[CP]}{2.74\times10^{-9} + 1.99\times10^{-3}[H_2O_2]^2} .$$

Based on this kinetic difference, molybdenum(VI) and tungsten(VI) can be determined differentially. The method developed here utilizes the initial rates measured at two different hydrogen peroxide concentrations and the corresponding rate equations. Their mixtures at approximately equimolar concentrations (in the 10^{-7} mol l^{-1} range) are determined with an error of ca. 10%. Although the interdependence of reaction variables in kinetic methods is commonly rather complicated, the rate equation accurately describes the quantitative dependence of the reaction rate upon the catalyst and all reactants and permits accurate prediction of the behavior of the reaction over a wide range of reaction conditions. Thus, the use of rate equations is the most favorable for systematically finding optimum conditions for differential determinations.

References

[1] H.L.Pardue, Anal. Chim. Acta, 216 (1989) 69.

[2] H.A.Mottola, Kinetic Aspects of Analytical Chemistry, Wiley, New York, 1988, pp.19-21.

[3] D.Perez-Bendito and M.Silva, Kinetic Methods in Analytical Chemistry, Ellis Horwood, Chichester, 1988, pp.190-247.

[4] K.-T.Lee, Anal. Chim. Acta, 26 (1962) 285.

[5] K.-T.Lee, Anal. Chim. Acta, 26 (1962) 478.

[6] I.S.Forrest, F.M.Forrest and M.Berger, Biochim. Biophys. Acta, 29 (1958) 441.

[7] H.S.Gowa and R.Shakunthala, Talanta, 13 (1966) 1375.

[8] M.H.Cordoba, P.Vinas and C.Sanchez-Pedreno, Analyst, 110 (1985) 1343.

[9] D.J.Cavanaugh, Science, 125 (1957) 1040.

[10] E.B.Sandell and I.M.Kolthoff, J. Am. Chem. Soc., 56 (1934) 1426.

[11] E.B.Sandell and I.M.Kolthoff, Mikrochim. Acta[Wien],1 (1937) 6.

[12] N.Yonehara, Bull. Chem. Soc. Jpn., 37 (1964) 1101.

[13] K.Oiwa, T.Kimura, H.Makino and Y.Kinoshita, Bunseki kagaku, 17 (1968) 805.

[14] S.Funahashi, M.Tabata and M.Tanaka, Anal. Chim. Acta, 57 (1971) 311.

[15] E.Jungreis and I.Gedalia, Mikrochim. Acta[Wien], (1960) 145.

[16] N.Yonehara, S.Kozono and H.Sakamoto, Anal. Sci., 7 (1991) 229.

[17] M.H.Cordoba, P.Vinas and C.Sanchez-Pedreno, Analyst [London], 110 (1985) 1343.

[18] P.Vinas, M.H.Cordoba and C.Sanchez-Pedreno, Talanta, 34 (1987) 351.

[19] T.Tomiyasu, H.Sakamoto and N.Yonehara, Anal. Sci., 10 (1994) 293.

[20] M.G.Evans and N.Uri, Trans.Faraday Soc.,45 (1949) 224.

[21] J.C.McCoubrey, Trans. Faraday Soc., 51 (1955) 743.

[22] H.A.Liebhafsky and A.Mohammad, J. Am. Chem. Soc., 55 (1933) 3977.

[23] T.Tomiyasu, Anal. Chim. Acta, 312 (1995) 179.

[24] A.Moreno, M.Silva, D.Perez-Bendito and M.Valcarcel, Anal. Chim.Acta, 15 7(1984) 333.

[25] A.Moreno, M.Silva and D.Perez-Bendito, Anal. Chim. Acta, 159 (1984) 319.

[26] S.Abe, T.Saito and M.Suda, Anal. Chim. Acta, 181 (1986) 203.

[27] S.Abe and M.Endo, Anal. Chim. Acta, 226 (1989) 137.

[28] T.J.Cardwell, D.Caridi and R.W.Cattrall, Anal. Chim. Acta, 192 (1987) 129.

[29] J.Alons, J.Bartroli, M.D.Valle and R.Barber, Anal. Chim. Acta, 219 (1989) 345.

[30] T.Kawashima, N.Hatakeyama and M.Kamada and S.Nakano, Nippon Kagaku Kaishi, 1981, 84.

[31] T.Tomiyasu, H.Sakamoto and N.Yonehara, Anal.Sci., 8 (1992) 293.

[32] T.Tomiyasu, H.Sakamoto and N.Yonehara, Anal. Sci., 12 (1996) 507.

[33] T.Tomiyasu, H.Sakamoto and N.Yonehara, Anal. Chim. Acta, 320 (1996) 217.

[34] T.Tomiyasu, H.Sakamoto and N.Yonehara, Anal. Sci., 10 (1994) 761.

[35] V.K.Pavlova, A.T.Pilipenko and R.N.Voevutskaya, Zh. Analit. Khim., 30 (1975) 2190.

[36] R.N.Voevutskaya, V.K.Pavlova and A.T.Pilipenko, Zh. Analit. Khim., 34 (1979) 1299.

[37] L.G.Sillen and A.E.Martell, Stability constants of metal ion complexes, supplement No 1, The chemical society, London, 1971, p.46.

[38] R.H.Smith and J.Kilford, Int. J. Chem. Kinet., 8 (1976) 10.

[39] T.Tomiyasu and N.Yonehara, Anal.Sci., 12 (1996) 1.

[40] T.Tomiyasu, Anal. Chim. Acta, 349 (1997) 43.

Acknowledgments

The author wishes to express his sincere thanks to Professor Norinobu YONEHARA, Faculty of Science, Kagoshima University, for his kind guidance throughout this study and for his criticism and helpful discussions.

The author wishes to express his sincere acknowledgment to Professor Takuji KAWASHIMA, Department of Chemistry, the University of Tsukuba, for his continuing interest and encouragement and for his valuable advice in the preparation of this manuscript.

The author is sincerely grateful to Professor Hayao SAKAMOTO, Faculty of Science, Kagoshima University, for his support of this work and many discussions.

The author is very grateful to Dr. Norio TESHIMA and Dr. Makoto KURIHARA, Department of Chemistry, the University of Tsukuba, for their help in the preparation of this manuscript.

The author would like to thank all his collaborators who contributed to this work with their warm assistance and advise.